# FES Joule Milestone 2009
## Fourth Quarter & Final Report
## September 30, 2009

**Annual Target**: Conduct experiments on major fusion facilities to develop understanding of particle control and hydrogenic fuel retention in tokamaks. In FY09, FES will identify the fundamental processes governing particle balance by systematically investigating a combination of divertor geometries, particle exhaust capabilities, and wall materials. Alcator C-mod operates with high-Z metal walls, NSTX is pursuing the use of lithium surfaces in the divertor, and DIII-D continues operating with all graphite walls. Edge diagnostics measuring the heat and particle flux to walls and divertor surfaces, coupled with plasma profile data and material surface analysis, will provide input for validating simulation codes. The results achieved will be used to improve extrapolations to planned ITER operation.

**Fourth Quarter Milestone**

Complete the necessary experiments, analysis, and modeling. Prepare a joint report on the empirical understanding gained, the comparison to simulation and identify critical research areas to improve extrapolation to ITER.

**Completion of 4th Quarter and Annual Milestone**

The 4th quarter milestone has been completed. Experiments, analysis and modeling have been carried out at the facilities. Joint research activities and results and highlighted here, and below the research results are organized by facility. Significant progress has been made towards better characterizing particle control and fuel retention in tokamaks. The facilities worked closely together to share and implement ideas on particle measurement techniques in order to best compare results across facilities using different wall materials. The facilities coordinated implementation of particle balance experiments using both the "static" and "dynamic" measurement method. The static technique is highly accurate but lacks time resolution, whilst the dynamic technique provides time resolved fuel retention, but can be prone to uncertainty in exhaust rates.

The main highlights of the joint work are:

1. Static and dynamic particle balance measurement techniques were successfully carried out on all three facilities (Alcator C-Mod, DIII-D and NSTX) with generally good agreement between the two techniques. This establishes a powerful and accurate set of tools to study particle balance across the three devices despite their significant differences in configuration and wall materials.

2. In DIII-D and C-Mod dynamic particle balance showed a very consistent trend, namely that the wall retention rate of fuel was very close to zero when the plasma reached a stationary condition in current flattop with density feedback control and divertor cryopumping. This similarity is despite the very different plasma-facing materials used: graphite/carbon in DIII-D and refractory metals (molybdenum and tungsten) in Alcator

C-Mod. This result could be encouraging for longer pulsed divertor plasmas with strong divertor pumping, such as ITER.

3. In contrast, NSTX finds a constant large rate of positive fuel retention to the wall during flattop. It is unclear if this difference is due to differences with Spherical Torus plasma transport, non-stationary density and/or the lack of divertor cryopumping. Furthermore NSTX finds only small differences in retention between graphite and Lithium-coated surfaces, although Lithium clearly reduces the recycling of fuel from the plasma-facing components. Ex-situ analysis of material samples from NSTX illuminated important surface chemistry processes that were occurring with the Lithium coatings and the underlying graphite/carbon. These insights helped explain NSTX results with respect to fuel absorption and release.

4. Dynamic particle balance indicates that wall fuel retention rates are strongest in the beginning phases of the discharge, and this phase typically leads to net wall retention when considered over the entire discharge in these modest pulse-length devices (1-5 seconds). Because the shot-averaged retention rates can be dominated by transient phases, such as plasma startup, the implications for very long-pulse devices, such as ITER and eventual reactors, remain uncertain.

<u>Exploring underlying processes controlling particle balance:</u>

5. In all three facilities it was found that shot-averaged retention organized well to incident ion fluence to plasma-facing surfaces. In discharges without strong external heating (ohmic) all facilities found significant and similar shot-averaged retention inventories. These inventories range from ~1-2% in C-Mod to 2-4% in DIII-D if normalized to the total incident ion fluence to the walls, and 6-7% in NSTX if normalized to only the ion fluence to the outer divertor.

6. Static and dynamic particle balance on Alcator C-Mod showed that disruptions, and the associated pulsed heating of wall material, can be used to effectively recover the retained fuel from the metallic surfaces, a technique which has been proposed for tritium recovery in ITER.

7. DIII-D showed that detached plasmas significantly reduced erosion sources of carbon, which is positive for ITER which must be operated with detachment to reduce heat flux. *(Ph.D. thesis)*.

8. NSTX results showed the positive effect of lithium actively pumping the deuterium fuel, resulting in a lower recycling edge and improved overall performance.

9. DIII-D showed that high energy confinement (H-mode) discharges with strong heating had consistently lower dynamic retention rates than ohmic dishcarges. In C-Mod confinement mode and heating did not strongly affect the near retention rate under stationary conditions. In NSTX the dynamic retention rate was high in both heated H-

mode and ohmic discharges. This indicates that it is difficult to separate the effects of confinement, which affects plasma fuelling requirements, from the effect of plasma heating which affect material temperatures, and hence, fuel retention.

10. C-Mod explored the depth profile of retained Deuterium in molybdenum, showing that the deuterium was deeper than the limit of ion beam detection (5 microns) and was present in the Mo at a concentration of D/Mo ~ 1%, much higher than expected and indicating that plasma bombardment was producing damage sites in the Mo where the deuterium fuel could then get "trapped" *(Ph.D. thesis)*.

11. The DIII-D and C-Mod results of ~zero real-time retention rates in stationary plasmas is not well understood. Material temperature is well known in laboratory measurements to be the primary controller of material interaction and retention with hydrogenic fuels. However, in these tokamaks without active cooling the material surface temperature continues to evolve even if the plasma conditions are stationary. Furthermore these two facilities use dramatically different materials: in C-Mod implantation and permeation should dominate retention in the refractory metals, while in DIII-D codeposition of the fuel with carbon layers should be most important. The results suggest that one should not view the plasma-material interaction in isolation, but rather include the plasma's self-regulation of fueling is which seems to play an important role in the fuel retention in these cases. This strongly suggests future research efforts in this area since such effects are not presently considered in models of fuel retention.

<u>Analysis and modeling of particle balance and control:</u>

12. C-Mod showed that actual pumping speed during a discharge at high divertor pressure is systematically lower than pumping speed obtained by gas only injections into the torus. DIII-D also found a similar difference in static versus dynamic inventories in their one case at higher density/divertor pressure. The reasons for this should be further investigated. These results clearly show the great advantage of combining static and dynamic techniques to improve the accuracy and time resolution of particle balance measurements.

13. DIII-D showed with carbon isotope tracer experiments that the carbon deposits, and accompanying fuel retention, were predominately at the inner divertor, although the details of the deposit location could vary with plasma conditions.

14. A dynamic particle balance model was used to study the wall pumping and outgassing during the discharge in NSTX. The wall was found to be in a pumping state in nearly all of the analyzed discharges. A measurable increase was found in the cumulative wall fuel inventory in lithium conditioned neutral beam heated discharges.

15. Numerical modeling of the permeation and trapping of the deuterium fuel in molybdenum metals was carried out. The model had success in replicating both the

retention of the fuel and its release by disruption heating, although the mechanism producing damage sites remains under investigation *(Ph.D. thesis)*.

**FIGURES: Results from Joint Experiments on DIII-D, Alcator C-Mod and NSTX**

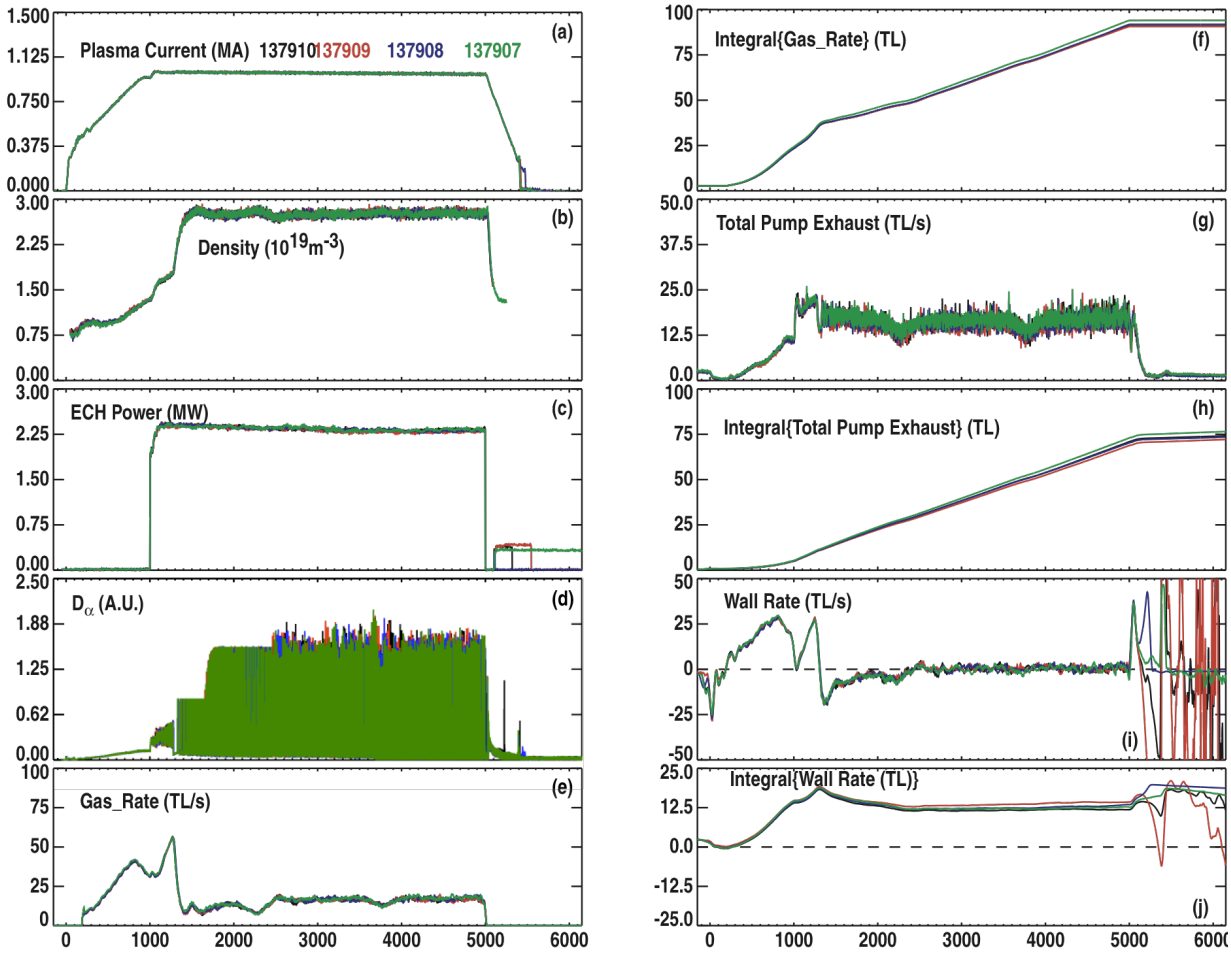


Figure 1 DIII-D particle balance experiment showing four repeated discharges. The fuel retention rate (i) is ~zero in the stationary conditions from 2500 -5000 ms.

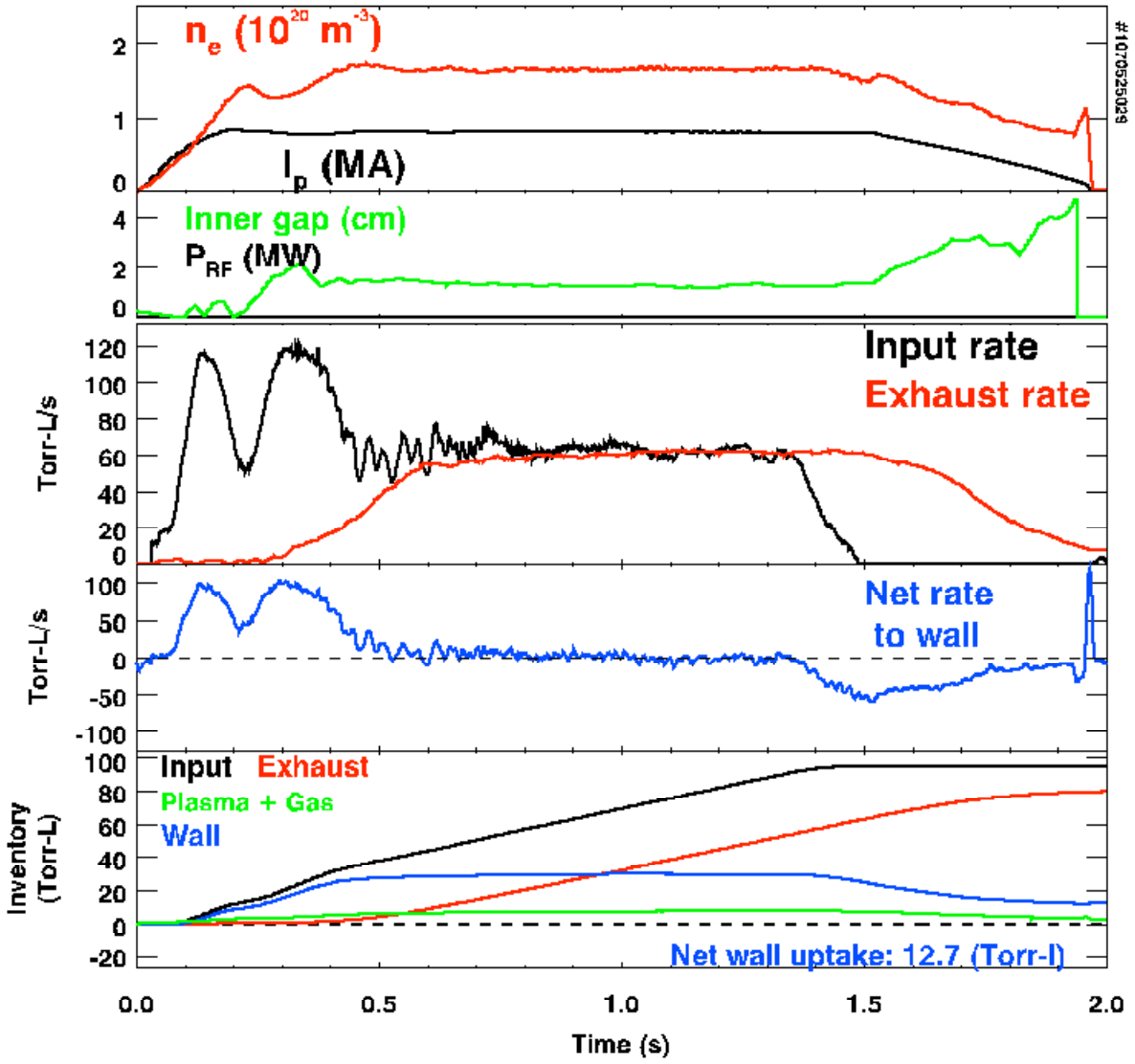


Figure 2 Alcator C-Mod particle balance experiment combining dynamic and static particle balance measurement. The fuel retention rate (third panel) is ~zero in the stationary conditions from 0.5 to 1.5 seconds.

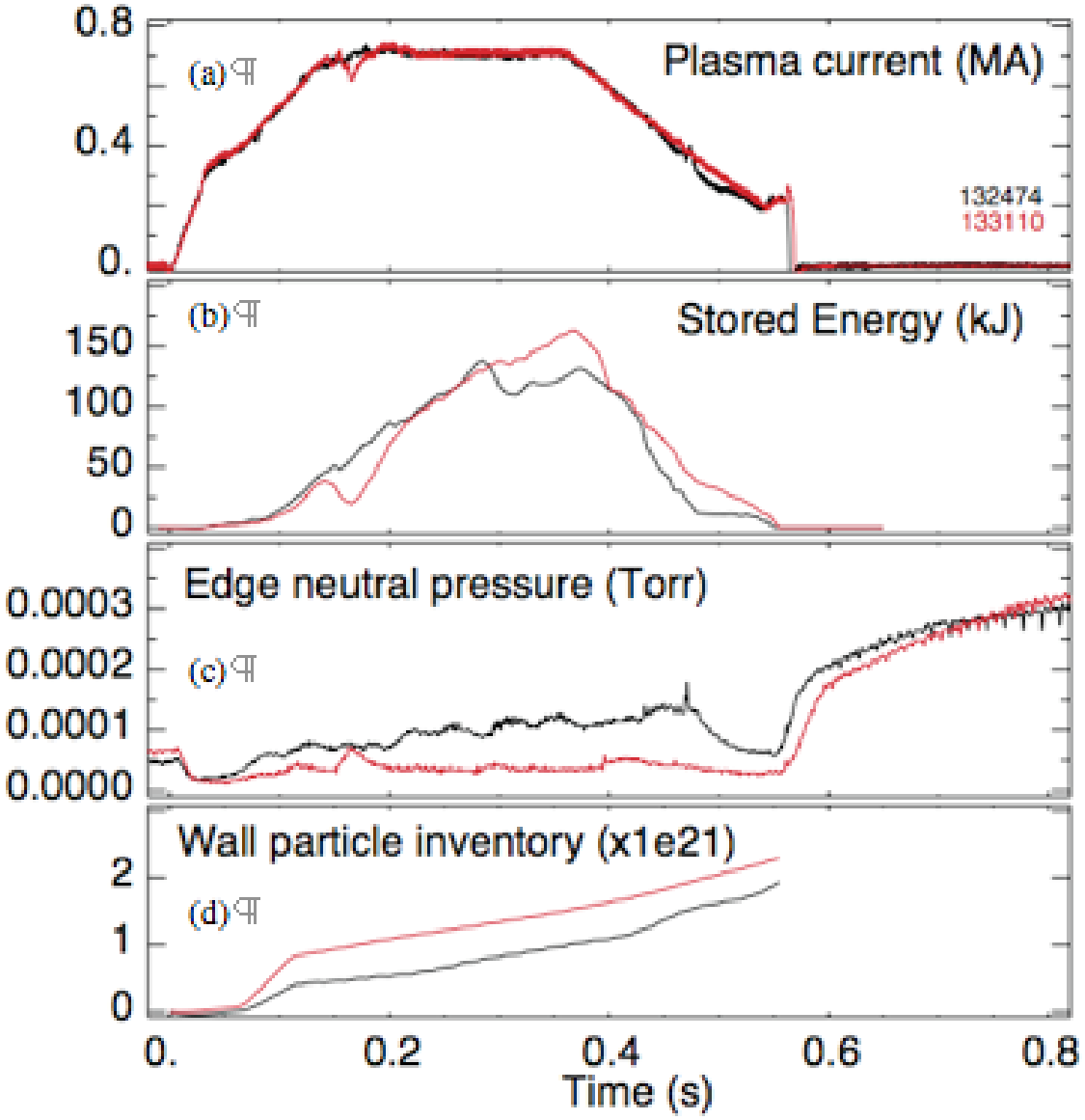


Figure 3 NSTX particle balance experiment using dynamic particle balance comparing matched discharges with graphite wall (black) and a lithium-coated wall (red). Note the constant retention inventory buildup in both ccases (d) while lithium lowers edge gas fuel pressure (c) and improves plasma energy (b).

# DIII-D Facility Report

GA–C26564

# PARTICLE CONTROL AND HYDROGENIC RETENTION WITH CARBON IN-VESSEL COMPONENTS: UNDERSTANDING AND CONTROLLING TRITIUM INVENTORY IN CO-DEPOSITED LAYERS (DIII-D CONTRIBUTION TO FY09 JOINT RESEARCH TARGET)

## FINAL REPORT

## Milestone 168

by
PROJECT STAFF

SEPTEMBER 2009

GENERAL ATOMICS

## DISCLAIMER

GA– C26564

# PARTICLE CONTROL AND HYDROGENIC RETENTION WITH CARBON IN-VESSEL COMPONENTS: UNDERSTANDING AND CONTROLLING TRITIUM INVENTORY IN CO-DEPOSITED LAYERS (DIII-D CONTRIBUTION TO FY09 JOINT RESEARCH TARGET)

## FINAL REPORT

## Milestone 168

by
PROJECT STAFF

Prepared for
the U.S. Department of Energy under
DE-FC02-04ER54698

GENERAL ATOMICS PROJECT 30200
DATE PUBLISHED: SEPTEMBER 2009

## DESCRIPTION OF DELIVERABLE

A critical ITER issue is the control of the in-vessel inventories of tritium and dust. DIII-D and other machines have demonstrated that co-deposition of hydrogen isotopes with eroded carbon is a potentially significant retention mechanism for ITER. DIII-D will systematically investigate hydrogenic retention and carbon/hydrogen co-deposition on divertor surfaces using a variety of techniques including $^{13}C$ methane injection followed by surface analysis at Sandia and MIT. Edge flow measurements, coupled with measurements of SOL and divertor plasma parameters along with other surface measurements, will be compared with edge simulation to better understand the physical mechanisms that govern hydrogenic retention. We will also investigate active control and/or removal of co-deposited carbon layers and dust using thermal oxidation (i.e., oxygen bake).

This is the DIII-D contribution to the FES Joint Research Target.

## DEFINITION OF COMPLETION

Final Report

# I. SUMMARY

For particle (fuel and/or tritium control), there are several important issues, including: a) measuring the rate of fuel retention by the wall, b) determining which processes influence the wall retention, c) determining the location of the retained fuel/tritium, and d) techniques to remove particles from the wall, either during or after the discharge. We have performed DIII-D experiments to address these questions with all-carbon walls, and provide results that can be compared with other machines with metal or lithium walls. Research on DIII-D has resulted in significant progress in answering these questions; the DIII-D contributions are the subject of this summary report and form the outline of the report.

1) "Dynamic" particle balance (particle sources and sinks calculated vs time in the discharge) yields similar results to "static" (calculated vs shot by pressure rise) particle balance.
2) DIII-D results show low wall retention in H-mode, compared with large retention during initial ramp-up and L-mode; dynamic particle balance is required for this determination.
3) The most tightly bound retained deuterium fuel has been found in the form of codeposits with eroded carbon. $^{13}C$ injection experiments have shown that most of the carbon in the plasma is deposited at the inner strike point of a SN divertor in L-mode, additional deposition in the private flux zone is present in H-mode. In addition, even moderate heating of graphite DiMES samples to 200°C results in a factor of 10 less deposition compared to room temperature.
4) The DiMES divertor surface station has been used to demonstrate that chemical erosion in the grahite divertor target is dramatically reduced in a cold, detached divertor, with important advantages for ITER.
5) Preparations for a DIII-D demonstration of removal of re-deposited carbon with an Air Bake have progressed and final reviews are in progress. An Air Bake of 10 Torr air for 2 h at 350°C is predicted to remove deposited $^{13}C$ layers in DIII-D. In ITER, removal of the carbon would also remove the co-deposited tritium.

In summary, DIII-D has made significant progress in addressing issues of carbon-facing materials in future tokamaks. Retention is nearly zero in ELMing H-mode, erosion is dramatically reduced for detached divertor operation, most of the eroded carbon is

deposited in the divertor region near the strike point, and effective means of removing co-deposits are being qualified. As no currently envisaged material is perfect for a fusion reactor, it is important to address the scientific issues of current materials such as carbon. More complete discussion of these key results follow.

## II. DYNAMIC AND STATIC PARTICLE BALANCE MEASUREMENTS AGREE

Scientists from DIII-D and C-Mod carried out particle balance experiments to measure wall retention with carbon Plasma Facing Components (PFCs) in DIII-D for comparison with similar experiments in C-Mod and NSTX. C-Mod has used a "static" particle balance technique where plasma discharges are carried out with a closed vessel and no pumping. Careful accounting of the gas input and pressure rise is used to determine the average particle balance on a shot by shot basis. Through a collaborative experiment with C-Mod scientists, this technique was used for the first time on DIII-D in ohmic discharges, and these results were presented in [1]. These DIII-D data showed that there was a significant influx of particles to the wall in unpumped ohmic plasmas, and modest retention ~ 20% during pumped ohmic discharges.

DIII-D has pioneered a "dynamic" particle balance technique [2] where the sinks and sources in the particle balance equation are calculated as a function of time from the plasma density, particle inputs, and particle exhaust. This time-dependent analysis allows for determining which part of the discharge is most responsible for fuel retention. DIII-D has 3 helium cryopumps that can provide pumping on the order of 20,000-30,000 T L/s each. Auxiliary heating with either ECH (no particle input) or neutral beams (with a particle input) can be compared. In a series of cryopumped H-mode experiments on DIII-D, the particle inputs and exhaust as measured by the dynamic technique were compared with the static technique. For the ECH H-mode shots, excellent agreement was observed between the two measurement techniques, as shown in column 5 of Table 1. In a given series of shots, the static exhaust was calculated from the pressure rise after the shot when the cryopump was regenerated (warmed). The dynamic exhaust was calculated during the discharge and integrated to obtain the total for each shot. The quantity show in column 5, {(Static Exhaust – Total Dynamic Exhaust)/Static Exhaust}, was used to compare the two measurement techniques. The percentage difference was on the order of 5% or less, showing excellent agreement between the two techniques. The quantity shown in column 6 of Table 1, {(Gas Input-Static Exhaust)/Gas Input}, yields the amount of gas retained was around 15%, which agrees well with the previous data shown in Fig. 1 (blue squares). As these discharges obtained H-mode with ECH heating, there were no additional particle inputs associated with the heating technique. It should be

emphasized that the 15% retention rate is for the total discharge, and includes the ramp-up, L-mode, and H-mode periods. We will see in the next section that most of the wall retention is during the ramp-up and initial L-mode, with very little wall retention during the ELMing H-mode.

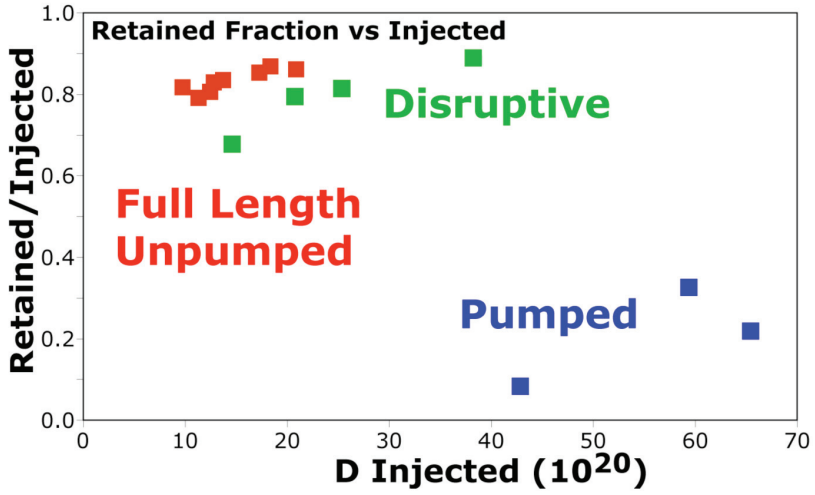


Fig. 1. Static particle balance measurements from ohmic discharges on DIII-D show high percentage retention without pumping, and are 10-25% with pumping. From [1].

Table 1: Summary of Dynamic and Static Exhaust for ECH H-mode with Cryopumping

| Shot Sequence | Total Gas Input | Dynamic Exhaust | Static Exhaust | (Static – Dynamic) / Static | (Gas-Static) /Gas |
|---|---|---|---|---|---|
| | | Calculated During Shot | Pressure Rise X Machine Volume | % Difference | % Gas Input Retained in Wall |
| 137903-137906 | 76+79+85+93= 333 TL | 66+64+68+67= 268 TL | 7 mT*V = 277 TL | 3% | 16% |
| 137907-137910 | 94+92+91+91= 368 TL | 75+72+71+72= 290 TL | 7.5mT*V = 297 TL | 2% | 19% |
| 137911 | 94 TL | 74 TL | 1.9 mT*V = 75 TL | 1% | 20% |
| 137912-137913 | 78+76= 154 TL | 67+64= 131 TL | 3.5mT*V = 139 TL | 6% | 10% |
| 137915-137918 | 85+83+84+79= 331 TL | 69+73+74+73= 289 TL | 6.9 mT *V= 273 TL | -6% | 18% |
| 137919-137921 | 101+72+79= 252 TL | 76+72+71= 219 TL | 5.4mT*V= 214 TL | -2% | 15% |
| 137922-137924 | 82+79+80= 241 TL | 69+69+73= 220 TL | 205 TL | -7% | 15% |
| Total | 1773 TL | 1491 TL | 1480 TL | -1% | 16% |

Measured Vessel Volume: V=39.6 $m^3$

## III. WALL UPTAKE IS SMALL OR NEGATIVE DURING H-MODE OPERATION

The advantage of the dynamic particle balance technique is that changes in the various particle balance terms can be tracked during the discharge. In Fig. 2 an ECH H-mode shot (red) is compared with a NBI discharge at the same power (black). First focus on the red ECH shot 137910 that is from the series in Table 1. The dynamic particle balance reveals a striking feature (panel g) that the wall uptake is ~20 TL/s during the period before 1 s, but then drops to nearly zero during the whole ELMing H-mode period of the discharge. Even though a small gas puff is required by the feedback system to maintain a constant density, note that the net wall inventory (panel f) calculated by the particle balance decreases during the H-mode. This is because the calculated wall retention flux is nearly zero. The red trace with ECH heating shows that ELMing H-mode discharges with cryopumping have very low wall retention, and it is important to discriminate between wall loading during the ramp-up, L-, and H-mode periods of the discharge.

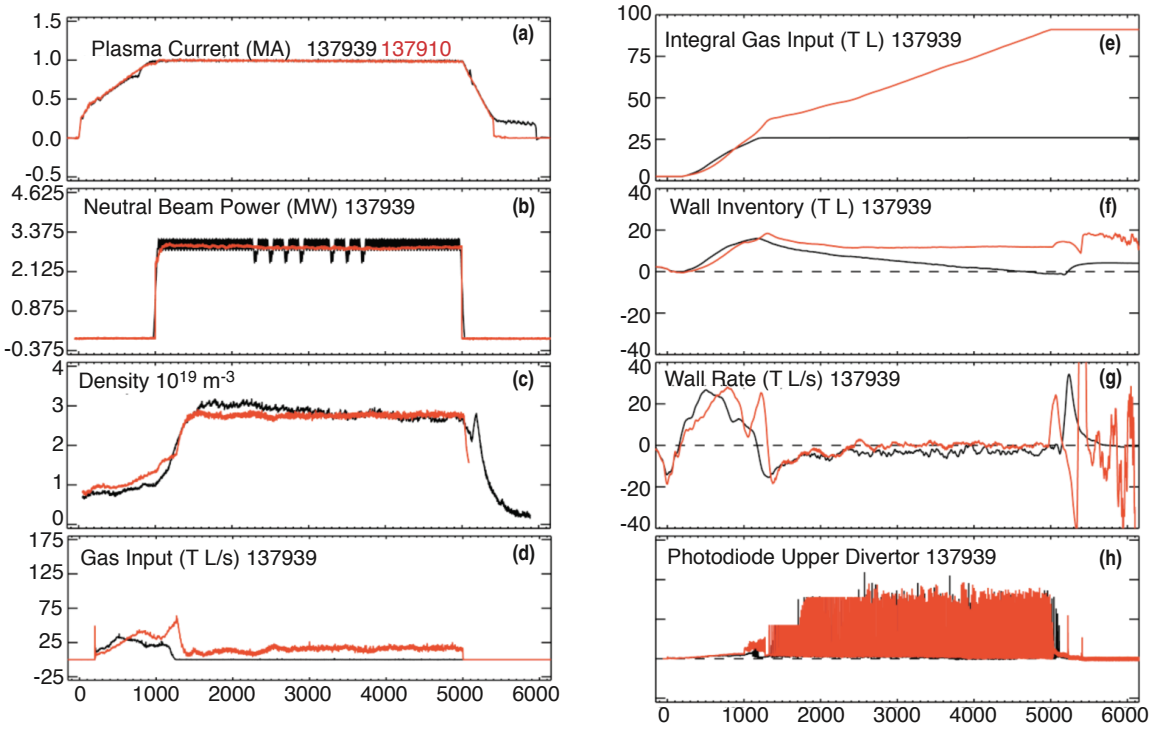


Fig. 2. ECH heated (red) H-mode plasma is compared with a NBI (black) discharge. The plasma current, neutral beam or ECH power, electron density, gas input, integral of the gas input; wall inventory and wall rate from the dynamic particle balance; along with the photodiode signal are compared with a neutral beam heated H-mode DIIID shot. Note that in both cases, the wall flux is quite large in the L-mode period, but during the ELMing H-mode, the wall flux is very close to zero.

If we use the dynamic particle balance to separately calculate the wall retention in the L-mode and H-mode periods of the discharge, we see that there is a net wall deposition during ramp-up and L-mode, but the particle inventory in the wall actually decreases during the H-mode.

| Ramp-up and L-mode | | | H-mode | | |
|---|---|---|---|---|---|
| Gas in | Wall Inv. Inventory | % Retained | Gas In | Change in Wall | % (+) Retained or Lost |
| 37 TL | 18 TL | 48% | 91 - 37 = 54 TL | 12 – 18 = -6 TL | -6/54 = -10% |

Shown in black in Fig. 2 is a discharge with NBI heating. Note that the plasma current and electron density were well matched with the ECH discharge. The neutral beams inject energetic neutrals, cold neutrals, and also have cryopumps for differential pumping. The Torus Isolation Valves for the neutral beams were opened and closed as close to discharge as possible. In contrast to the ECH case in Fig. 2, there was no gas injection in the NBI case {note that (panel e, black) is flat}. As the gas input during the NBI H-mode is zero, the wall flux is slightly negative and the wall inventory *decreases* during the shot, reaching nearly zero by the end of the discharge. In comparing the two discharges, the ELMs are much more rapid and very regular in the ECH heated H-mode, evidently resulting in an additional plasma exhaust. After the second day of the experiment, the bake resulted in a pressure rise of about 25 mTorr, so about 1000 TL was removed from the wall (recall the experiment was started with an "average" wall).

## IV. CARBON DEPOSITION MAXIMIZES NEAR THE INNER STRIKE POINT IN LSN DISCHARGES

Even though the wall retention is extremely small in H-mode, there can be some retention during ramp-up, L-mode, and disruptions. The most tightly bound of this retained fuel is codeposited with eroded carbon. For this retained fuel, it is important to minimize the D/C ratio of the co-deposits. Specifically, the D/C ratio of the co-deposited layers can be high (~0.8) at room temperature, but is low (0.2) at higher temperature. Shown in Fig. 3 is DIII-D data from DiMES showing that the amount of deuterium deposited in a graphite DiMES sample in the divertor at 200°C is nearly 10X less than that at ambient temperature. Thus, operation of the divertor plates at high temperature will reduce the amount of deposited carbon and deuterium fuel codeposited with it.

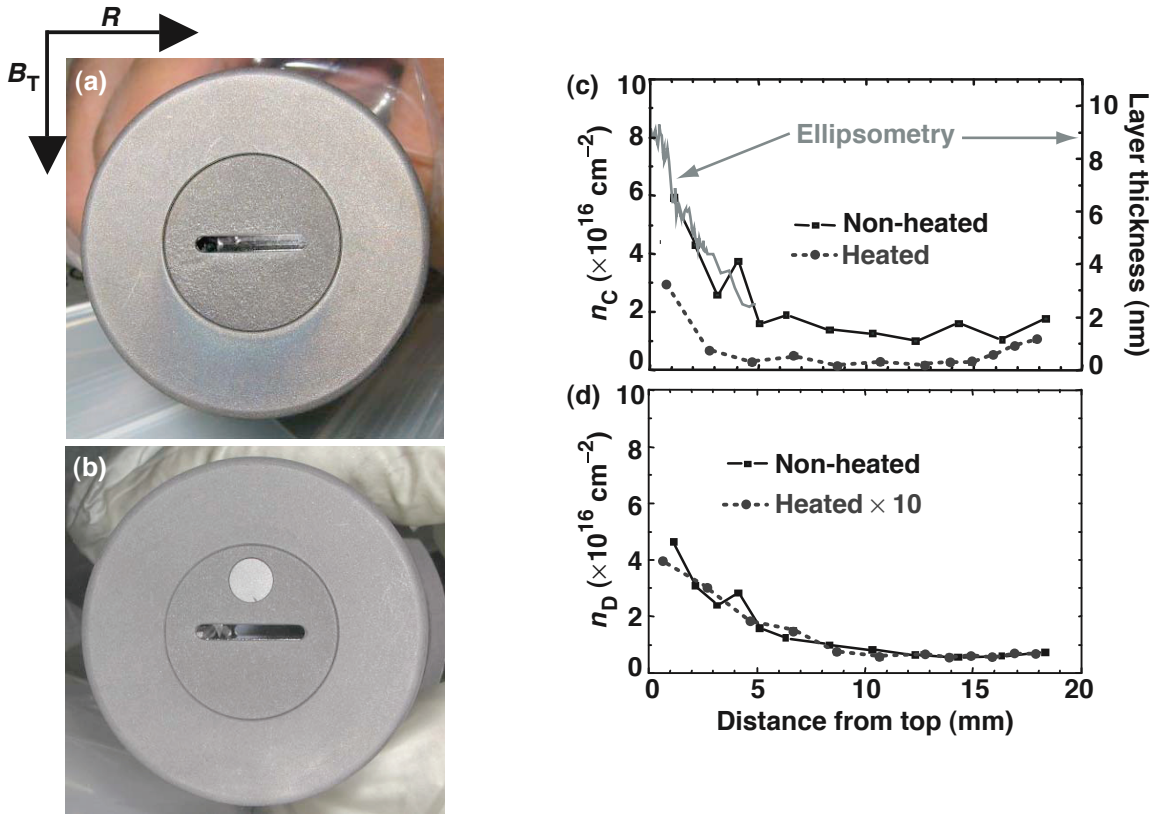


Fig. 3. Plasma-facing surface of the tile-gap sample after plasma exposure at ambient temperature (a) and pre-heated to 200°C (b). Profiles of the carbon (c) and deuterium (d) areal density measured by IBA versus the distance from the gap entrance for the ambient temperature (squares) and pre-heated (circles) exposures. The thickness profile measured by ellipsometry for the non-heated case [grey line in (c), scale on the right] compares well with IBA data.

In addition, it is important to determine the location of the co-deposits, and we have used $^{13}C$ injection in DIII-D to map these deposits in a tokamak plasma [4]. Over three run campaigns, $^{13}C$ was injected into plasmas and then tiles were removed and measured to determine where the carbon was deposited. The $^{13}C$ injection was from a toroidally symmetric plenum in the upper divertor, simulating carbon arriving in the SOL from the divertor on its way to the main chamber. The first experiment used a series of repeated L-mode shots. When the tiles were removed and analyzed by Sandia National Laboratory, it was found that most of the $^{13}C$ was deposited near the inner strike point of the lower divertor in Lower-Single-Null (LSN) plasmas (Fig. 4). The next year, the experiment was repeated with detached ELMing H-mode plasmas, and in addition to the peak at the inner strike point, there was deposition in the private flux region. The two cases are compared in Fig. 4, which shows the Sandia surface analysis results. A final experiment was done with injection into an unbalanced (downward) double null plasma

in an attempt to determine how much is deposited in the upper (inactive) divertor, these tiles are currently being analyzed.

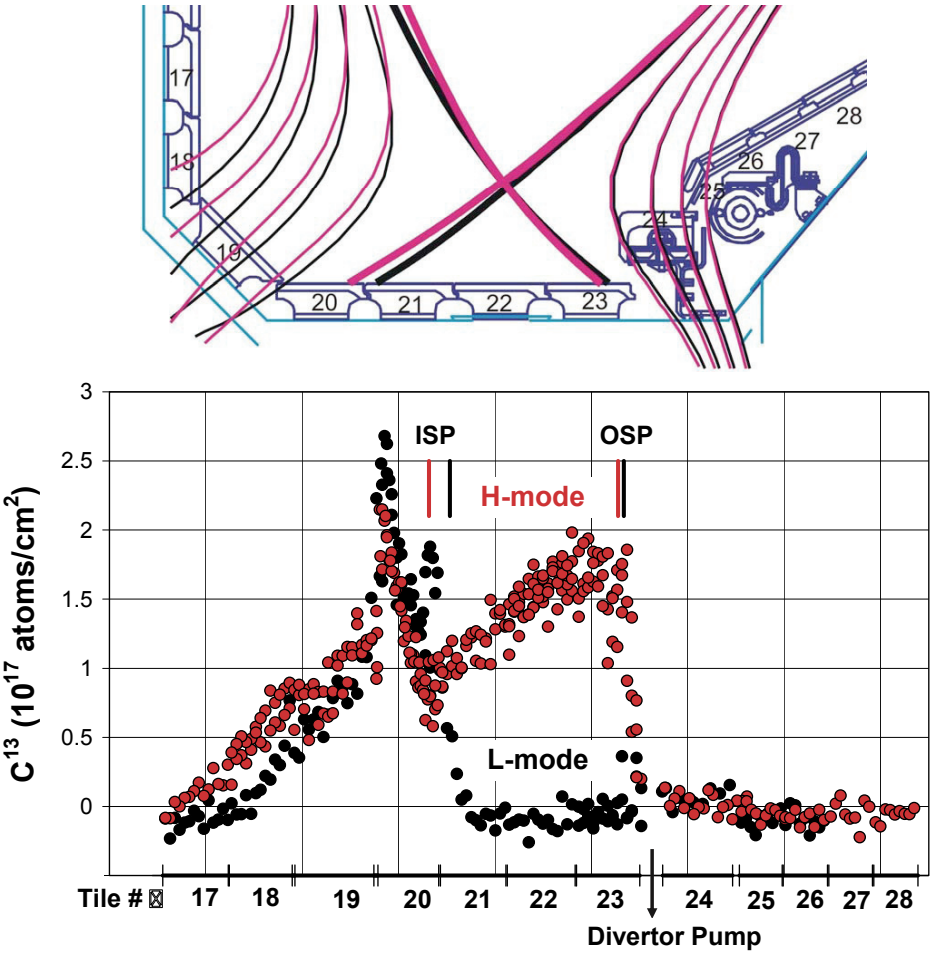


Fig. 4. The $^{13}C$ distribution measured by Sandia NRA analysis for L-mode and ELMing H-mode discharges. Note that the highest concentration is near the inner strike point, and there is additional deposition in the private flux region in H-mode.

## V. CHEMICAL EROSION IS DRAMATICALLY REDUCED IN DETACHED DIVERTOR OPERATION

A potentially large source of carbon is due to erosion of the divertor plate; erosion also determines the lifetime of the divertor plate. The erosion in the region can be due to either physical or chemical sputtering, and the relative rates are not well established in tokamak plasmas. Current estimates of tritium retention by co-deposition with hydrocarbons in ITER place potentially severe restrictions on operation. However, up

until recently, estimates have been based on excessively conservative assumptions, due to a limited understanding of cold, detached divertor plasmas (1-5eV) which involve complex atomic and molecular processes not present in attached conditions. A novel set of experiments was carried out on DIII-D to improve the accuracy of sputtering measurements, and thereby to obtain better erosion estimates. The results are summarized in a recent PhD thesis [5]. Hydrocarbon injection through a unique porous graphite plate was used to measure chemical erosion in the DIII-D divertor plasma. This Porous Plug Injector (PPI), mounted on the DiMES probe, realistically simulates secondary reactions of hydrocarbons with a graphite surface. For the first time in a divertor, measurements were made at extrinsic $CH_4$ injection rates comparable to the expected intrinsic chemical erosion rate of C, with the resulting spectroscopic emissions separated from those of the intrinsic sources. Under cold plasma conditions the contribution of carbon produced by chemical erosion (CE) relative to total C sources in the divertor declined dramatically from ~50% to <15%. Photon efficiencies for products from the breakup of injected $CH_4$ were greater than previous measurements at higher puff rates, indicating the importance of minimizing perturbation to the local plasma. At 350 K, the measured CE yield near the outer strike point was ~2.6% in attachment dropping to only ~0.5% in cold plasma; results are consistent with some theoretical predications and lab studies. Under full detachment, near total extinction of the CD band occurred, consistent with suppression of net C erosion. These findings have potentially major impact on projected target lifetime and tritium retention in future reactors, and for the PFC choice in ITER.

## VI. DIII-D PREPARATIONS FOR THE DIII-D AIR BAKE DEMONSTRATION

For the regions in the tokamak that have deposition, and hence co-deposited tritium, it is important to develop techniques to remove co-deposited graphite. The Univ. of Toronto has quantified [6] the effectiveness of the thermal oxidation removal technique. This is basically baking the graphite in a high partial pressure of oxygen. Their research has also shown air can be used, when accounting for the ~20% partial pressure of oxygen. Their results in Fig. 5 show that the removal rate is a strong function of temperature. These results were used to determine the process parameters for a demonstration experiment on DIII-D: 10 Torr air at either 250 or 350°C (achieved by two experiments). As DIII-D does not have tritium, the experiment will examine removal of a co-deposited $^{13}C$ layer to determine the effectiveness of thermal oxidation; the pronounced toroidal symmetry of the measured deposition patterns makes it possible to sample a subset of tiles. At the end of a run campaign, a $^{13}C$ injection expereriment will be performed, and the deposition pattern will be measured in a similar manner to that in

Fig. 4. One poloidal sample of tiles will be removed for analysis and then the 10 Torr, 250 degree Air Bake will be carried out. After this, a second poloidal sample of tiles will be removed, followed by a 10 Torr, 350 deg bake. After this bake, a third poloidal set of tiles will be removed. These three sets of tiles use the toroidal symmetry of the $^{13}C$ injection to assure that all sets of tiles start with a similar layer of deposited $^{13}C$. These three sets of tiles before the Air Bake, a 250 deg bake, and a 350 deg bake will be analyzed for $^{13}C$ to determine the efficiency of the bakes for removing carbon deposits. After the Air Bake, the tiles will be replaced and plasma operations will be resumed. It is anticipated that this experiment will take place at the beginning of the 2010 LTOA-II, where there will be longer than the usual time to recover plasma operations and the conditions of the vacuum chamber.

In preparation for these experiments, tests of DIII-D components were carried out at U. of Toronto and a new Air Bake chamber was constructed at DIII-D by LLNL. The overall goal was to identify systems that could be damaged by the Air Bake. The cryopump components were tested and it was determined that the cryopump operation should not be affected. Several other systems, including the ECH antennas, diagnostic mirrors, and other internal components were also tested. The largest concern is with copper components, which could have a heavy oxide coating. In the case of the Fast Wave antennas, there is sufficient concern that they may have to be removed before the Air Bake to minimize the need to remove the oxide layers from surfaces that are difficult to access. The LLNL Air Bake test stand at DIII-D and examples of components that have been tested are shown in Fig. 6.

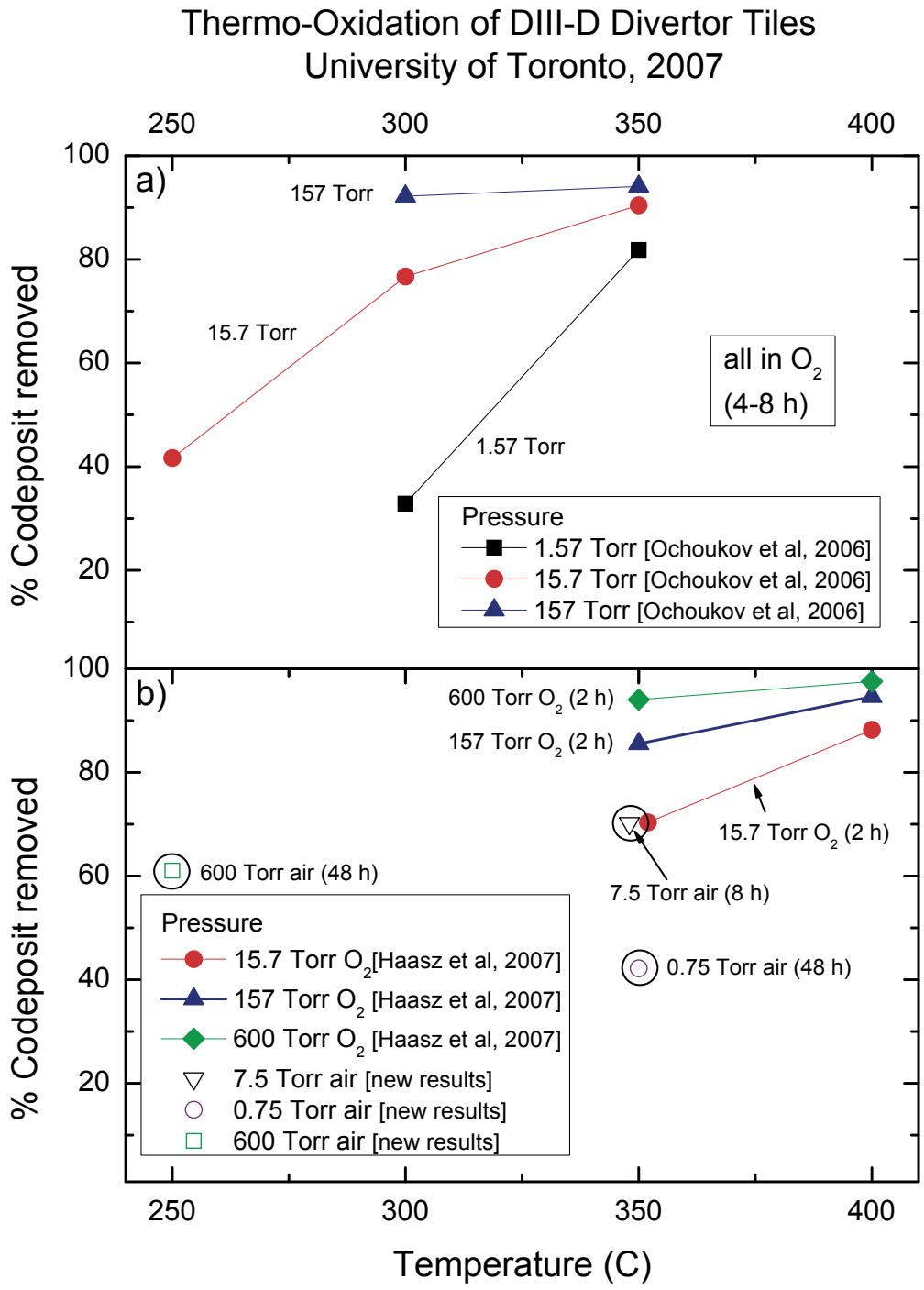


Fig. 5. Carbon removal rates as a function of temperature; the U. of Toronto group measured similar graphs for oxygen pressure. These were used to set the DIII-D Air Bake parameters of 10 Torr air, 350°C.

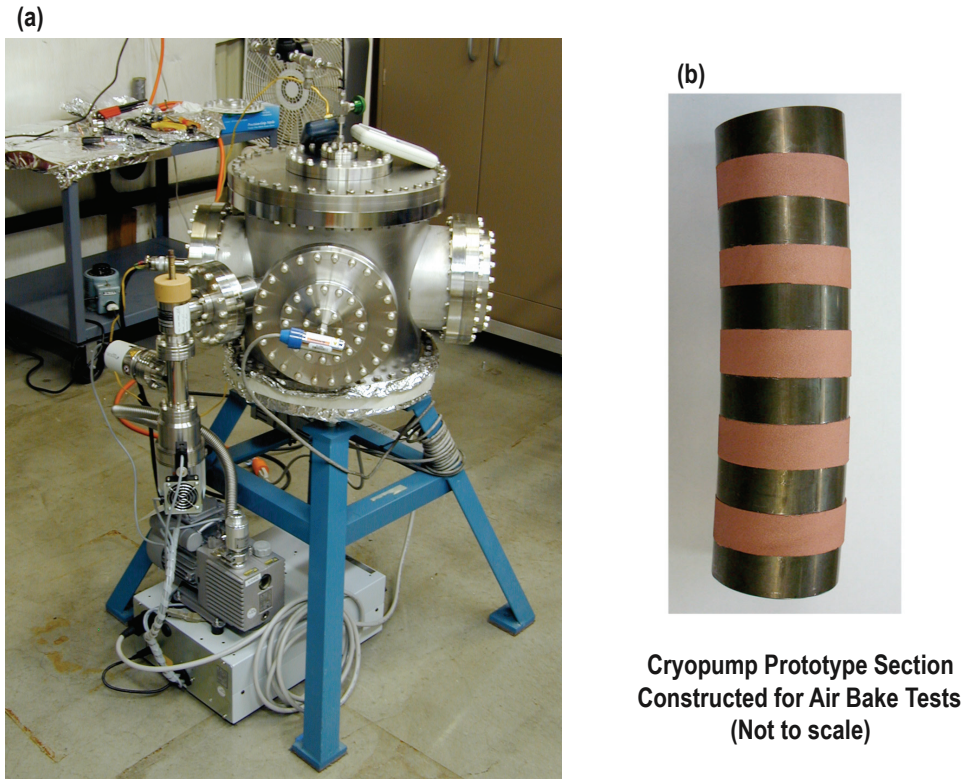


Fig. 6. The LLNL Air Bake Test Stand at DIII-D (right) a section of the cryopump was constructed for Air Bake tests.

## VII. FUTURE DIRECTIONS

These experiments have shown that in the DIII-D machine with all-graphite walls, the particle retention of the wall can be very small during ELMing H-modes produced by either ECH or NBI injection. Both the "dynamic" time-resolved particle flux and the "static" pressure rise techniques yielded nearly identical results. In this particular experiment, there was not sufficient time to perform a bake both before and after the plasma discharges. For the 2009-10 campaign, we are proposing one run day that would start and finish with a well-baked graphite wall. This would provide a better comparison of the wall fluxes during the plasma experiment with the particles that are removed during the subsequent bake and better determine the fraction of retained fuel that must be removed by more aggressive means such as an Air Bake. To demonstrate minimal retention, there are times in the latter part of the ECH and particularly the NBI H-modes when the integrated wall flux is close to zero or negative. For the USN case considered

here, we did not optimize the pumping configuration by sweeping the strike point towards and away from the pump openings. It may also be possible to obtain stronger exhaust with the lower cryopump alone, or by optimizing the separatrix location In either case, we may be able to achieve zero or negative wall flux for extended periods, as has been reported previously on DIII-D. This would establish that plasma operation with cryopumping can affect the particle inventory in the wall.

Recent research on DIII-D by Unterberg [6], has also shown that the wall retention is also small during ELM control with the RMP coils, an important result for the ITER design.

# REFERENCES

1. Phil West, *et al.*, Bull. Amer. Phys. Soc **53**, "Gas Balance in Ohmic Discharges in DIII-D", paper JP6-63 (2008) 140.
2. R. Maingi, *et al.*, Nuclear Fusion **36** (1996) 245.
3. D L Rudakov, *et al.*, Phys. Scr. **T128** (2007) 29–34.
4. S.L. Allen, *et al.*, Proc. 2006 IAEA Conference, "Transport And Deposition Of $^{13}C$ From Methane Injection Into L- And H-Mode Plasmas In DIII-D."
5. A. McLean, PhD thesis, University of Toronto, 2009.
6. J.W. Davis, A.A. Haasz, Journ. Nucl. Mat. **390-391** (2009) 532.
7. E. A. Unterberg, *et al.*, "Demonstration Of Particle Exhaust Control During Elm Suppression By Resonant Magnetic Perturbation In DIII-D," (2009), submitted to Nucl. Fusion Letters.

Milestone 168 is the DIII-D contribution to the 2009 FES Joint Research Target.

> **2009 FES Joint Research Target**: Conduct experiments on major fusion facilities to develop understanding of particle control and hydrogenic fuel retention in tokamaks. In FY09, FES will identify the fundamental processes governing particle balance by systematically investigating a combination of divertor geometries, particle exhaust capabilities, and wall materials. Alcator C-Mod operates with high-Z metal walls, NSTX is pursuing the use of lithium surfaces in the divertor, and DIII-D continues operating with all graphite walls. Edge diagnostics measuring the heat and particle flux to walls and divertor surfaces, coupled with plasma profile data and material surface analysis, will provide input for validating simulation codes. The results achieved will be used to improve extrapolations to planned ITER operation.

# APPENDIX A: DETAILS OF 2009 PARTICLE BALANCE EXPERIMENT

We have completed analysis of the particle balance experiments that were carried out on DIII-D. These experiments were carried out by scientists from DIII-D and C-Mod to measure wall retention with carbon PFCs in DIII-D for comparison with similar experiments in C-Mod and NSTX. Data were obtained from ohmic, L-mode, and H-mode phases in discharges heated by NBI and in discharges heated by EC. Dynamic (calculated during the discharge) and static (calculated after a series of discharges) particle balance techniques were shown to be in quantitative agreement. The wall retention rate was greatest during ohmic ramp-up and L-mode. Nearly zero wall retention rates in graphite during both EC and NBI heated H-modes were measured. Particularly in ECH H-modes, the ELMs played an important role in the exhaust. Negative wall fluxes (i.e. the wall is a sink of particles) were observed in neutral beam discharges. We are planning one more DIII-D experiment in the FY09-10 campaign (October 2009) to repeat these experiments with a fully baked wall both before and after the plasma shots.

D. Whyte and B. Lipschultz from MIT played key roles in the planning and execution of this experiment. The goal was to compare two techniques of particle balance and thereby compare particle transport in the DIII-D machine with carbon walls and the C-Mod tokamak with all-metal walls. C-Mod has pioneered a “static” particle balance technique where plasma discharges are carried out with a closed vessel and no pumping. Careful accounting of the pressure rise and removal of particles is used to determine the average particle balance on a shot by shot basis. This technique was used for the first time last year in L-mode discharges, and the analysis was presented in an APS poster. DIII-D has pioneered a “dynamic” particle balance technique where the sinks and sources in the particle balance equation are calculated as a function of time from the plasma density, particle inputs, and particle exhaust. DIII-D has 3 helium cryopumps that can provide pumping on the order of 20,000-30,000 T L/s each. Auxiliary heating with either ECH (no particle input) or neutral beams (with a particle input) can be compared. There was some doubt by the staffs of both C-Mod and DIII-D that these two techniques yielded similar results, and so a major goal of the DIII-D experiment was to use both measurement techniques in an ELMing H-mode plasma heating with ECH. It is anticipated that a second experiment will be carried out on C-Mod later in the FY.

The experimental plan was developed through a series of videoconferences held on several dates, including April 16, April 28, May 5, and May 21. A detailed plan was developed which necessitated extensive interaction with the DIII-D operations group as

the tokamak would be operated in a new way for the static particle balance measurements. The concept was to close off all the vessel cryopumps and neutral beams and create an ECH H-mode. This was felt to be a simpler configuration, as it did not involve the particle inputs (both energetic and room temperature) of the neutral beams. The cryopumps would be used to exhaust particles for several discharges, and then the cryopumps would be warmed up so that the product of the pressure rise and the vessel volume could be used to calculate the particles that were not retained in the walls. This required the technical staff at DIII-D to develop new techniques to rapidly warm the helium cryopumps by introducing helium and then nitrogen gas into the pumps to regenerate them. Qualification of this technique required a design review, modification of the cryopump system, and tests before plasma operations.

Another facet of the experiment that emerged from the discussion between the two experimental groups was a bake of the tokamak at the end of the day (with no pumping) after plasma operations to estimate the total number of particles that were retained in the wall. DIII-D routinely bakes to ~350°C for a weekend with pumping, but this plan envisioned a bake after plasma operations without pumping, and then cool down with experiments on the next day (with a clean wall). This also required the DIII-D operations group to develop a new baking and cool-down technique. In short, this experiment utilized the full operational flexibility of DIII-D, and required careful planning and execution by the operations group. The timeline for the experiment is shown in Fig.A1.

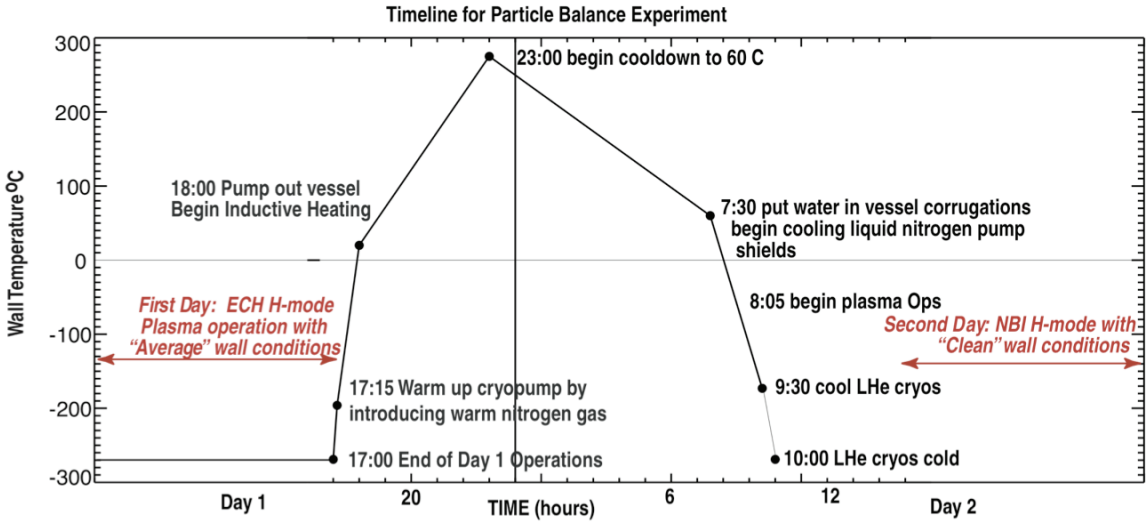


Fig. A1. Timeline for DIII-D particle balance experiment. After considerable discussion, the team decided to start with "average" wall conditions, and make groups of ECH H-mode shots. This run day was followed by a bake, and then NBI H-mode shots were carried out on the second day.

For the first run day, reproducible H-modes with only ECH were used for particle balance studies. As discussed above, as ECH heating does not also introduce particle like Neutral Beam Injection (NBI), the team felt that this would be the most straightforward set of discharge to compare. After a few test shots, the cryopumps were regenerated by flowing nitrogen gas through the helium channel in the cryopump. The pump was then cooled with Helium and the turbopumps were closed. Shown in Fig. A2 are the first four shots in the plasma sequence: shots 13907 through 13910.

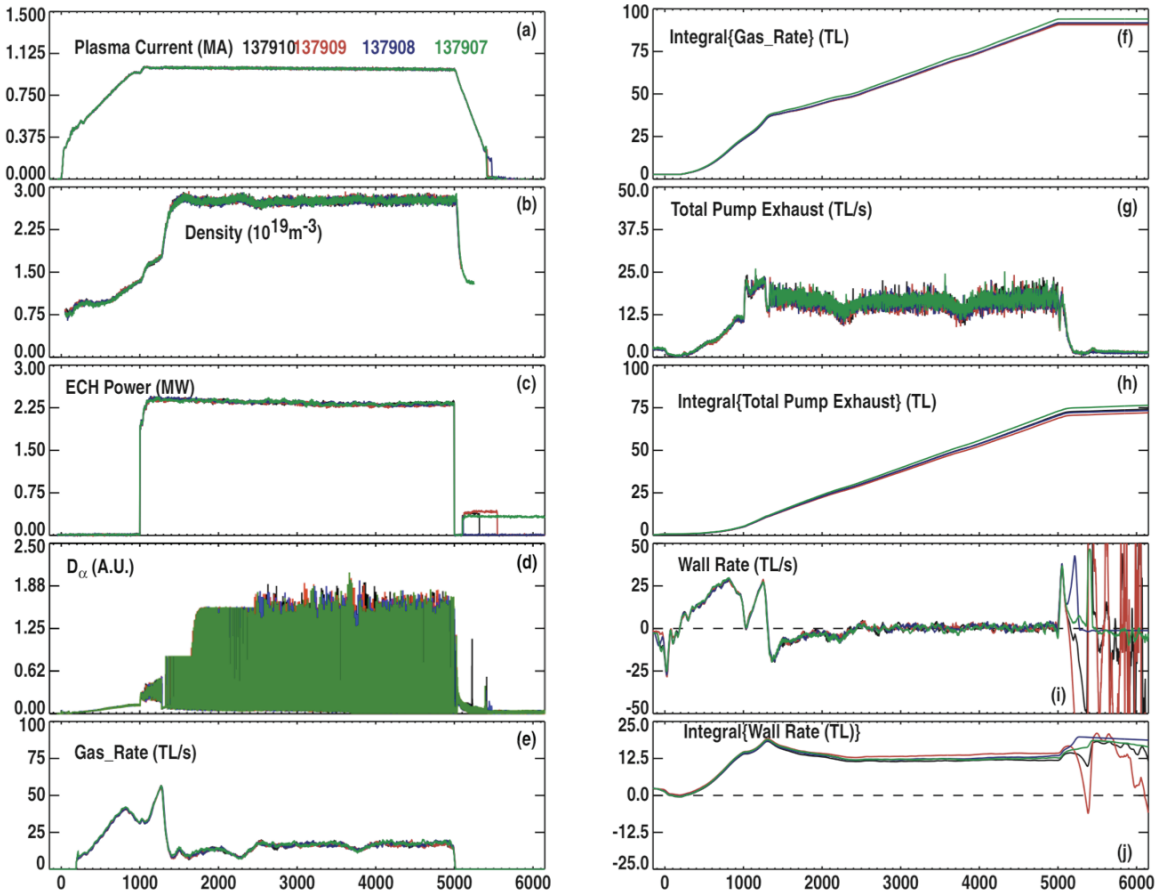


Fig. A2. The first four shots of ECH H-mode. The plasma current, density, and $D_\alpha$ emission in the upper divertor are shown. The particle balance terms are then calculated for the dynamic particle balance: the gas input rate (and integral), the total pump exhaust (and integral), and the wall flux (and integral). Note that the wall flux is large during the ohmic and L-mode periods, but then drops to nearly zero during the H-mode period of the discharge.

During each shot, the terms in the particle balance were calculated; this analysis was first established on DIII-D by Maingi, and more recently, by Unterberg.

$$Sources = Sinks$$

$$Gas\_Input + NBI\_Input + Neutrals = Pump\_Exhaust + Plasma\_Density\_Rise + Wall\_Flux$$

$$\Gamma_{GAS} + \Gamma_{NBI} + \Gamma_{Neutrals} = \Gamma_{Pumps} + \frac{\partial(nV)}{\partial t} + \Gamma_{Wall}$$

where:

Gas_Input is the input gas flow rate measured in TL/s.

NBI_Input is the particle input due to neutral beams, for ECH this term is 0.

Neutrals is the increase in the neutral pressure in the vessel, this is small because we are cryopumping.

Pump_Exhaust is the measured pressure rise in each pump plenum times the pumping speed of the cryopump. We operated with three cryopumps for these experiments – an inner and outer in the upper divertor, and an outer pump in the lower divertor.

Plasma_Density_Rise is calculated from the measured line-average density times the plasma volume obtained as a function of time from EFIT. Note that this is a "sink" term because the system we are considering is the neutrals contained by whole vacuum vessel, and particles temporarily "stored" in the plasma are removed from the system.

Wall_Flux is calculated as the remainder that is required to balance the equation. This also includes measurement error and any inadequacies of the particle balance model. A positive term indicates particle lost from the system (to the wall), and a negative term indicates that particles are being removed from that wall.

In Fig. A2, note that the four shots were very reproducible H-mode discharges. There was no glow discharge cleaning between these shots, and the turbopumps were closed. The cryopumping was not specifically optimized for this shape, as we were also trying to perform "picture frame" analysis of these shots. This is a technique where most of the plasma-wall interaction is at a well-defined, toroidally symmetric surface and then the plasma flux can be measured with a probe close to or outside this surface. The plasma shape was an upper-single null divertor, as shown in Fig. A3. The approximate aiming of the ECH heating gyrotrons are shown; a broad, off-axis heating profile was used to obtain a constant discharge without long ELM-free periods (based on other exerperiments). After the ohmic and L-mode periods of the shot (up to about 1500 ms), note that the gas input is decreased dramatically (feedback control) and the density remains constant. The total pump exhaust is also relatively constant, resulting in a dramatic decrease in the

$\Gamma_{wall}$ required to balance the equation. This is maintained throughout the rest of the discharge, and is repeatable on all four of the plasma discharges.

After these four shots, we then performed the "static" particle balance measurement. The cryopumps were regenerated by introducing nitrogen gas in the helium lines. Barotrons were used to measure the resulting pressure rise in the DIII-D vessel with the turbopumps closed. For this series of four shots, the vessel pressure rise was 7.5 mTorr on the Barotron. Multiplying this by the measured DIII-D vessel volume of $39.6\ m^3$ (with an estimated uncertainty of about $0.23\ m^3$) results in 297 TL or about 300 TL of exhaust. Referring to Fig. A2, the integral of the exhaust at the end of the shot is approximately 75 TL for each shot, for a total of 300 TL for 4 shots. This is remarkable agreement, and provided a check that the exhaust from the dynamic particle balance (calculated during the discharge) was in agreement with the "static" technique obtained by the total pressure rise after a series of four plasma shots. The reason that four plasma shots were used was to increase the total pressure rise to reduce the error in the Barotron calibrated pressure measurement.

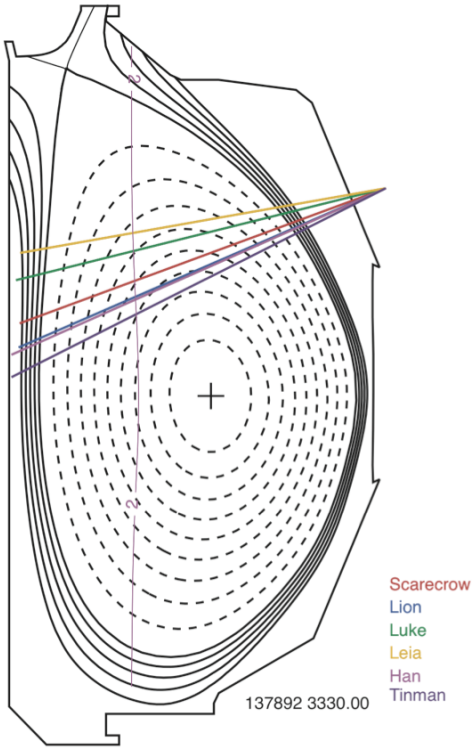


Fig. A3. The plasma shape used for both the ECH and NBI H-mode experiments. The approximate rays for each of the gyrotrons is indicated; a broad, off-axis heating profile was chosen for a steady H-mode discharge, and no optimization of the H-mode was performed. Each colored ray corresponds to a particular gyrotron.

As a single-shot test, the cryopumps were regenerated after a single discharge (137911). The dynamic particle balance for this shot is shown in Fig. A4. The pressure rise measured by the Barotron was 1.9 mTorr, which multiplied by the DIII-D volume is about 75 TL. As seen in Fig. A4, the integral of the total exhaust at the end of the discharge from the dynamic balance was also 75 TL.

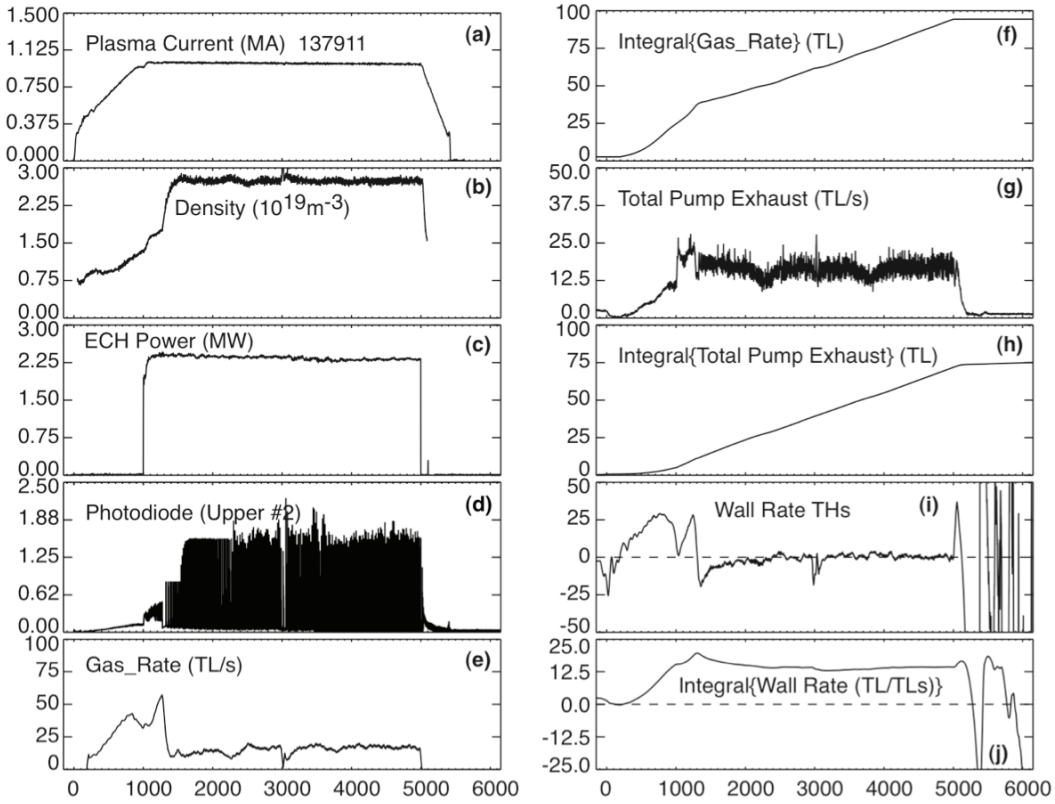


Fig. A4. Dynamic particle balance for a single discharge in ECH H-mode, Shot 137911. The integral of the exhaust is 75 TL from these analyses, which agrees well with the static of 75 TL.

Another sequence of four shots (137915 through 137918), similar to the previous series, was next obtained as shown in Fig. A5. In this series, the wall rate remains low during H-mode. Furthermore, the integral of $\Gamma_{wall}$ changes- the lowest is for shot 137917. This particular discharge also has a small unexplained particle input at 3000 ms. At this point, we are starting to see some change in the integral of $\Gamma_{wall}$; in particular, it is decreasing and approaching zero for several of the shots.

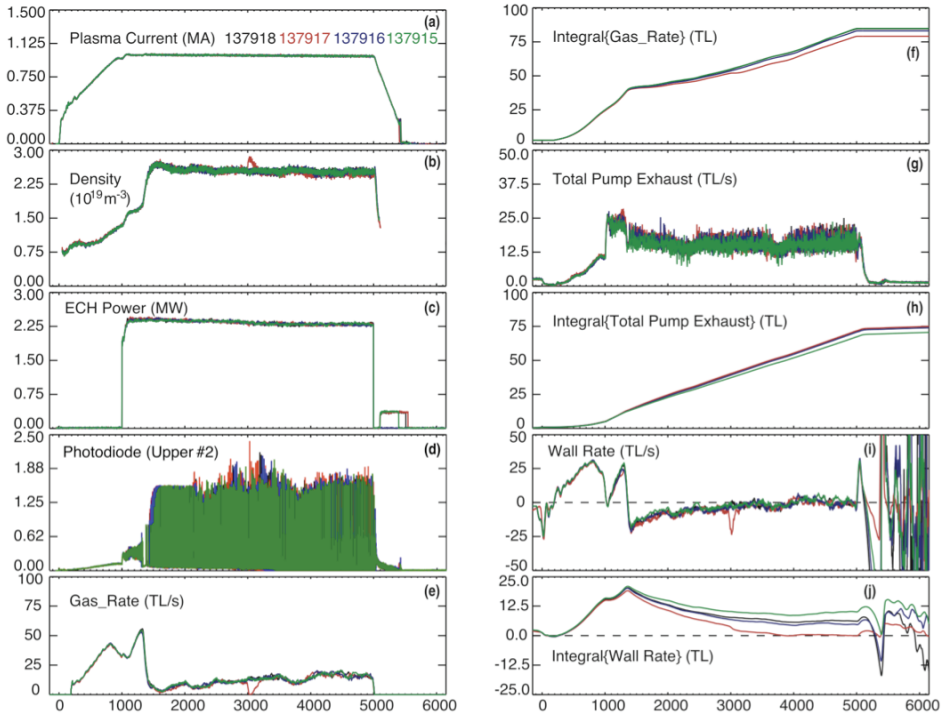


Fig. A5. Shots 137915 through 137918 were another series of reproducible shots. The sum of the exhaust for the two discharges is 299 TL, and the static particle balance yields 273 TL. However, the integral of the wall rate is changing for this series of shots.

Similar results were found when the plasma conditions were varied. In a 3-shot series, 137919-21, (Fig. A6), the toroidal field was decreased slightly from 1.69 to 1.6 T, and the density feedback control target was decreased. The integral of the exhaust for each shot was about 75 TL, for a total of 225 TL. The measured static pressure rise was 5.44 mTorr, resulting in 200 TL. For these shots, the lower density shots resulted in a small negative wall rate and hence the integral was close to or less than zero. Recall the sign convention is that a negative wall rate is a source to the system, so a source is required to balance the particle balance equation. We attribute this to a wall source, i.e. removing particles from the wall.

After this series of shots, the cryopumps were regenerated (both the liquid helium and the liquid nitrogen shields were purged with nitrogen gas) and a bake of the machine started that lasted for about 5 hours and reached an average temperature of roughly 280° C. During the bake, the rough pressure rise was 25 mTorr, which multiplied by the vessel volume is roughly 1000 TL. As we started the day with an “average” wall, a careful accounting with the total pump exhaust is not possible, but it is of the same order of magnitude. A subject of a future experiment is to repeat this experiment with a bake both before and after the experiment.

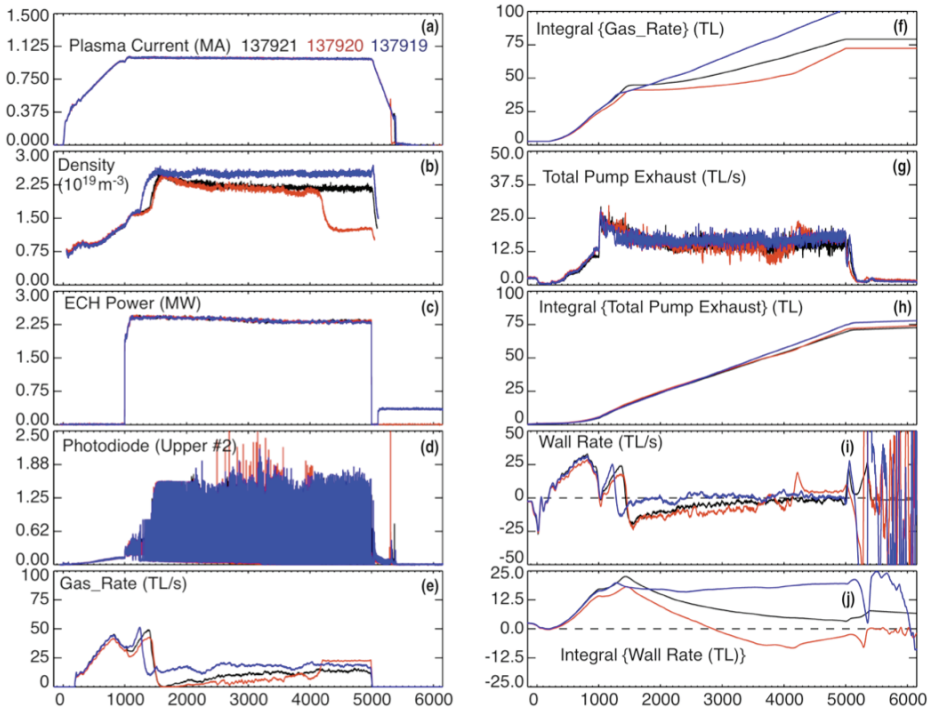


Fig. A6. Shots 137919 through 137921 were another series of shots with an attempt to change parameters. The toroidal field was decreased slightly from 1.69 to 1.6 T. The integral of the exhaust is about 75 TL for each of 3 shots, for a total of 225 TL. The static pressure rise when the pump was regenerated was 5.44 mTorr, which is 200 TL.

Table 1: Summary of Dynamic and Static Exhaust for ECH H-mode

| Shot Sequence | Dynamic Balance | Static Balance |
|---|---|---|
| 137903-137906 | 300 TL | 300 TL |
| 137911 | 75 TL | 75 TL |
| 137912-137913 | 135 TL | 139 TL |
| 137915-137918 | 300 TL | 275 TL |
| 137919-137921 | ~200 TL | 215 TL |
| 137922-137924 | 220 TL | 205 TL |
| Total | | 1209 TL |

On the second day of the experiment, the wall was baked according to the sequence shown in Fig. A1 and the team decided to attempt the same comparison with NBI heated ELMing H-modes. This meant that the operations team had to develop a discharge scenario where the Torus Isolation Valves (TIV) for the NBIs were opened very shortly before the discharge. This is because the each NBI has a cryopump to provide differential pumping between the high pressure neutralizer and the plasma. As a result, each NBI provides some net pumping on the torus.

Because of the time required to bake the machine and then cool down, along with the development of the NBI discharge sequence, the second day had fewer plasma shots. Shots 137931 through 137937 had no cryopumping and no glow discharge, and were remarkably reproducible. The first sequence of NBI shots with cryopumping was 137938 and 137939, and shown in Fig. A7. Note that the integral of the wall rate is very close to zero or negative for both of these shots.

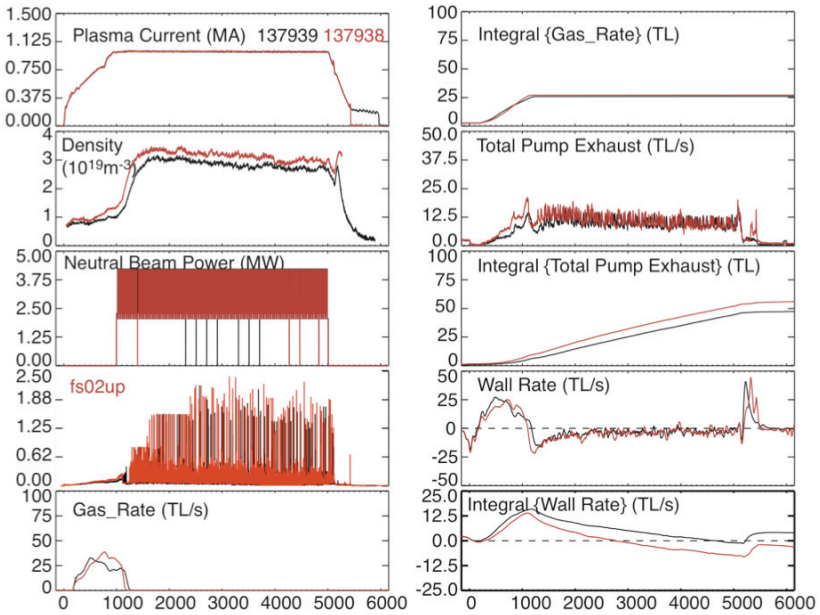


Fig. A7. Shots 137938 thru 137939 were NBI ELMing H-mode shots. The static pressure rise was 2.8 mTorr resulting in 112 TL, and the sum of the exhaust from the dynamic was 103 TL. Again notice that the wall rate is very low during the ELMing H-mode period of the shot.

The next series of shots used four shots to increase the amount of pressure rise and reduce the measurement uncertainty due to the Barotron pressure rise. Shown in Fig. A8, this is sequence 137940 through 137943. Again in this case, the wall flux is very low during the H-mode period of the discharge, and the integral of the wall flux is slightly increasing during the shot sequence.

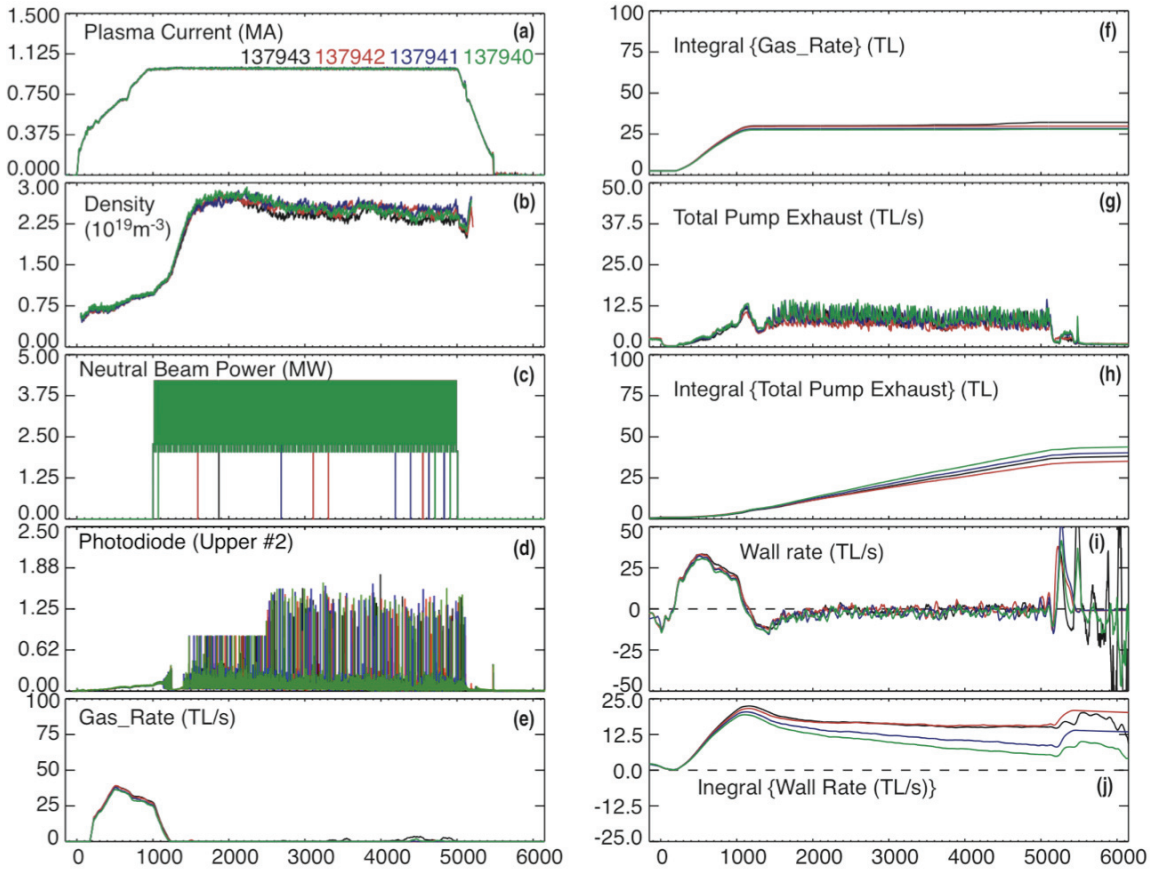


Fig. A8. Shots 137940 thru 137943 were NBI ELMing H-mode shots. The static pressure rise was 4.05 mTorr resulting in 160 TL, and the sum of the exhaust from the dynamic was 160 TL. Again notice that the Wall Rate is very low during the ELMing H-mode period of the shot.

We then tried to make adjustments to raise the plasma density, but at the same time, a large influx of impurities resulted in degradation in the discharge quality. The following shot would not initiate, and so we regenerated the pumps at this stage. The static balance was difficult to interpret on these shots, but the static yielded 3.16 mT (125 TL). At this point, we were forced to use a 10-minute glow discharge to recover conditions. However, after two shots with glow discharge, we were able to obtain one last sequence of NBI heated ELMing H-mode shots (with no glow discharge, and using the normal sequence for all of the other shots). These are shown in Fig. A9, and are the discharge sequence 137948 through 137950.

We compare the dynamic particle balance for similar discharges with ECH and Neutral Beam heated H-mode in Fig. A10. The duty cycle of the neutral beams was adjusted to yield nearly the same power as the ECH heated case. Note that there was not sufficient time to optimize the H-mode in these discharges and this will be the subject of

future research. The *wall retention rate* in the L-mode part of the discharge is very similar and large, while the *wall retention rate* during the H-mode portion of the shot is nearly zero.

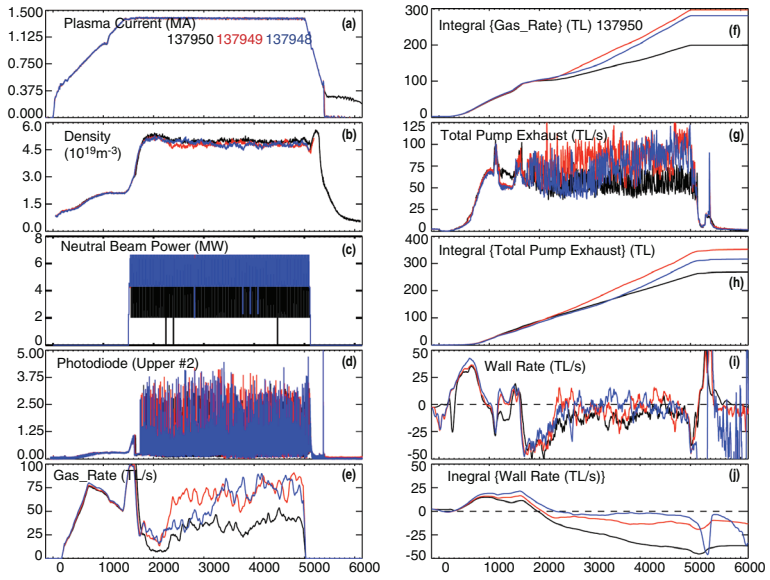


Fig. A9. Shots 137948 through 137950. The static pressure rise was 18.1 mTorr or 715 TL. The dynamic is 941 TL. This is the largest discrepancy that we observed during the experiments.

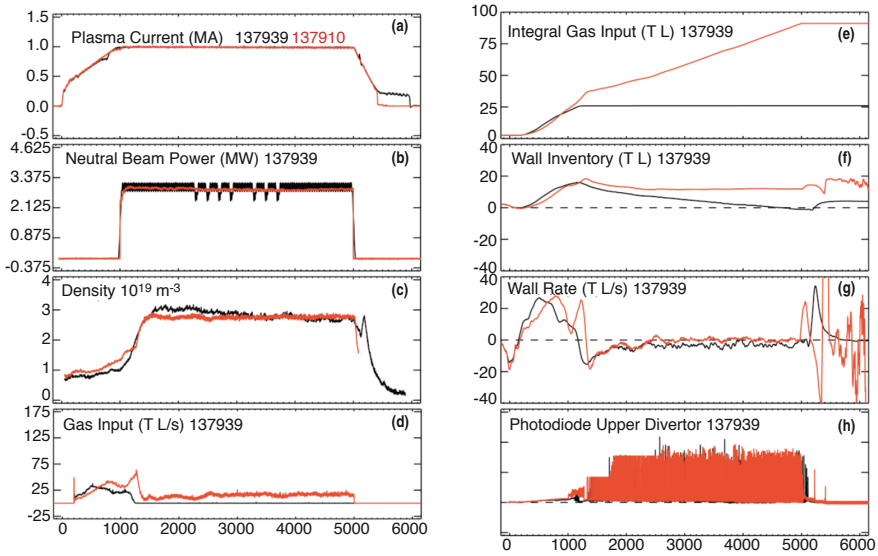


Fig. A10. The plasma current, neutral beam or ECH power, electron density, gas input, integral of the gas input; wall inventory and wall rate from the dynamic particle balance; along with the photodiode signal are compared with a neutral beam heated H-mode DIIID shot. Note that in both cases, the wall flux is quite large in the L-mode period of the plasma, but during the H-mode, the wall flux is very close to zero.

As shown in Fig. A11, the ELMs in the H-mode influence the particle exhaust. Particularly in the NBI case (right), the particle exhaust in the upper pumps is modulated in concert with the ELMs. In the ECH case, the ELMs are very regular and uniform, and result in a more constant particle exhaust. This is seen in more detail in Fig. A12, comparing two ECH and two NBI shots.

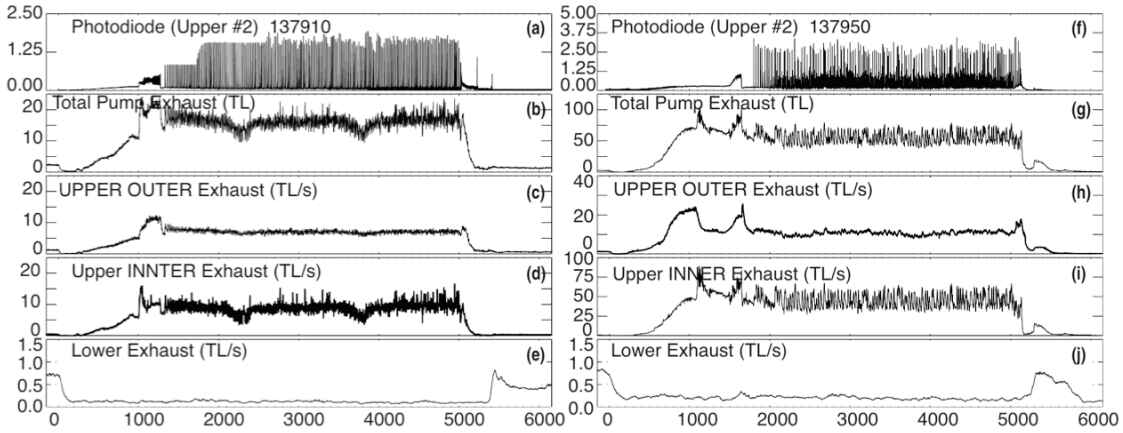


Fig. A11. The ELM character for similar ECH (left) and NBI (right) H-modes is compared, along with the particle exhaust from each of the pumps. Note that most of the exhaust is from the upper pumps (the active divertor in USN configuration). Particularly in the NBI case, modulation in the particle exhaust is observed with the ELMs.

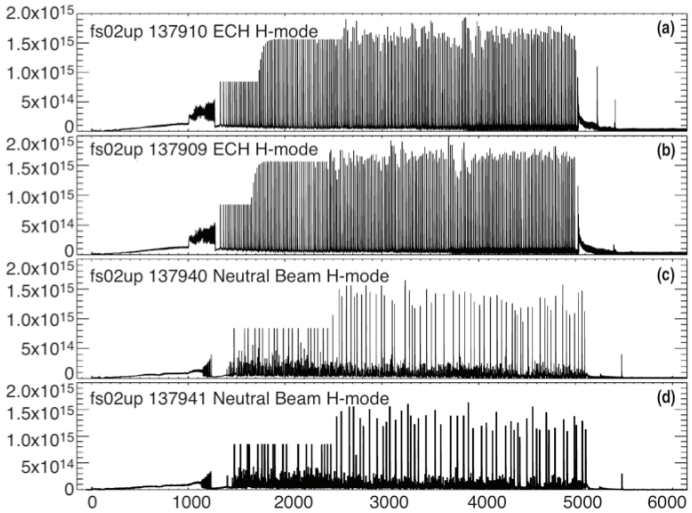


Fig. A12. ELMs from two sequential ECH H-mode shots (137910-11), compared with two NBI shots (137940-1). Note how regular the ELMs are in the ECH case.

A section of each shot is expanded in Fig. A13. A Fourier decomposition of shots 137909-10 shows that there is a very regular pattern of ELMs at approximately 60 Hz.

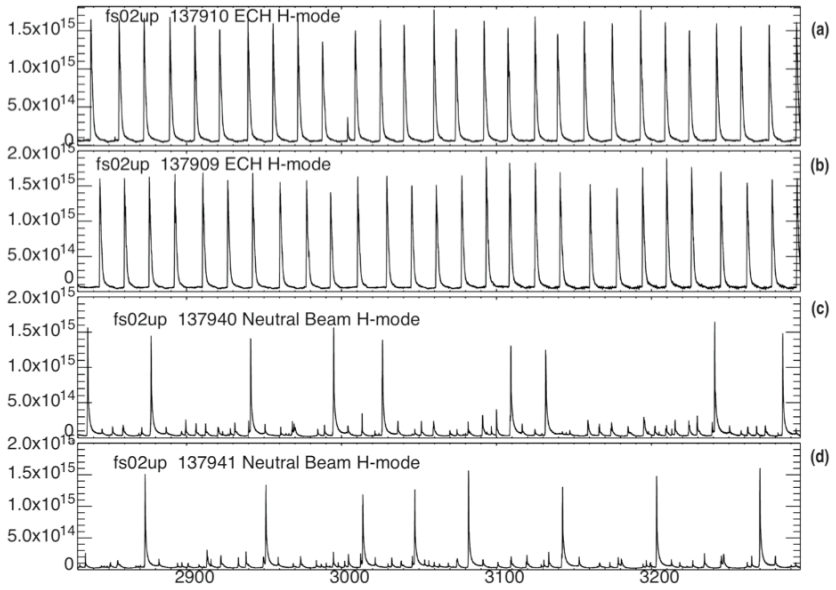


Fig. A13. ELMs from two sequential ECH H-mode shots (137910-11), compared with two NBI shots (137940-1). Note how regular the ELMs are in the ECH case.

As the ELMs play an important role in the particle exhaust, it is also interesting to explore the particle balance during ELM mitigation experiments with the RMP coils. As shown in Fig. A14, the particle flux to the wall is also small in this case.

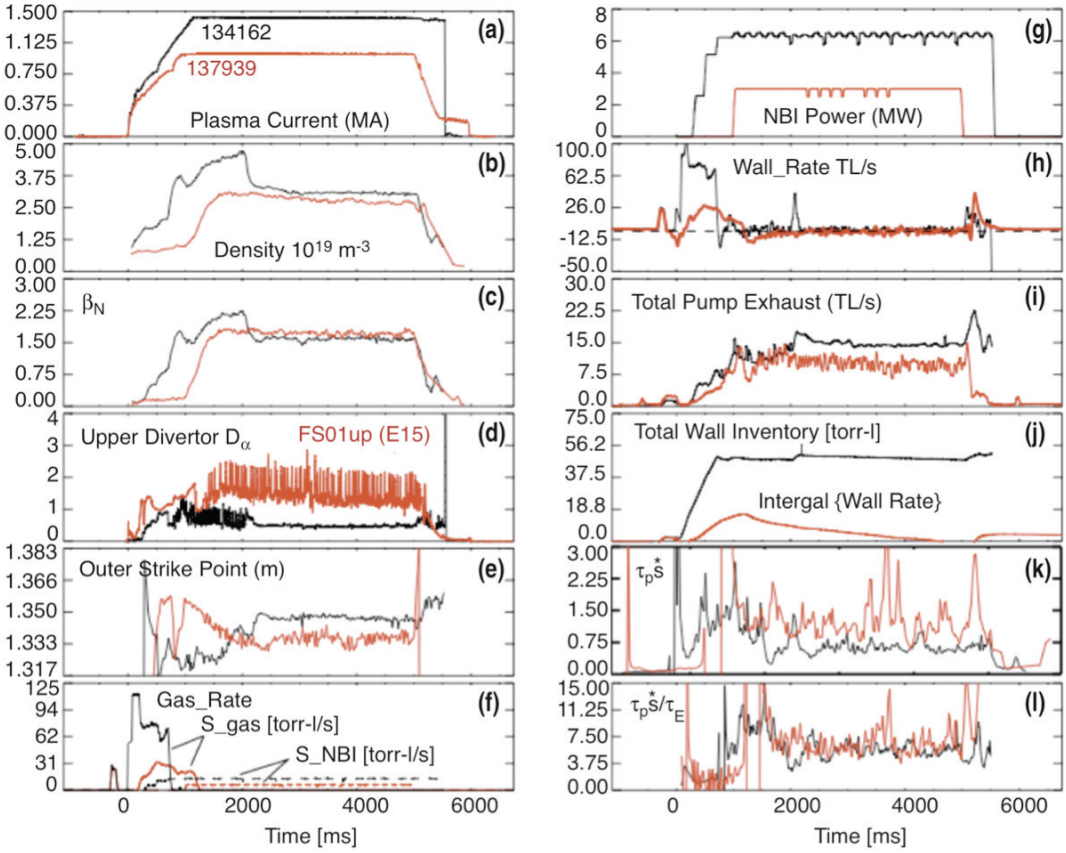


Fig. A14. Particle Balance (Unterberg) for an ELM control shot with RMP (black) compared with an ELMing H-mode. Note that the S_wall in both of these discharges is small, indicating that the flux to the wall is small.

# IV. FUTURE DIRECTIONS

These experiments have shown that in the DIII-D machine with all-graphite walls, the particle retention of the wall can be very small during ELMing H-modes produced by either ECH or NBI injection. Both the "dynamic" time-resolved particle retention and the "static" pressure rise techniques yielded nearly identical results. Furthermore, the wall retention is small during ELM control with the RMP coils. In this particular experiment, there was not sufficient time to perform a bake both before and after the plasma discharges. For the 2009-10 campaign, we are proposing one run day that would start and finish with a well-baked graphite wall. This would provide a better comparison of wall retention during the plasma experiment with the particles that are removed during the subsequent bake.

In addition, there are times in the latter part of the ECH and particularly the NBI H-modes when the integrated wall flux is close to zero or negative. For the USN case considered here, we did not optimize the pumping configuration by sweeping the strike point towards and away from the pump openings. It may also be possible to obtain stronger exhaust with the lower cryopump alone, or by optimizing the separatrix location (Fig. A15). In either case, we may be able to achieve zero or negative wall flux for extended periods, as has been reported previously on DIII-D. This would establish that plasma operation with cryopumping can affect the particle inventory in the wall.

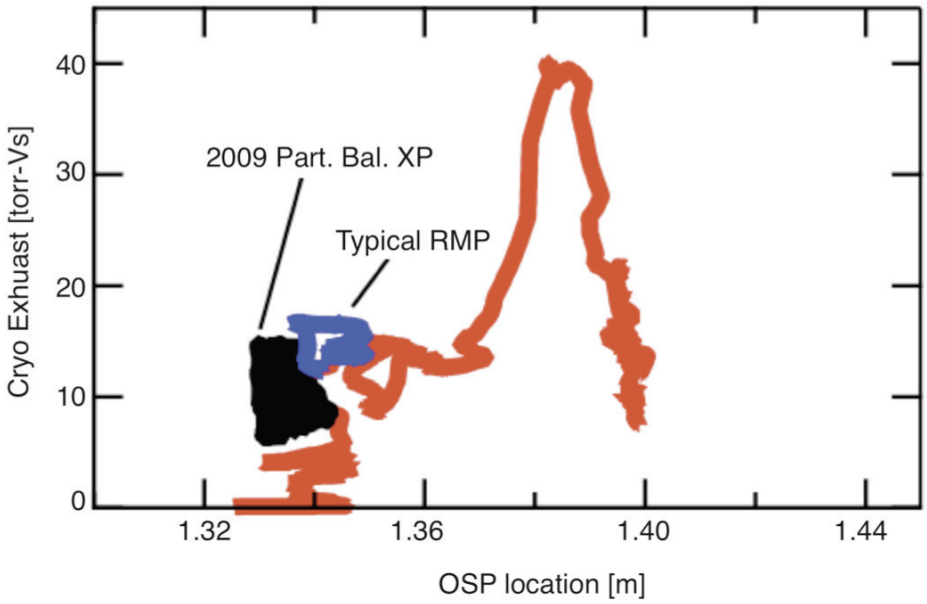


Fig. A15. Particle exhaust as a function of outer strike point location from experimental data. The exhaust in the present experiments can be increased by over a factor of 2 by optimizing the strike point location.

# ACKNOWLEDGMENT

This is a report of work supported by the U.S. Department of Energy under Cooperative Agreement No. DE-FC02-04ER54698.

# Alcator C-Mod Facility Report

## 1. Alcator C-Mod Summary

Alcator C-Mod has carried out extensive experiments on global fuel retention using both the static and dynamic particle balance technique with refractory metal plasma-facing components of molybdenum and tungsten [1-5]. Tungsten (W) is being used in the ITER divertor to provide simultaneously good heat removal capability and low tritium storage capacity. Worldwide, C-Mod is the only divertor tokamak using solid refractory metal plasma facing components. Using the highly accurate static measurements, a technique pioneered on C-Mod, it is found that in the absence of disruptions deuterium (D) fuel retention is constant from shot-to-shot, i.e. the wall continues to absorb D fuel particles and not release them. The rate of retention scales ~ 1% of the total D ion fluence incident on the divertor and main wall plasma-facing components (PFCs). This behavior was confirmed out to ~30 seconds of plasma exposure (about 15 shots) with no indication that the wall reservoir was saturating. A series of studies using different magnetic divertor geometries, Helium plasmas and the external applications of Boron films [1] strongly imply that the D is being retained at the outer divertor of Alcator C-Mod; a location which is known to be in net erosion and have "bare" Mo and W surfaces (i.e. the Boronization films are quickly eroded from this region by plasmas).

Dynamic particle balance measurements, which provide intra-shot time resolution to the particle balance measurements, have been carried out with the Alcator C-Mod upper divertor cryopump. A surprising result is that in most discharges the real-time retention rate of D drops from large values in plasma rampup, to a constant and near zero value in the steady-state portion of the discharge. This would seem to imply that the D uptake is dominated by the early phases of the discharge. However this is inconsistent with the total retention variations with stikepoint position, divertor film thickness, etc. Furthermore, a constant (or zero) fuel retention rate is surprising because the wall temperature is varying throughout the discharge. This dynamic behavior is nearly identical to the results of DIII-D with a graphite wall. The conclusion is that the static balance provides accurate information to the global retention on a shot-averaged basis. However the dynamic, coupled response of the wall and edge plasma are extremely important (if not yet well understood) particularly under stationary plasma conditions.

The long-term retention rate in the C-Mod metallic molybdenum tiles was investigated using ex-situ ion beam analysis. The deuterium was found to be trapped at an atomic concentration ~ 1% D/Mo, much higher than expected from intrinsic trap fractions in Mo ~ $10^{-6}$ D/Mo [4], suggesting a damage mechanism under plasma bombardment that increases the Mo capacity to hold D fuel. This was experimentally investigated in laboratory plasma, DIONISOS, which showed similar results, although the details of the damage mechanisms are unclear.

Nevertheless the cumulative campaign-averaged retention in C-Mod Mo tiles was small in all investigations. It was found by examining particle balance in large sets of discharges that this was caused by disruptions removing and recovering the D fuel retained in the Mo tiles. Dedicated experiments and modeling were carried out to investigate and confirm this effect was dominated by rapid surface heating during the disruption which allowed for a "flash" recovery of

the majority of retained fuel. This technique has been proposed for ITER to recover tritium fuel [2].

## 2. Particle Balance and Fuel Retention Processes in Metallic Plasma-Facing Components

Alcator C-Mod pioneered a method to obtain highly accurate global particle balance [1] of which an example is shown in Fig. 1. All active pumping is stopped for the duration of the plasma shot (1-3 seconds) and the following 5-10 minutes. Following the discharge the wall returns to uniform temperature (~300 K) and the deuterium (D) fuel gas pressure comes to a constant value. The difference of the fuel injected to the fuel recovered must be located in the plasma-facing components in the device. The method is very accurate because it only requires the difference between highly accurate pressure gauges in static conditions of neutral pressure and vessel temperature. This "static" method will be later compared to the "dynamic" particle balance obtained using varying pressures and conditions, a technique pioneered by DIII-D.

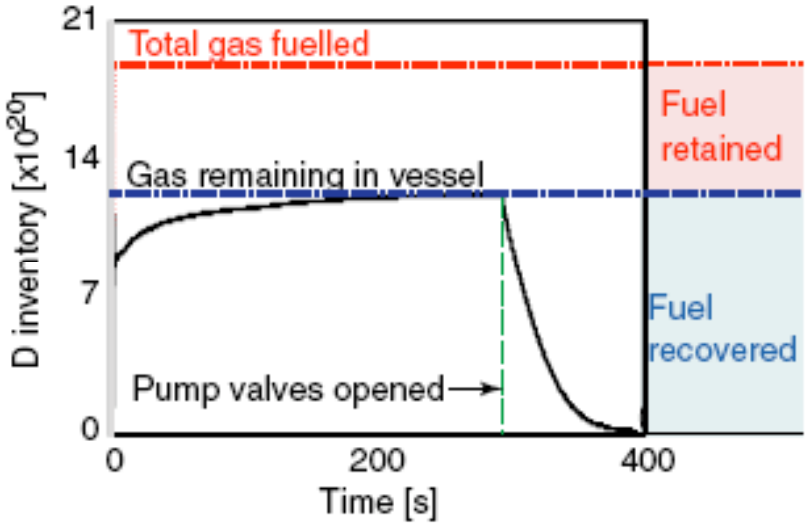


*Fig. 1 Example of the static fuel balance method. The discharge occurs from t=0-2 seconds without active pumping. The vessel pressure is allowed equilibrate for several minutes and then the Deuterium fuel gas is removed. The technique is accurate to < 1% because retention is obtained by comparing only static pressure differences.*

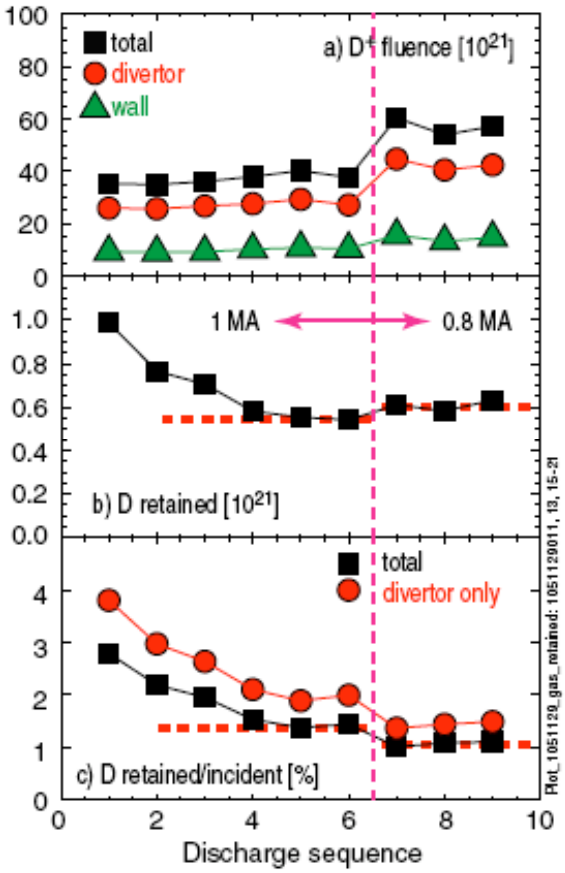


*Fig. 2 Deuterium fuel retention on C-Mod in a sequence of non-disruptive repeated discharges obtained using the static particle balance method [1].*

The major results of the static particle balance measurements, in the absence of divertor cryopumping, are shown in Figs. 2-5. Details of the experiments and analysis are to be found in a recent Nuclear Fusion paper [1]. It is found that the metallic wall exhibits net fuel retention on a highly repeatable basis as long as the discharge does not terminate in a disruption (Section 3). No change in shot-averaged retention was found for repetitive discharges with ~30 seconds cumulative plasma exposure. The retention rate did not depend on the presence of a thin boron film from boronizations as long as the outer divertor had been eroded clean of this layer (verified with spectroscopy [1]). Retention varied as a function of plasma den(sity, and was found to scale approximately with the total D ion fluence to the PFCs during a shot rather than to the amount of gas injected for fueling requirements (Figs. 2-3). The retention did not depend strongly on the confinement regime (Fig. 3). The retention was found to depend on divertor strikepoint location. If the strikepoint was moved, with constant core plasma conditions, the retention would adjust within one shot and then be constant thereafter (Fig. 4). The retention was lowest if the strikepoint was placed on atypical divertor locations (Fig 4b) where thick boron layers were known to exist. Retention in helium diverted plasma was zero or negative compared to matched D divertor discharges (Fig. 5a-b). Deuterium plasmas which remained in the limiter configuration (inner wall limited) showed very low or zero retention (Fig. 5c).

The cumulative results of Figs. 2-5 strongly suggested that the retained deuterium was located at outer divertor locations of relatively clean metals (Mo and W). Some aspect of the deuterium surface chemistry and/or interaction with the Mo was affecting the Mo since inert helium was not being retained. Simple particle accounting indicated that very high atomic fractions of D/Mo (~1%) extending tens of microns into the divertor material were required to provide a sufficient particle reservoir.

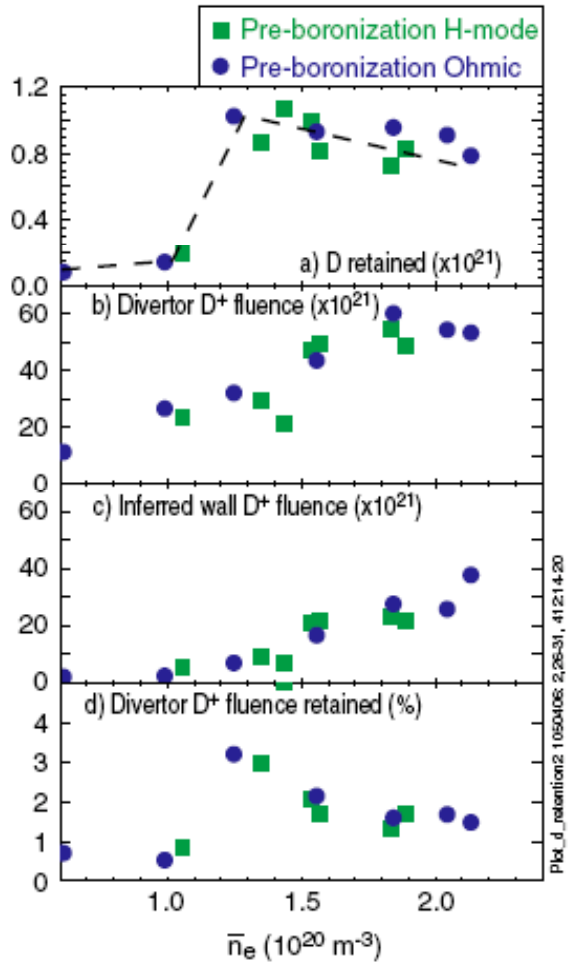


*Fig. 3 Fuel retention from the static method as a function of plasma density. Retention is not affected by confinement mode (Ohmic versus H-mode with RF heating). The total retention is found to scale as ~1-3% of the total deuterium ion fluence to the walls.*

In other words, the deuterium was finding a way to permeate deeply into the Mo and be stored there at a a very high fraction (intrinsic solubility of D in Mo is less than one part per million << 1%). This is in stark contrast to carbon PFC tokamaks which find the long-term retention is dominated by codeposition in plasma-deposited films at the inner divertor. Codeposition in boron was ruled out in C-Mod by doing experiments where all B films had been removed. These observations were partially supported by ex-situ analysis of the D (Section 3). Post-exposure analysis of C-Mod Mo tiles showed a volumetric concentration of 1% down to the limit of the ion-beam analysis detection (~4 microns). Such long-term storage of D in Mo takes place in traps, i.e. sites of potential energy wells within the Mo from which the D cannot escape at thermal energies once it falls into the well; however the stated natural trap density in Mo is ~$10^{-5}$

trap/Mo [4], much lower than seen in the C-Mod tiles. Experiments in DIONISOS [4] also showed that D/Mo ~1% could be obtained when the Mo was damaged by energetic ions from the plasma and/or by high-energy beams. This suggested that the Mo was somehow being damaged in C-Mod under high particle flux bombardment from the plasma as to create trap sites.

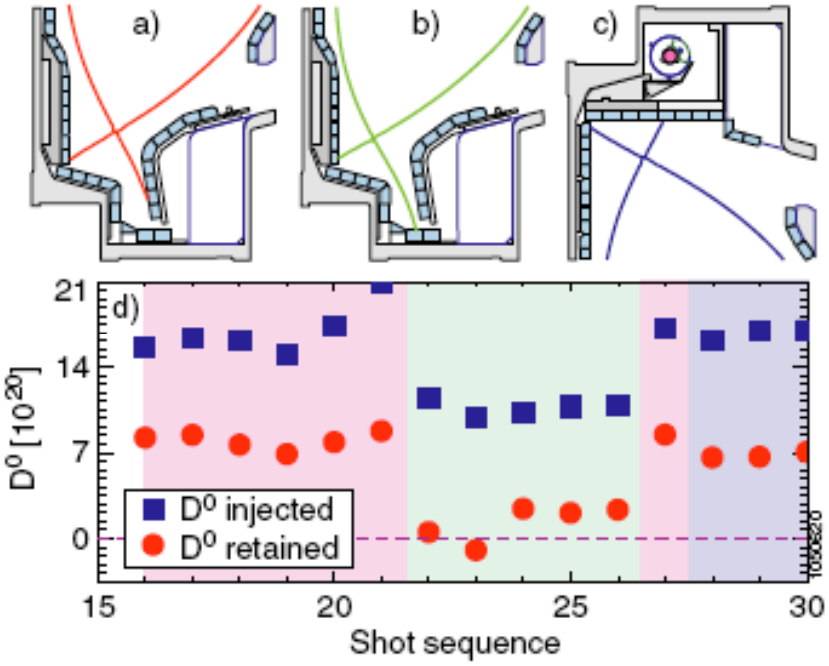


*Fig. 4 Static particle balance (injected and retained) with constant core plasma conditions but varying divertor strikepoint locations. Retention is similar for conventional (a)lower-null (inclined plates) and (b) upper null (flat-plate), but is nearly zero for (c) lower null slot.*

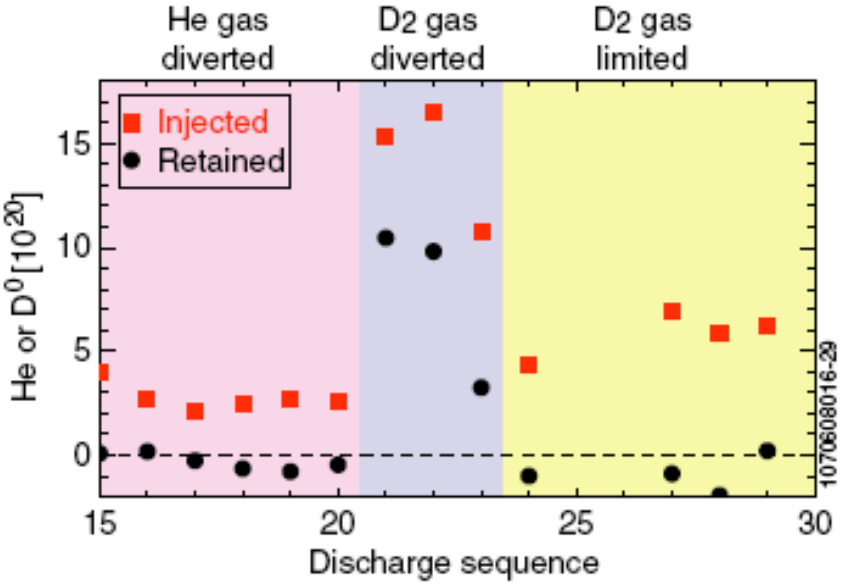


*Fig. 5 Sequence of static particle balance shows ~zero fuel retention in matched helium plasmas compared to deuterium plasmas. Also deuterium plasmas that remained limited through the flattop show no shot-averaged fuel retention.*

Alcator C-Mod has also carried out an extensive set of "dynamic" particle balance experiments. While the static particle balance method is very accurate it lacks direct information about *when* in the shot the retention is occurring (although this can be inferred through changing plasma conditions or geometry). The dynamic particle balance technique, developed at DIII-D, exploits the fact that the external particle exhaust rate into divertor cryopumps can be well characterized through the measured divertor plenum pressure and its calibrated (usually constant) pumping speed. Therefore differences between cyropump particle exhaust rate and gas injection rate provides *time-resolved* wall retention rates.

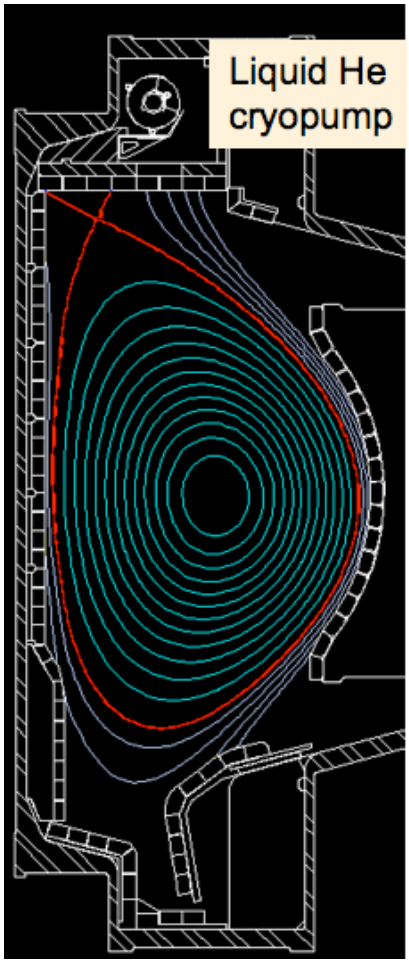


*Fig. 6 Example discharge shape for dynamic particle balance using the upper divertor cryopump in Alcator C-Mod. The cryopump is toroidally continuous while the Mo tiles immediately below the pump have 50% toroidal coverage in order to allow plasma recycling gases to enter the cryopump chamber.*

The dynamic technique was adapted to C-Mod with the use of the upper divertor cryopump (Fig. 6). The cryopump pumping speed of D2 gas was provided by constant, calibrated gas injection into the vessel with no plasma. The cryopump pumping speed was calibrated versus divertor pressure by varying the gas injection rate. The calibration covered divertor gas pressures ~0.1–5 mTorr (measured with a cold pump), which spans the pressures obtained during plasma discharges. As expected the pumping speed was quite constant versus pressure (~15% variation from 0.1 to 5 mTorr). For dynamic particle balance discharges (Fig. 7), all external pumping was

closed during and after the shot. Therefore the exhaust rate to the pump could be directly calculated from the divertor pressure and calibrated pumping speed (third panel of Fig. 7). Following each pulse the cryopump was regenerated, i.e. allowed to increase to liquid N temperatures, thus releasing all the particles it pumped during the shot into the un-pumped vessel. By measuring the resulting static pressure the inventory of exhausted fuel was obtained. Since this provides us the *actual* amount of pumped D during the shot, the calculated pumped inventory is normalized to assure that the dynamic exhaust rates integrate through the shot to the proper value. *Effectively, we have combined the best features of the static and dynamic particle balance techniques*.

An example analysis of particle balance is shown in Fig. 7. The input gas rate is obtained from the pressure change in calibrated fueling plenums. The real-time inventory of D in the plasma and gas in the vacuum chamber (divertor and main chamber) are obtained from core plasma density and distributed pressure gauges respectively, although this inventory tends to be small compared to input and exhaust inventories (compare the green line to blue and red lines in lower panel of Fig. 7). The net wall rate, or rate of retention, is the difference between the input and exhaust rate, corrected for any finite time derivative of the plasma plus + gas inventory.

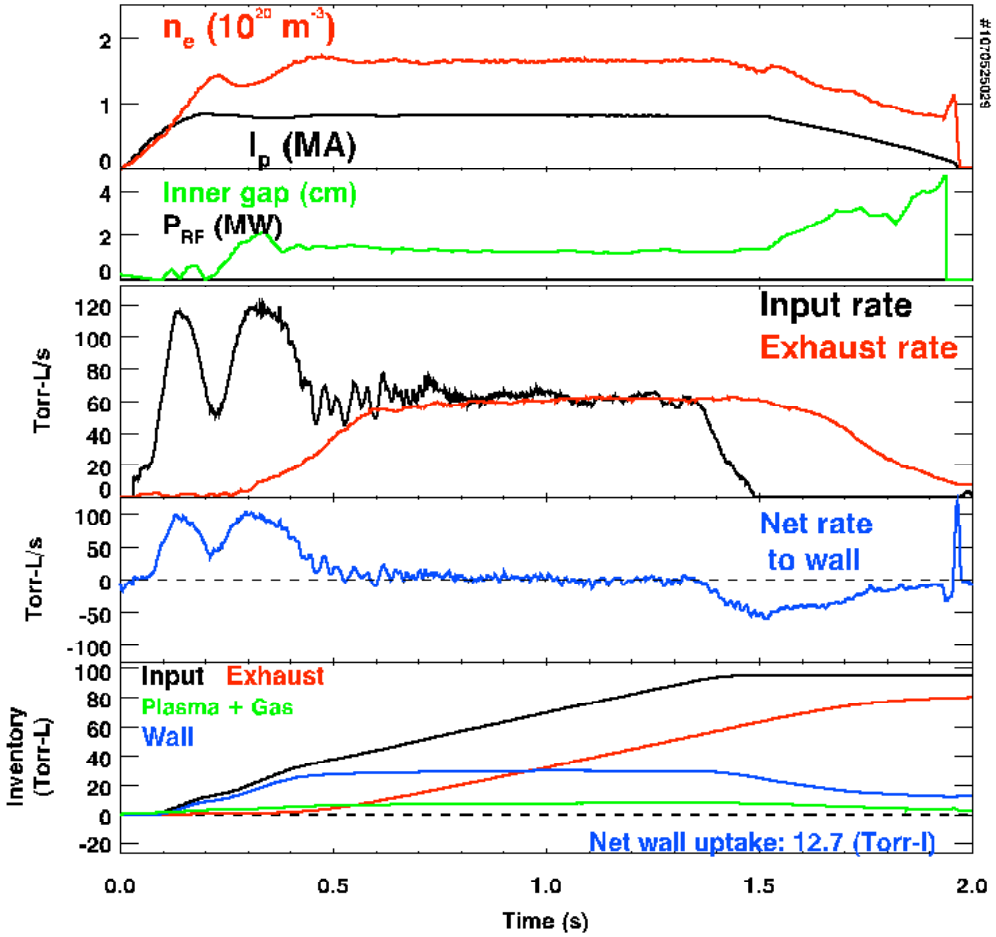


*Fig. 7 Example of dynamic particle balance for a C-Mod shot with stationary balanced double-null plasma. The shot-averaged static particle retention is 12.7 Torr-L obtained from cryopump regeneration (bottom panel). 1 Torr-L of $D_2$ gas at room temperature = $7x10^{19}$ D atoms.*

The example shown in Fig. 7 is very typical of the particle balance obtained when the plasma conditions are stationary during current flattop (0.5 -1 .5 s) and strong divertor pumping is used (i.e. the dominant strikepoint is near the cryopump). Large net retention rates are found to the wall in the early phases of the shot, first when the plasma is limited (inner gap is zero, 2nd panel) and then when the plasma density is being established. *However during the stationary period of the discharge, when the plasma and neutral gas inventories are not changing by definition, the input and exhaust rates are almost exactly balanced and therefore one concludes that real-time retention rate to the wall approaches a constant value near zero*. In the plasma rampdown active fueling is terminated and the cryopump recovers D from the walls. So while the static balance shows that the wall retained ~12 Torr-L (~ $10^{21}$ D atoms), the dynamic particle balance indicates this did not take place during the stationary portion of the discharge, and was instead dominated by startup and shutdown phases. *This has a striking resemblance to the DIII-D dynamic particle balance experiments*.

Several more examples of dynamic particle balance are shown in Figs. 8 – 10 to examine possible trends.

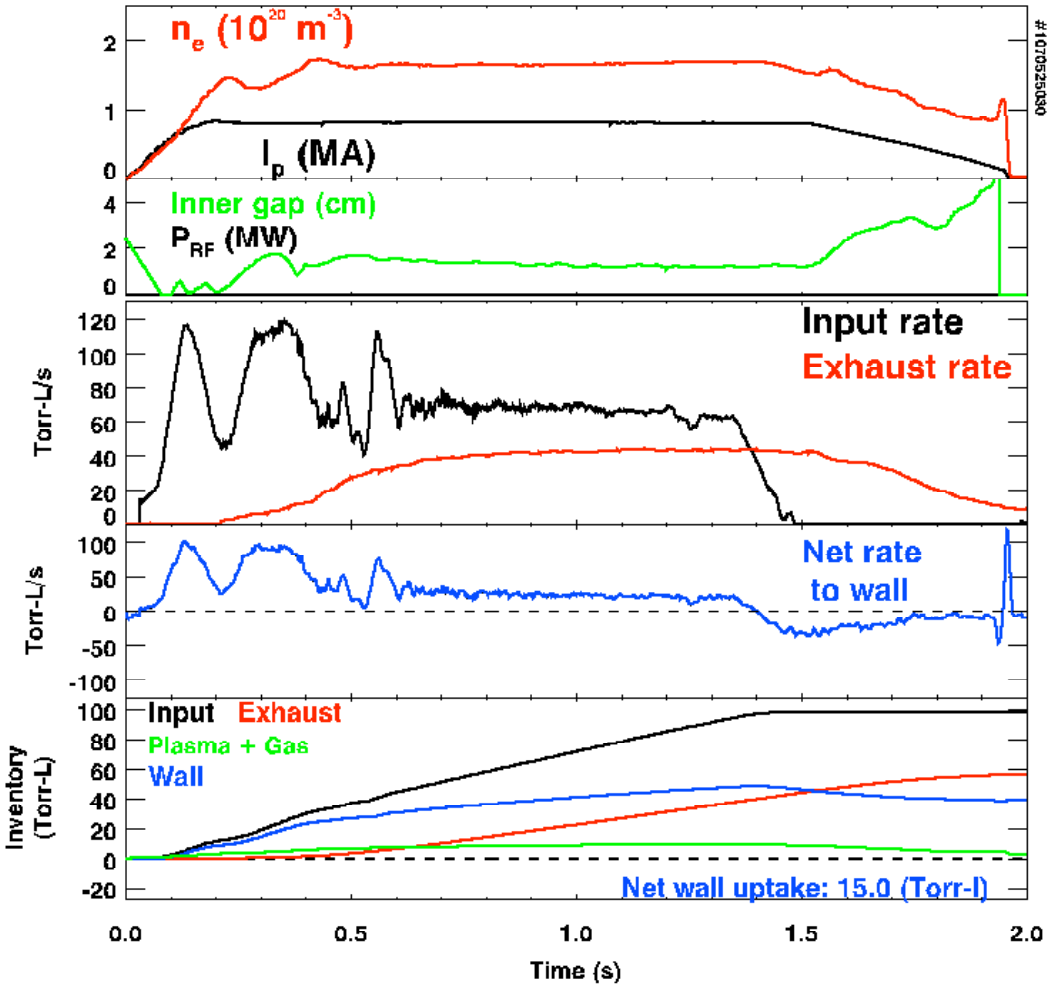


*Fig. 8 Repeat of stationary plasma conditions in Fig. 7 but with lower null shape (magnetic separation 3 mm). The shot-averaged static particle retention is 15 Torr-L but the lower pumping efficiency leads to a constant net wall retention rate ~ 20 Torr-L/s.*

Figure 8 shows a repeat of the core plasma conditions in Fig 7 but has its dominant strikepoint in the lower divertor, i.e. away from the cryopump. As a result the upper divertor pressure and exhaust rate are reduced. The net wall rate again reaches a constant value, but in this case has positive value. The static retained inventory also increases with respect to Fig. 7. This indicates some dependence of the dynamic wall rate on the pumping location and/or efficiency.

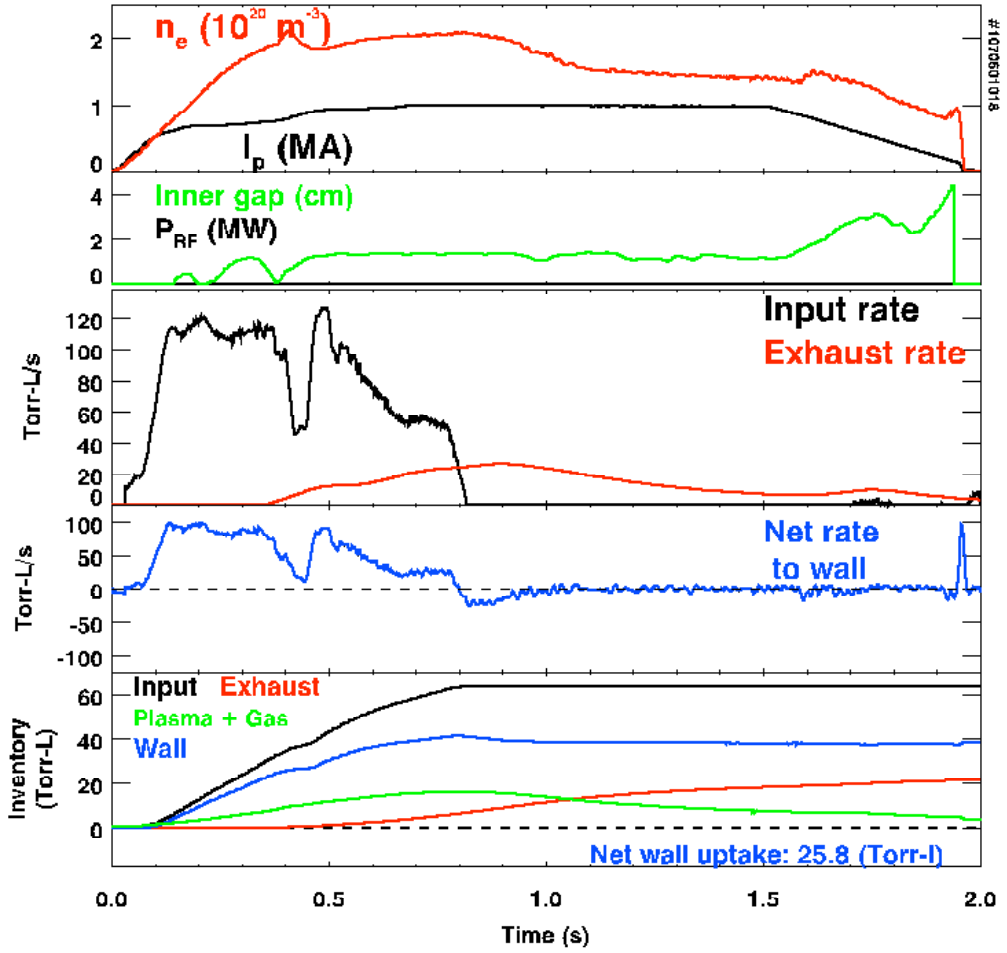


*Fig. 9 Upper-null discharge where active fuelling was terminated after 0.75 s and the cryopump was used to reduce the plasma density. The exhaust rate to the pump matches the changing particle inventory in the core plasma and in-vessel neutral gas, resulting in ~zero uptake by the wall after 1 second.*

In several cases the cryopump was not used to achieve stationay conditions, but rather to test its ability to achieve low density core plasmas. Such an example is shown for an upper-null discharge in Fig. 9 where active fuelling was forced off after 0.75 s. The divertor exhaust continues to be finite, yet the net wall rate is ~zero! This is because the time derivate of the plasma+gas inventory is exactly matched by the pump exhaust rate (or vice versa).

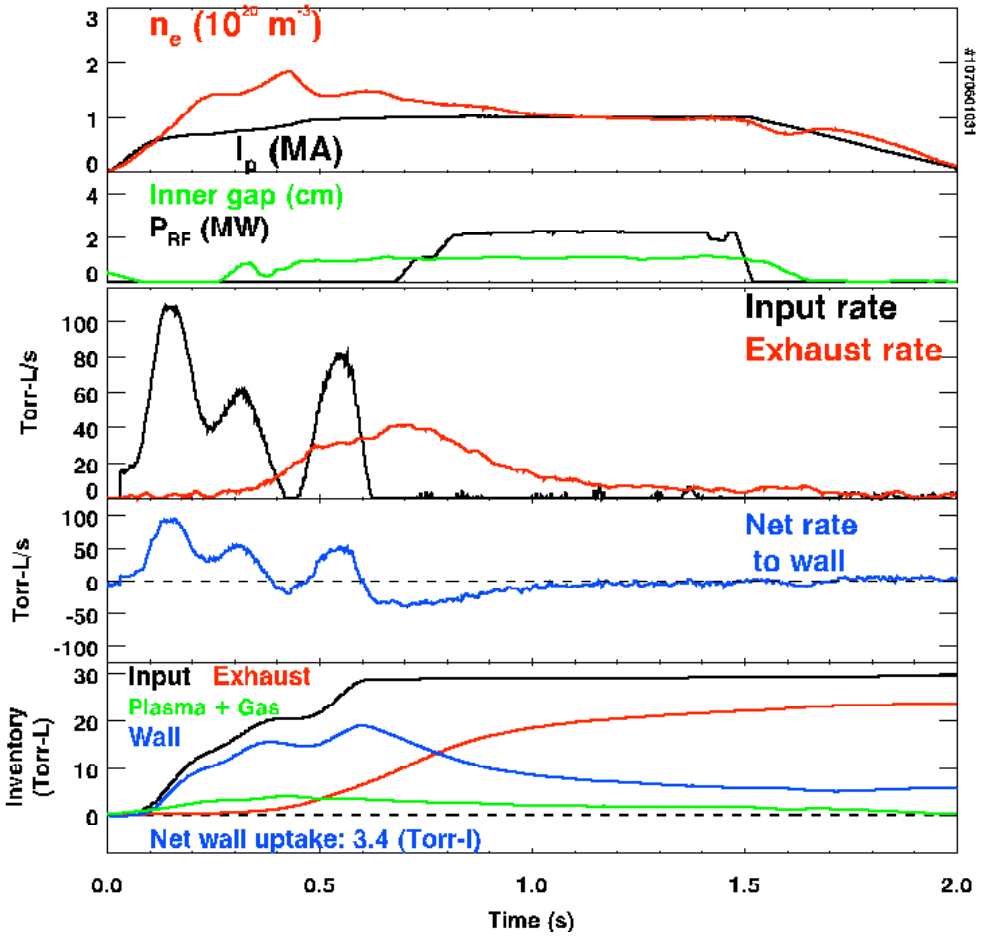


*Fig. 10 Example dynamic particle balance with RF heating in an upper-null shape.*

The effect of RF heating is shown in Fig. 10. The 2 MW of ICRF heating was applied simultaneously with an attempt to reduced the plasma density by turning off fueling. H-mode was not achieved due to the unfavorable grad-B ion drift direction in this upper-null discharge. Again the net wall retention rate goes to ~zero within the noise of the dynamic particle balance, as is the case without RF heating (Fig. 9).

A database of 67 cryopumped discharges was assembled in order to provide a more thorough assessment of wall retention rates; the major results of which are shown in Figs. 11-13.

The net wall retention rate versus time in the shot is shown in Fig. 11. The only selection criteria for these timeslices are constant current (non-disruptive) and stationary plasma density ($dN_p/dt <$ 0.05 Torr-L/s), so this reflects large variations in divertor shaping, absolute plasma density, etc. Nevertheless, the average trend is clear: the wall rate tends from positive values early in the discharge to near constant ~zero values in the latter phases of the discharge.

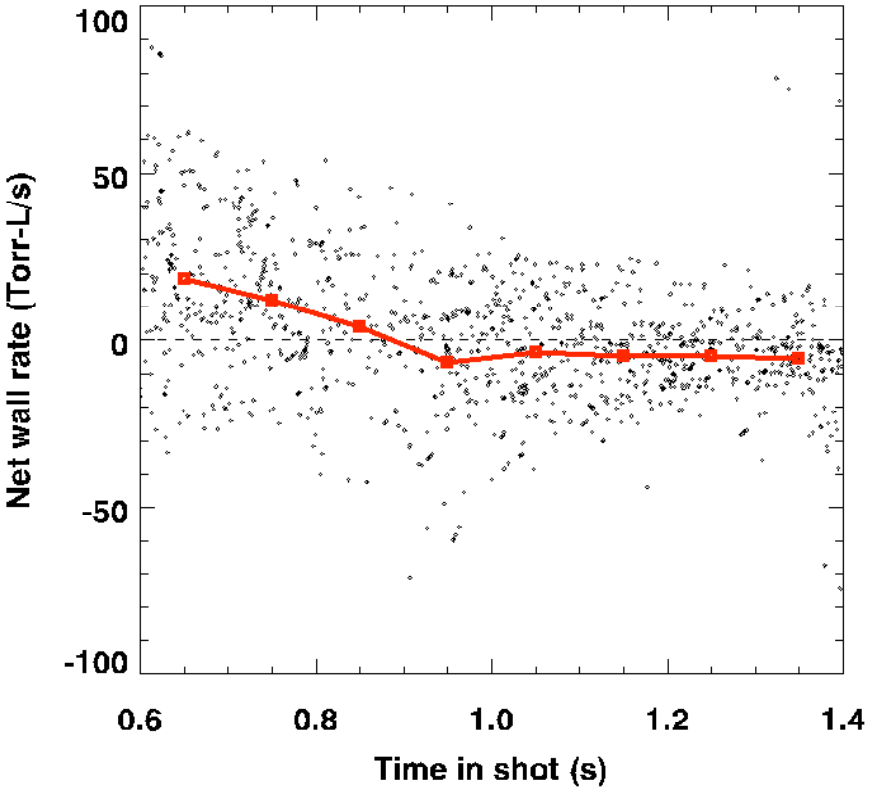


*Fig. 11 Dynamic particle balance database results using divertor cryopumping: Net wall retention rate as a function of time in the shot with the only selection requirements being steady core plasma density and plasma current. Dots are all results. Red squares are average results with 0.1 s time binning. As the shot progresses the net wall rate statistically approaches ~zero.*

The results of Fig. 7-11 provide a very different picture of the controlling periods for fuel retention than those obtained from static particle balance (Figs 2-6). The static results clearly point to D permeation into the Mo/W tiles of the active divertor, and therefore should be dominated by the steady-state diverted periods. However dynamic particle balance counter-indicates this picture showing that overall the net retention rates go to ~zero in those periods. Yet the overall static results of un-pumped discharges (Figs. 2-6) are actually supported by the shot-averaged retention rates in the cryopumped discharges. Fig. 12 shows that non-disruptive shots with active cryopumping typically retain ~10-20 Torr-L (~1-2 x$10^{20}$ D) and that the retention increases with divertor recycling, completely consistent with the un-pumped discharges.

This mixture of observations from comparing static and dynamic results likely informs us that we are missing an important process controlling fuel retention in C-Mod. First we note that generally shot-averaged absolute retention is weakly affected by cryopumping. However if we stated the retention rate as a fraction of fueled particles, the retention would be much lower since in the pumped case the external fueling is much larger. But this reduction is "false"; the same number of deuterons are retained in the vessel and this is what matters. This suggests that the retention process is controlled by exposure conditions to the materials; for example ion fluence. Yet at the same time we see that the dynamic particle balance *is* affected by the strength of external pumping (Figs. 7-8)! The most compelling observation is that when the plasma tends

towards stationary conditions, the dynamic net wall rate follows suite (Figs. 6-11). This occurs despite the fact that the exposure conditions are not constant; the Mo/W tile surface temperatures are continually evolving due to the plasma heating and absence of active cooling. Lab studies show that temperature is easily the dominant factor in controlling D permeation and retention in Mo [4]. So how can these observations be made consistent? A preliminary, and highly speculative, conclusion must be that the plasma is somehow self-regulating the wall uptake via a complex feedback loop. In other words, while the retention at each wall location is set by its exposure conditions, the plasma boundary is adjusting those conditions to assure a particle "neutral" wall. It is well known that the plasma boundary has strong non-linear responses to "upstream" conditions, and because of this the edge plasma varies greatly in order to satisfy power balance. It may be that an analogous effect is occurring for particle balance. A speculation is that if the external (and therefore unavoidable) exhaust becomes sufficiently strong compared to the overall recycling/refueling loop then the wall is not "allowed" to be a strong sink or source of fuel particles. In reality, because the wall recycling is the dominant fueling source, this would mean that the edge plasma is forced into overall balancing of the wall rates, even though locally this may not be the case. In the C-Mod cases the pump exhaust rate is significant: ~10% of the divertor recycling rate, and comparable to or higher than the net core fuelling rate ~20 Torr-L/s. This condition is also met in DIII-D which could help explain their very similar results despite the huge differences in plasma-facing materials. In NSTX the pumping is not external (*except small amount of cryopumping by beam ducts*) but is rather set by lithium coating of the surfaces. It seems clear that further investigations are required of this speculative plasma-controlled feedback loop of wall retention.

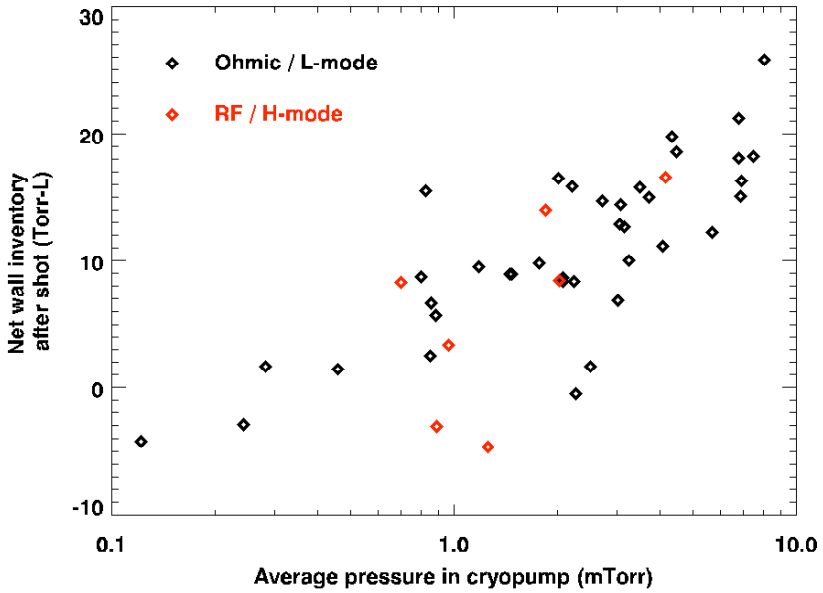


*Fig. 12 Shot-averaged total wall inventory uptake from static particle balance for cryopumped, non-disruptive shots. Results are plotted versus average divertor gas pressure which indicates plasma recycling rate. RF heated and H-mode shots (red) show no significant difference. The results generally agree with static particle balance in unpumped shots (Figs. 2-4)*

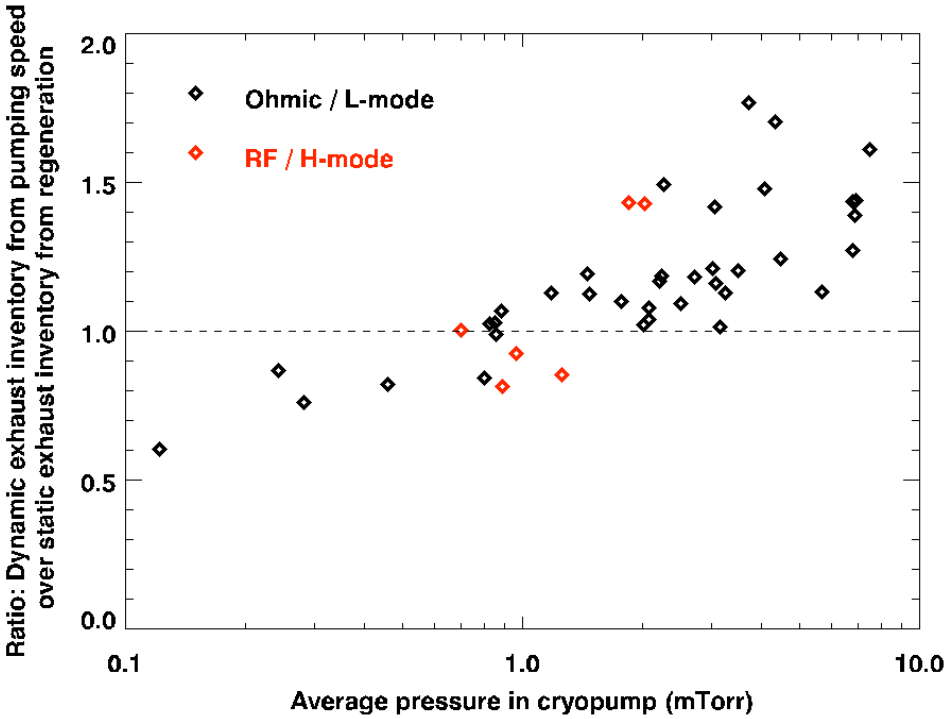


*Fig. 13 Ratio of dynamic particle exhaust in cryopump to actual pumped inventory from pump regeneration after each shot. The calculated pumping speed from gas-only calibrations overestimates actual pumping speed at higher divertor pressure / plasma recycling, indicating that the presence of the plasma is having an effect on pumping speed.*

A comparison of calculated exhaust inventories (based on calibrated pumping speeds with gas only) to the actual exhaust inventory from pump regeneration is shown in Fig. 13. There is a clear trend that as the divertor cryopump pressure increases (i.e. increased recycling), sthe dynamic calculations over-estimates particle exhaust (note this effect has been removed from the C-Mod dynamic particle analysis by renormalizing calculated exhaust rates). This shows that the effective pumping speed is somehow different when the neutrals are produced by plasma recycling, rather than by simple gas injection into the chamber.

## 3. Long-term Retention & Recovery of Retained Fuel with Disruptions

The long-term retention of deuterium fuel in metal walls has been examined on C-Mod. Ex-situ ion beam analysis of Mo tiles (Fig. 14) shows that the D can be retained at an atomic fraction ~1% in the Mo, to depths which are larger than the penetration of the ion beam. This is consistent with the requirements of D reservoirs in Mo from the particle balance experiments (Section 2). However overall accounting of the retained D in Mo tiles using ion beam analysis and TDS showed a global inventory ~100-1000x times smaller than expected from 1-2% of incident ion fluence integrated over a run campaign [1].

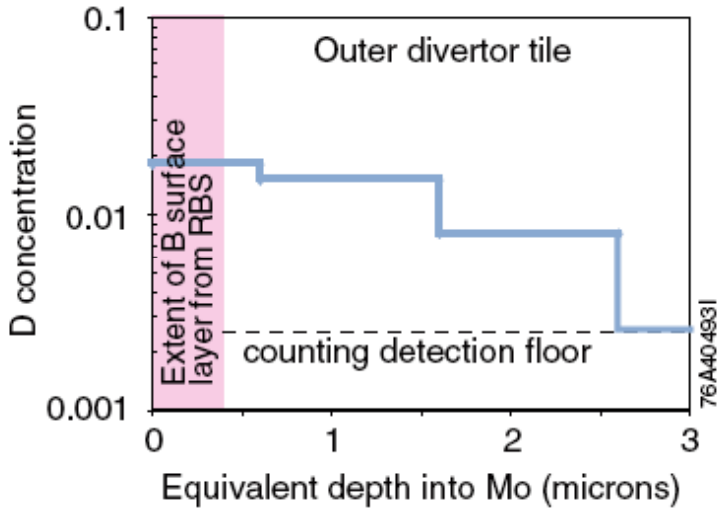


*Fig. 14 Ion beam analysis of retained D/Mo concentration vs. depth for a C-Mod Mo tile removed after several run campaigns.*

This result is largely explained by disruptions, which were carefully avoided in the static particle balance experiments. Disruptions appear to play a major role in limiting global retention in C-Mod. An examination of particle balance over a span of 300 shots [1] (Fig. 15) shows that the net wall uptake is limited to ~zero solely due to the natural occurrence of disruptions. On average, disruptions at full current (~15% of all discharges) lead to release of 6-7x the amount of D retained in a single non-disruptive shots (all discharges in the previous discussion on retention were non-disrupting).

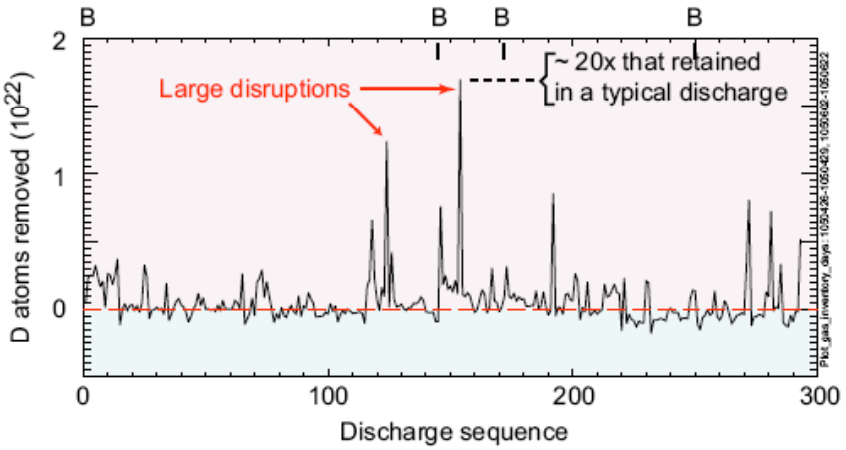


*Fig. 15 Shot-to-shot static particle balance in C-Mod. B marks times of boronizations [1]. Large disruptions are seen to produce a net recovery.*

Intentional disruptions were used to better characterize this effect (Fig. 16). Significant recovery of fuel was only found when the plasma stored energy passed some critical value, after which the recovered fuel inventory increased exponentially. This is in fact consistent with the expectation that the disruptions are causing rapid heating of Mo/W surfaces which force the trapped deuterium to be released. This hold promise as a technique to used controlled plasma disruptions to recover tritium in ITER [2,3].

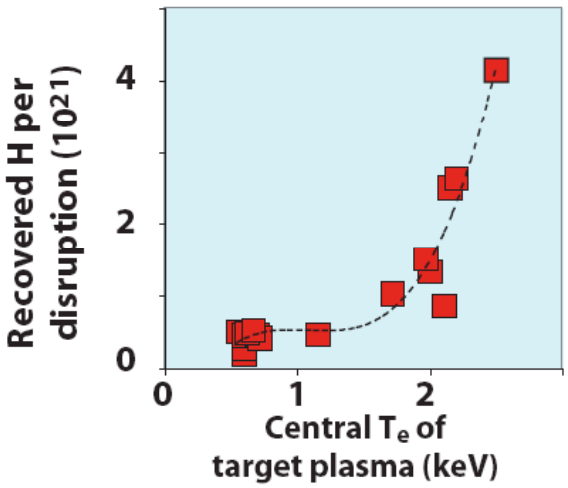


*Fig. 16 Hydrogenic fuel recovery on C-Mod following intentional disruptions with increasing target plasma $T_e$ (at constant density) and plasma stored energy. [3]*

The observation of sudden release of the retained fuel caused by the disruption is corroborated by the dynamic particle balance experiments. In Fig. 17 an example (unplanned) disruption is shown. Note that the net wall inventory is positive up to the point of the disruption. The large recovered inventory all occurs after the end of the plasma discharge.

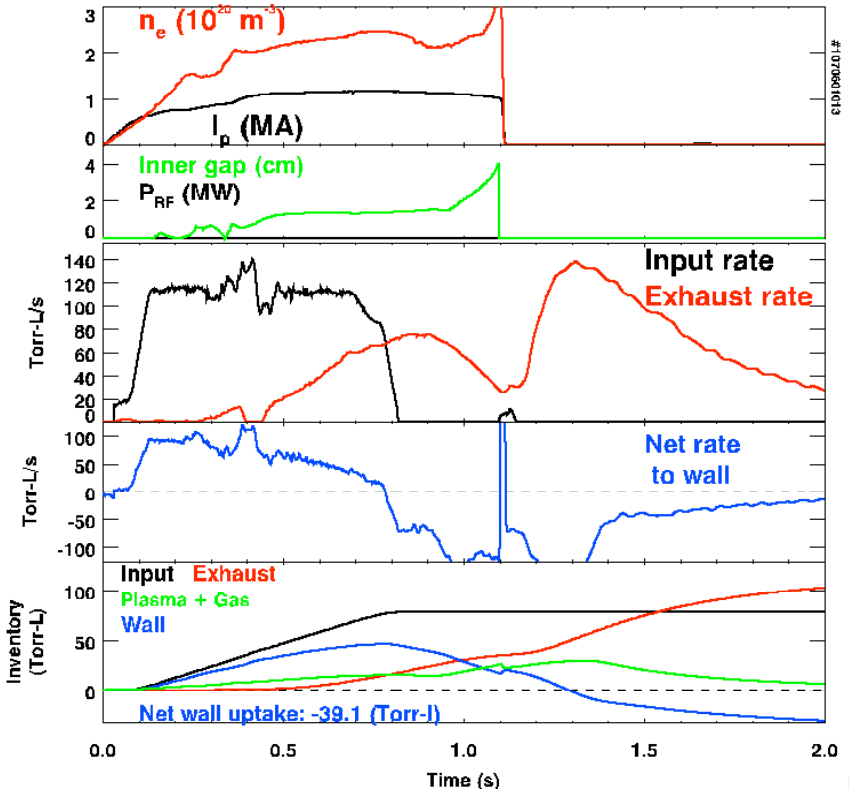


*Fig. 17 Example of dynamic particle balance on an ohmic (no RF) shot which ends in disruption. Note that the wall inventory is positive at the time of the disruption, but overall ~39 Torr-L is recovered **after** the disruption occurs at 1.1 seconds.*

The dynamic particle database was further used to examine the disruption recovery of fuel. Fig. 18 shows a comparison of the net wall D inventory immediately before the disruption and the inventory after the disruption and recovery by the cryopump (i.e a negative wall inventory). The wall inventory is generally positive up to the point of the disruption, but the recovered amount is significantly larger than retained inventories. This is particularly true for full current disruptions (0.5-1.5 s) that are earlier in the discharge. This is qualitatively consistent with the expectation that the recovery will be more efficient when the D has only permeated shallow distances. Modeling of this effect is described in Section 4.

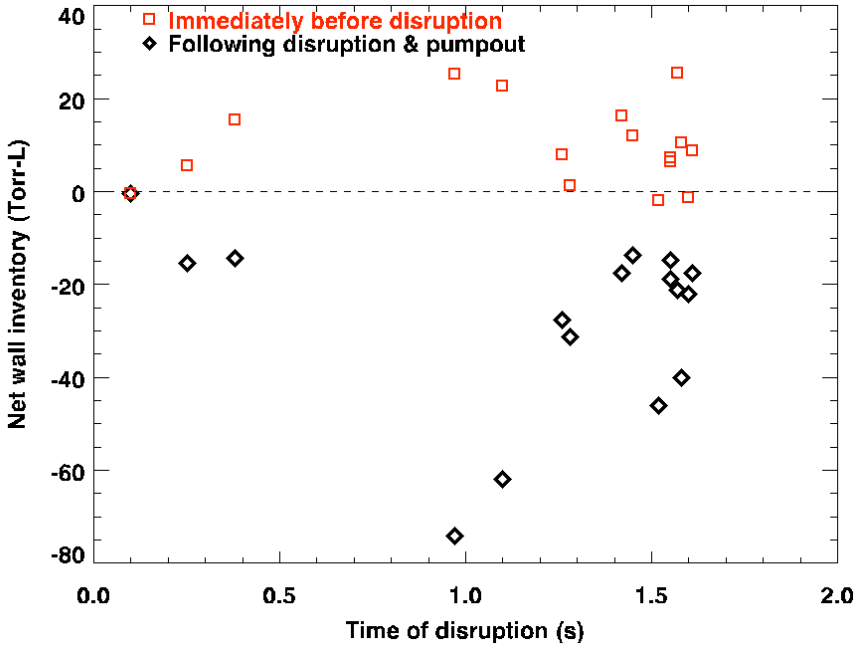


*Fig. 18 Database of disruptive shots (negative wall inventory means fuel reovery). (Red) Net wall inventory built up in that shot before the disruption. (Black) Net wall inventory through disruption and neutral gas pumpout.*

## 4. Modeling of Fuel Retention

Numerical modeling has been applied to deuterium retention and release in molybdenum, based on C-Mod particle balance experiments [1,3]. The numerical model solves the time-dependent coupled particle continuity equations for D transport and trapping in refractory metals like W and Mo using accepted temperature dependent rate coefficients from literature (details can be found in [4] and [5]). At this stage, the purpose of the modeling is to ascertain whether the observations of D retention and release in C-Mod are consistent with the known interactions of H fuels in molybdenum (Mo). Unique among divertor tokamaks in the world, C-Mod plasma-facing components are made entirely of bulk refractory metals (99% Mo, <1% W). There are two principal observations of D fuel retention in Mo that we are particularly interested in modeling:

1) A constant rate of D fuel retention in the Mo divertor at ~ 1% of the incident ion fluence, and 2) Substantial release of retained D from the wall caused by disruptions.

Given this background the numerical model is used to examine how the Mo surface in the C-Mod divertor would respond to typical incident ion flux so as to match the experimental results. The most important process is diffusion; the plasma deuterons are implanted at a shallow depth (~10 nm) and then diffuse both back to the surface and into the bulk where they can find vacant traps and therefore be retained. The model uses laboratory measured temperature dependent diffusion coefficients. Also important is the assumed density of empty traps and their distribution in the material. Based on the tile analysis we set the maximum trap density at 1% volumetric concentration relative to Mo. We show two simulation examples.

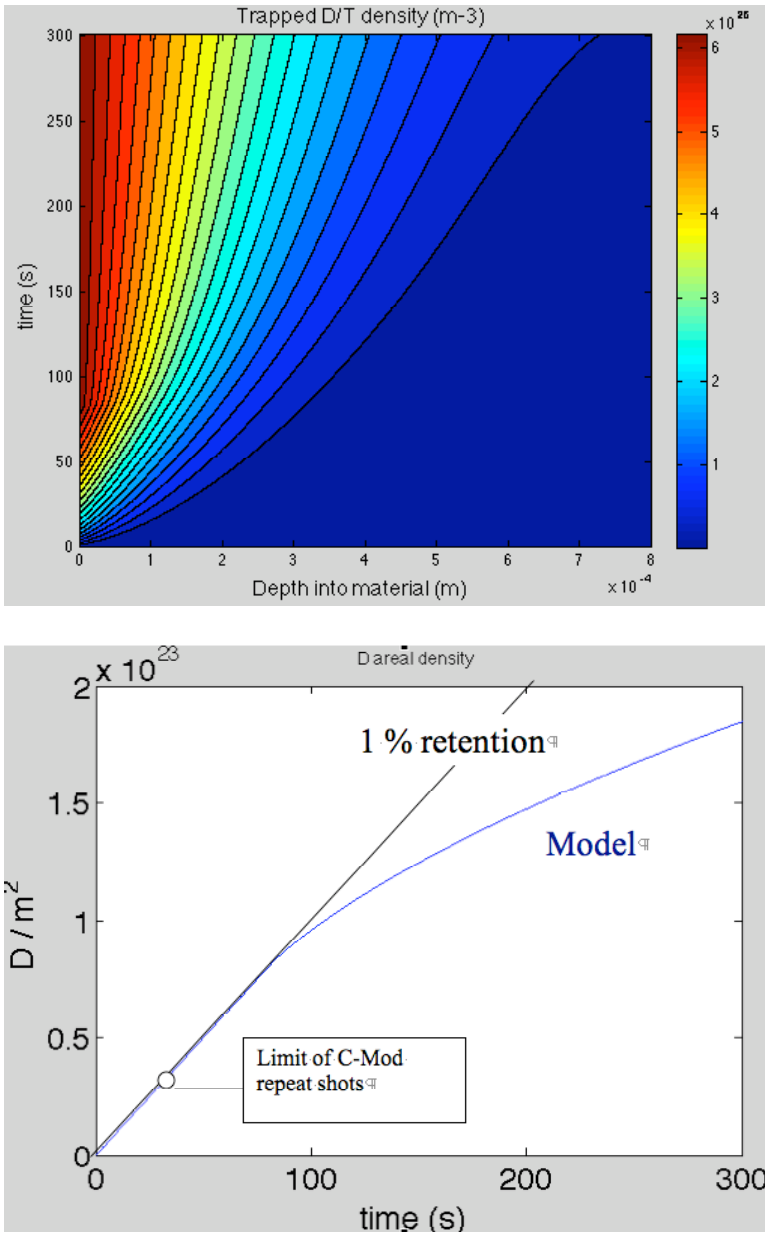


*Fig. 19 Numerical simulation of D retention in Mo at divertor with surface trap production and mobile traps. (Top) Contour of trapped D versus time and depth into Mo (Bottom) Integrated D fluence retained.*

The first example (Fig. 19) assumes that the traps are being produced at the surface by the D bombardment itself, at a rate of 1% traps per incident ion (there is also a possibility the damage is caused by low-Z impurity ions in the plasma). The traps are therefore only produced at the surface and are then assigned a diffusion coefficient equal to that of the solute D. It is well known from laboratory experiments that the traps have finite mobility in the Mo [4] but this is certainly an over-simplification. An average temperature of 600 K is assigned for the outer divertor of RF heated discharges, and for the typical measured ion flux density ~$10^{23}$ ions/s/m$^2$ is used. The simulation shows that the D and trap diffusion is sufficiently fast that up to ~30s the retained D is linearly increasing at a rate of 1% of incident ion fluence (of course this is somewhat "forced" by our imposition of 1% trap production efficiency). While this linear retention with fluence is valid to the limits of the C-Mod experiments (~30 s), the model suggests the retention should begin to slowly saturate starting at ~100s; at that time the diffusion starts to limit the D access to deeper locations and since 1% is

the maximum allowed concentration, this is required to store more D. This suggests the retention would be limited at this temperature for very long pulses, which is positive for devices like ITER. At the same time a concern is that the D is stored so deeply in the Mo, ~50 microns even for the short timescales of C-Mod experiments, raising a concern that recovery of this D will be difficult.

The second simulation example (Fig. 20) shows that if the trap concentration is 1%, but immobile, then the retention should appear to follow permeation and increase with square root of time on the C-Mod shot timescales ~30 s. This does not occur in the experiments (Figs. 2-4), highlighting the importance of trap mobility in this process.

The conclusion of simulating the retention is that it is physically possible for the Mo to retain deuterium as seen in the C-Mod experiments, mainly by allowing access of the deuterium to deeper trap sites through diffusion. However there are many unanswered questions as to the production and mobility of the traps, which seems to be the most important processes occurring in setting the retention level.

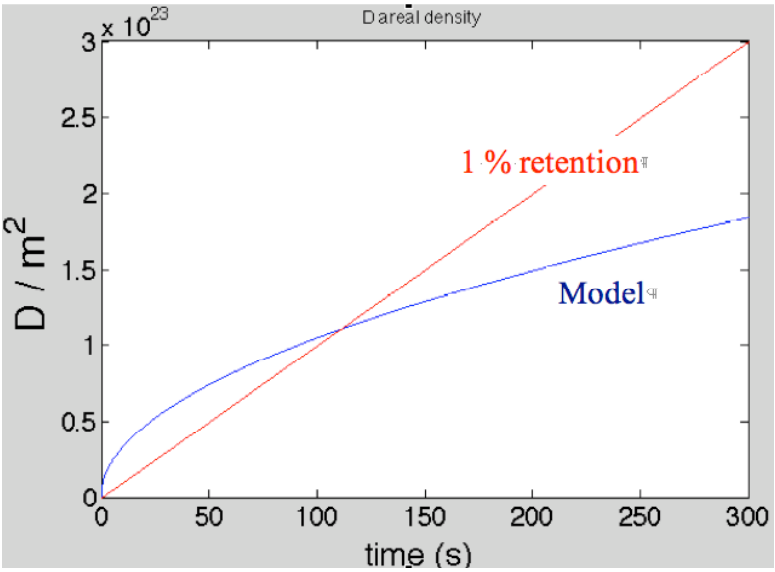


*Fig. 20 Numerical simulation of D retention in Mo at the divertor with immobile traps at 1% concentration.*

We now move to the second overall observation from C-Mod: disruptions release large amounts of the retained hydrogenic (H or D) fuel (Section 3). Rapid heating of the Mo is the underlying reason for the D release. In order to thermally release the D from trap sites (typical trap energy ~1.4 eV) the temperature must be elevated substantially above room temperature, while at the same time the D diffusivity rapidly increases, allowing the liberated D to "escape" to the surface, where it can recombine, and be released as $D_2$ molecules. These critical rates (de-trapping, diffusion, recombination) are governed by the Arenhhius relationship and are therefore exponentially sensitive to temperature. This suggests that a minimum amount of energy density is required in the short timescales of disruptions (1 ms) to sufficiently heat the Mo, or else minimal D will be recovered. This expectation is supported by C-Mod experiments (Fig. 16) where the stored core energy/temperature of planned disruptions was slowly increased. When the

core T exceeded ~ 2 keV (stored energy 40 kJ) the release of H from the walls increases exponentially.

The numerical simulation is used to model the release of D during disruptions (Fig. 13). The D is assumed to be retained at 1% D/Mo up to 50 microns depth as suggested by the retention modeling. A trap energy of 1.4 eV is assumed based on laboratory experiments. Taking typical plasma stored energy (thermal + magnetic) in C-Mod suggests a range of surface temperatures above 1000 K could be obtained for the divertor tiles in a 1 ms heat pulse due to a disruption. Fig. 21 shows that temperatures above 1000 K are sufficient to strongly deplete the stored D, even on a 1 ms timescale, although the depletion is strongly dependent on temperature assumptions. This simulation result is then qualitatively consistent with the observation that rapid heating during a disruption is sufficient to recover the D retained over 10's of seconds of regular C-Mod discharges. This also suggests controlled disruptive heating can be a useful tool to limit retention on ITER, as previously proposed [2].

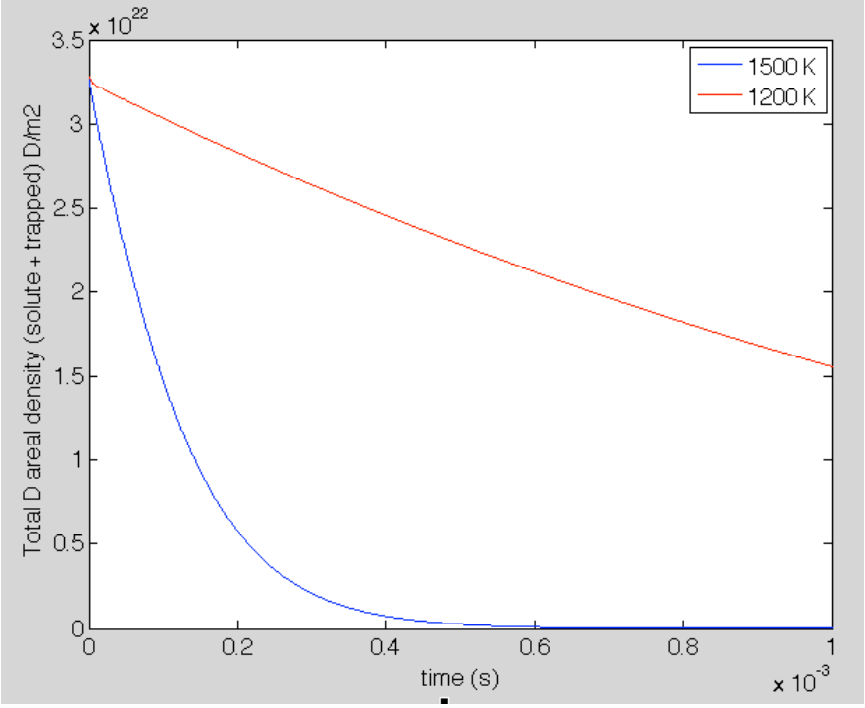


*Fig. 21 Numerical simulation of disruption-heating induced reduction of retained D in Mo for two different assumptions of surface temperature.*

In summary the numerical simulations have shown consistency with the experimental C-Mod results on D retention and release, although many details need to be resolved. In particular the mechanism of trap formation and mobility in the deuterium need to be understood much better.

**REFERENCES**

[1] B. Lipschultz, D.G. Whyte, J. Irby, B. LaBombard, G. Wright *Nuclear Fusion* **49** (2009) 045009.

[2] D.G. Whyte, J.W. Davis, J. Nucl. Mater. **337-339** (2005) 560.

[3] D.G. Whyte, *et al*. Proc. 21st IAEA Fusion Energy Conference, Chengdu, China, October 2006, EX/P4-29.

[4] G.M.Wright Ph.D. Thesis U. Wisconsin 2007.

[5] D. G. Whyte, J. Nucl. Mater. **390-391** (2009) 911.

# NSTX Facility Report

# FES Joule Milestone 2009

## Fourth Quarter Report

## September 30th, 2009

### *Annual Target:*

Conduct experiments on major fusion facilities to develop understanding of particle control and hydrogenic fuel retention in tokamaks. In FY09, FES will identify the fundamental processes governing particle balance by systematically investigating a combination of divertor geometries, particle exhaust capabilities, and wall materials. Alcator C-mod operates with high-Z metal walls, NSTX is pursuing the use of lithium surfaces in the divertor, and DIII-D continues operating with all graphite walls. Edge diagnostics measuring the heat and particle flux to walls and divertor surfaces, coupled with plasma profile data and material surface analysis, will provide input for validating simulation codes. The results achieved will be used to improve extrapolations to planned ITER operation.

### *Quarter 4 Milestone*

Fourth Quarter - Complete the necessary experiments, analysis, and modeling. Prepare a joint report on the empirical understanding gained, the comparison to simulation and identify critical research areas to improve extrapolation to ITER.

### *Completion of 4$^{th}$ Quarter Milestone*

The 4$^{th}$ quarter milestone has been completed by analyzing results from earlier experiments carried out at the facilities. Research progress and activities are organized by facility below.

## *NSTX*

### Summary:

Fundamental processes governing deuterium retention in lithium conditioned graphite were identified in dedicated gas balance and surface analysis experiments. The amount of deuterium fuel that was retained at the end of a NSTX discharge was high (~ 90%). With lithium conditioning the retention was moderately higher, but the additional retained deuterium was released immediately after a discharge. In the long term, the retained deuterium is released by outgassing, some rapidly and some on a time scale that can extend to weeks or longer. During this time the deuterium gas can undergo isotope exchange with intrinsic hydrogen also released from the tiles. The graphite surface can also pump molecular deuterium in some cases.

Insights into deuterium retention in lithiated graphite were obtained from surface analysis of NSTX tiles and samples exposed in dedicated experiments at NSTX and Purdue University. A simple picture of lithium-deuterium bonding in LiD was not supported by the data. Instead the analysis identified important chemical functionalities associated with deuterium irradiation of a graphite surface conditioned with lithium suggesting that the interaction of deuterium atoms is by indirect electrostatic interactions with Li atoms. The key finding is that with sufficient lithium the binding or retention of D atoms during the plasma interaction is *fundamentally different* from that of non-conditioned graphitic surfaces. In particular, D atoms are weakly bonded in regions near lithium atoms bound to either oxygen or the carbon matrix.

Significant correlations were found between gas balance and surface analysis data. Gas balance data indicated the retention increases with increasing lithium dose and this was correlated with changes in chemical functionalities found with x-ray photoelectron spectroscopy. In addition, the evidence for deuterium weakly bound to lithium conditioned graphite found in thermal desorption spectroscopy of exposed samples was mirrored by the prompt recovery of this deuterium after lithium conditioned NSTX discharges.

### Introduction:

The first deuterium particle balance experiments at NSTX were performed in FY2008 and described in the 2$^{nd}$ quarter Joule milestone report. For ohmic discharges with the pumping

valves closed, the preliminary estimate of deuterium retention was high: 97% - 100% with- or without lithium wall conditioning. Outgassing in the subsequent 12 – 24 h after the discharge reduced this number to 50% (60% with Li) of the deuterium fuel of the last discharge. These experiments were greatly expanded in the 3rd quarter of FY2009 together with extensive calibrations of the pressure gauges, residual gas analyzers, and measurements of the neutral beam cryopump and turbomolecular pumping speeds. To investigate the lithium/carbon surface chemistry a novel PMI (or sample) probe was commissioned that enabled the exposure of 4 samples to NSTX discharges, and withdrawal for analysis in a chamber next to the vessel without exposure to air. This report documents the analysis of the particle balance and PMI probe data and the insights gained into deuterium retention in graphite and lithium-conditioned graphite.

## 4. Deuterium particle balance: (section numbering to be adjusted in final document)

The deuterium inventory was tracked on 4 dedicated run days on NSTX. These were devoted to:

(i) ohmic discharges pre-lithium conditioning with the pumping valves closed,

(ii) neutral beam heated discharges pre-lithium where the particle inventory on the neutral beam cryopumps was tracked,

(iii) ohmic discharges with lithium conditioning with the pumping valves closed,

(iv) neutral beam heated discharges with lithium conditioning where the particle inventory on the neutral beam cryopumps was tracked.

In each case the PMI probe was used to expose samples to 6 or 8 discharges for subsequent analysis.

D retention in ohmic discharges before- and with lithium conditioning.

For these experiments the vessel was closed with no pumping and the vessel pressure rise with an ohmic discharge compared to fueling the vessel in a gas-only 'shot' without a plasma. This is the 'static' particle balance technique described in earlier quarterly reports, and enables a straightforward measurement of retention by comparison of the vessel pressure. This method is independent of pressure gauge calibrations (provided they are linear over the range used) and

does not need estimates of the pumping speed. The disadvantage is that it cannot be used for neutral beam heated discharges (described in the next section).

Baseline discharges were developed with the outer strike point on the outer divertor, close to the PMI probe (see Fig. 2 in 3rd quarter report). The ramp down in plasma current was controlled to avoid a minor disruption that would heat the tiles and possibly influence the retention. Fig. 4.1 shows results from an ohmic discharge with lithium conditioning.

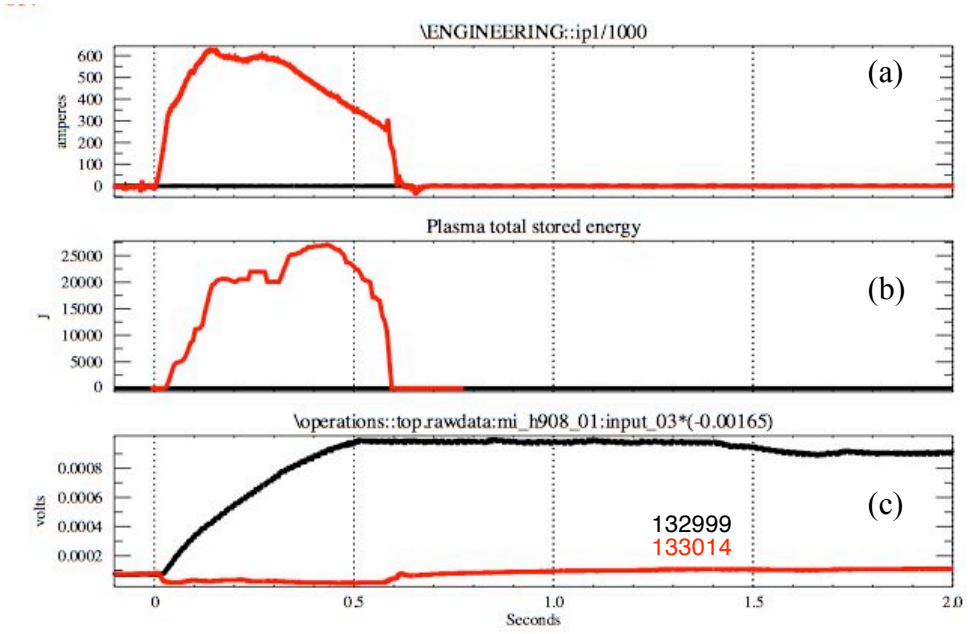


Fig. 4.1 (a) Plasma current, (b) stored energy and (c) in-vessel pressure for gas-only 'shot' and ohmic discharge (red trace) with lithium conditioning.

The deuterium retention after the ohmic discharge was estimated from:

$$\text{Retention (ohmic)} = 1 - \frac{\text{pressure after discharge}}{\text{pressure after gas-only shot}} \quad \text{x ratio of D input.} \qquad (1)$$

The deuterium input was programmed to be the same for gas-only and plasma discharge so the second factor, calculated from the experimentally measured input, is close to one. The retention for 133014 (Fig. 4.1) immediately after the discharge at 0.65s is 94.3%. This may be compared to the pre-lithium retention in 132489 (shown in Fig. 3a in the 3rd quarter report) of 92.8% also immediately after the discharge. The gas fueling for this pair of discharges was similar: 29.3 torr-liters for 132489, 23.3 torr-liters for 133014. Discharge 132489 was immediately preceded by 8 minutes of He glow discharge cleaning (He-GDC), discharge 133014

was immediately preceded by 48 mg of Li evaporation but no He-GDC (unnecessary with Li conditioning). The question is whether the small ~ 2% difference between the average of pre-Li (92%) and with-Li discharges (94%) is significant and attributable to lithium. The value of the retention was quite reproducible (within 1%) in a sequence of nominally identical discharges used to expose the PMI probe. However the retention is sensitive to the discharge ramp down. For example a shot in the sequence with Li, 133017, had a tail end minor disruption and the retention was reduced to 87%. We also note that the 2008 discharges described in the third quarter report had preliminary estimates of higher retention (in the 97% - 100% range). We conclude that the post-discharge retention difference between pre-Li and with-Li ohmic discharges is small (probably of order 2 %) and is less than other effects such as variations in PFC heating. This difference is larger with neutral beam heated dicharges that had 3x higher lithium evaporation (next sect.). For comparison a 80% wall uptake was estimated for a DIII-D ohmic shot in the Q2 report.

Fig. 4.2 shows a comparison of the in-vessel pressure on 133014 (from fig 4.1 above) with the pre-Li discharge 132489 shown in the 3rd quarter report fig. 3. It can be seen that the in-vessel pressure during the discharge is substantially reduced with lithium conditioning but rises to approximately the same value immediately after the discharge. Evidently the additional deuterium pumped by the lithium conditioned wall is released promptly after the discharge. The same effect was seen in neutral beam heated discharges (Fig. 4.4). This result is consistent with independent TDS measurements of chemical binding of D in lithium conditioned graphite discussed in section 5.3.

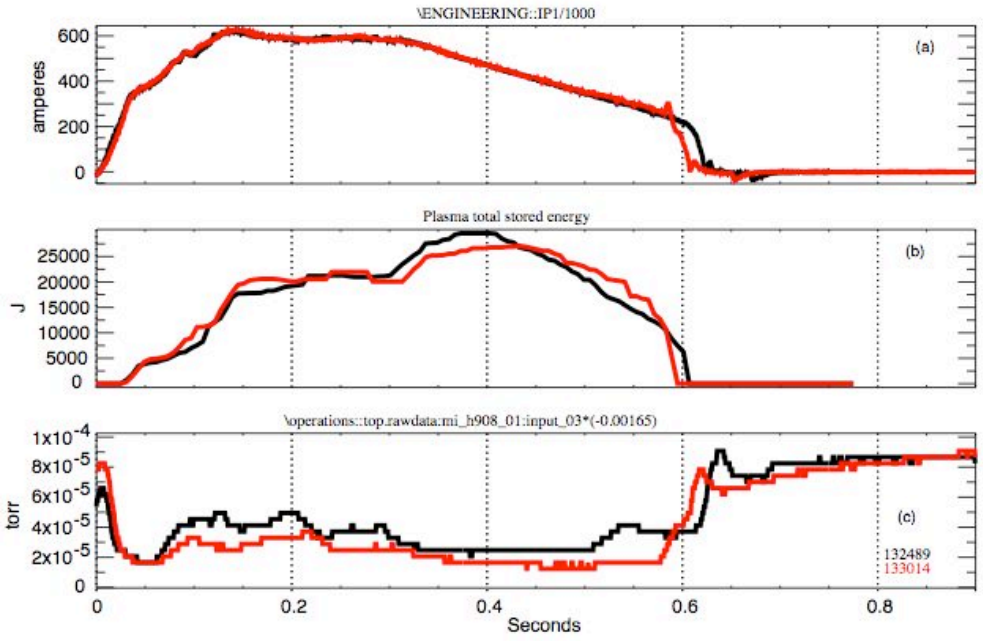


Figure 4.2 (a) plasma current, (b) stored energy and (c) in-vessel pressure for pre-Li (black) and with-Li (red) ohmic discharges.

The retention rate can also be expressed as a function of ion fluence to the wall. Fig. 7 in the Q3 report showed the rate of retention in Alcator C-mod was ~ 1-3% of the total D ion fluence incident on the Mo divertor and main wall PFCs[1]. On NSTX the ion flux density (ions/$m^2$/s) was derived from the ion saturation current at the two Langmuir probes on the outer divertor. D-alpha emission was also recorded from the divertor, though this was not absolutely calibrated. Under the approximation that the D-alpha profile was proportional to the ion flux profile, the Langmuir probe data was combined with the divertor D-alpha emission profile to construct an ion flux density profile for the outer SOL extending from the outer strike point to major radius (R) = 1.0 m. The ion flux density was integrated over the outer divertor to derive the outer divertor particle flux (particles/s) for each time slice. This was then integrated over the whole discharge duration to obtain the total ion fluence (particles) incident on the divertor. For the ohmic pre-lithium discharge 132489 this was 2.4 x$10^{22}$ D ions and for the ohmic with-lithium discharge 133014 this was 2.65 x$10^{22}$ D ions. The deuterium retention measured by gas balance

[1] B. Lipschultz et al., Nucl. Fus. 49 (2009) 045009.

on this pair of discharges was 1.9 x$10^{21}$ and 1.5 x$10^{21}$ D atoms, which corresponds to 8% and 6% of the outer divertor ion fluence measured by Langmuir probe and D-alpha. This does not include D flux to the inner divertor, the center stack or outer vessel wall[2] so the number for the retention rate as a function of the total ion fluence to the wall and divertor will be less.

D retention in neutral beam heated discharges before- and with lithium conditioning.

Retention in discharges heated by neutral beams was measured by tracking the balance between input and exhausted deuterium. These discharges were developed with the outer strike point on the outer divertor, close to the PMI probe. The ramp down in plasma current (Ip) was programmed so that the final Ip drop was at very low stored energy to avoid tile heating that could possibly influence the retention. The pre-Li discharges were ELMy H-mode. The post-lithium discharges were mostly ELM-free H-mode. The lithium reduced the density, increased the temperature, and stored energy in most cases, by 20-30%.

A simple comparison of the in-vessel pressure during the discharge to that of a similar gas-only 'shot' is shown in Fig. 4.3 and indicates that there is high retention in these discharges. However a quantitative estimate of retention needs to take into account the details of the fueling and pumping.

These discharges are fueled by both low field side (LF) gas injection and high field side gas injection from the centerstack (CS). Because of space constraints the CS injection tube is narrow (~3 mm i.d.) with low conductance and the CS gas valve is 3 m from the injection point. The pressure rise after the discharge from 0.6 s to 1 s in Fig. 4.3 ((c) red curve) is mostly due to residual gas exhausting from the CS gas tube. The subsequent pressure decrease is due to pumping by the neutral beam cryopanels.

[2] V. Soukhanovski et al., J. Nucl. Mater., 390-391 (2009) 516.

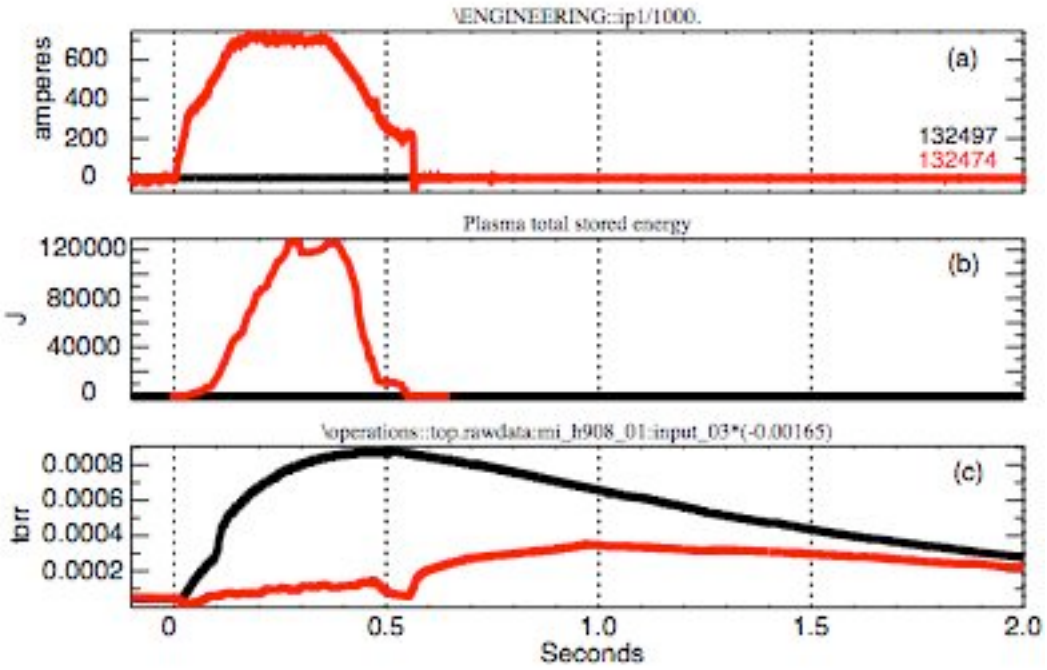


Fig. 4.3 (a) Plasma current, (b) stored energy and (c) in-vessel pressure for gas-only 'shot' and neutral beam heated discharge (red trace) before lithium conditioning. The gas fueling was programmed to be the same in both cases.

The amount of low field side gas injection used at the beginning of the discharge is estimated from the drop in pressure and the volume of the supply plenum. The CS gas injector was calibrated by injecting gas into the vessel without plasma, and monitoring the vessel pressure rise with time. Only the quantity of CS gas injected during the plasma current duration was counted as fuel. An additional complication is a small amount of fueling by cold deuterium gas that is an intrinsic part of neutral beam operation. This was measured separately by operating the neutral beam without the accelerator voltage and with the calorimeter retracted. The cold gas pulse caused the vessel pressure to rise before being pumped by the NB cryopanels. The integral of the deuterium pressure (torr-s) was multiplied by the NB cryopanel pumping rate (liters/s) (see next paragraph) to obtain the total quantity of cold gas fueling in torr-liters (1.77 torr-liters in 1.6 s). The fueling rate was multiplied by the plasma current duration to estimate the quantity of NB cold gas entering the plasma.

The neutral beam cryopanel pumping speed was measured by injecting a known quantity of gas in a 25 ms pulse from the lower dome gas injectors. The turobomolecular pumps were closed. The vessel pressure rose and then decreased with a time constant of approximately 0.9 s

governed mostly by the conductance through the neutral beam duct. The time constant was calculated by curve fitting the pressure data as it decreased over a given pressure range. This time constant increased with the transition from viscous to molecular flow below 1e-4 torr. The cryopanel pumping speed (liters/s) was calculated by multiplying the decay time constant by the NSTX vessel volume. For the range of interest, 1e-5 to 1e-4 torr, the cryopump speed was 32,680 liters/s.

The in-vessel deuterium pressure was monitored by micro-ion gauges[3] that were calibrated against a high accuracy baratron with calibration traceable to NIST. The small change (~ 6%) in response due to the toroidal field was measured separately. The micro-ion gauges were mounted on the vessel wall and had a fast (~5 ms) time response. The quantity of deuterium pumped by the cryopanels during the plasma was estimated by integrating the in-vessel pressure from t = -0.42 s before the pulse to the time of end of the plasma current and multiplying this quantity (torr-s) by the cryopanel pumping speed (liters/s). Finally the quantity of neutral deuterium remaining in the vessel was calculated from the pressure at the end of the plasma and the vessel volume. The retention was calculated from equation 2:

$$\text{Retention (NB)} = \frac{\text{Total D fueling during plasma less D pumped and D remaining in vessel}}{\text{Total D fueling during plasma}} \quad (2)$$

The different methodologies of equation 1 and equation 2 were checked against each other by measuring the retention of similar ohmic discharges (pre-Li) both ways i.e. in one case with the NB valve closed and in two discharges with the NB valve open. These discharges had similar plasma current, stored energy and in-vessel pressure during the discharge. The retention calculated by equation 2 was R = 89.5% and R = 90.0% in the NB valve open cases and for comparison, the average value calculated by equation 1 was R = 92.0% for the valves closed case. This close agreement validates the comparison of retention as measured by the two methods.

[3] R Raman et al., Rev. Sci. Instrum., 74 (2003) 1900.

The retention for the before-lithium neutral beam heated discharge in figure 4.3 was calculated by eqn. 2 to be 88%. As in the ohmic case, this number would change if minor disruptions heated the wall. The retention in a discharge that was programmed to be the same, but that experienced a minor disruption, decreased to R = 75% in one case. Discharges without minor disruptions had reproducible retention viz: R = 86%, 86%, 88%, 85%.

Similar discharges were run with lithium conditioning. These had an average of 137 mg of lithium evaporation in between discharges, substantially higher than the 48 mg of Li used for the ohmic case. No intershot He-GDC was used with lithium conditioning (compared to 9 minutes of intershot He-GDC before Li). The with-lithium retention measured by the eqn. 2 methodology detailed above for 6 discharges ranged from R = 92.5% to 94.5% distinctly higher than the retention before lithium. The average values of the retention are shown in table 1.

| End of discharge retention | Before Li | With Li |
|---|---|---|
| Ohmic | 92% | 94% |
| NB heated | 87% | 93% |

Table 4.1. Retention measured immediately following ohmic and neutral beam heated discharges before and with lithium conditioning. The values are averaged over 3-8 discharges.

The lithium conditioning caused a substantial decrease in in-vessel pressure during the discharge. Fig. 4.4 shows a comparison of a neutral beam heated discharges before- and with lithium conditioning. The gas fueling during the plasma for this pair of discharges was similar: 37 torr-liters for 132474, 41 torr-liters for 133110. With lithium the in-vessel pressure decreases to 40% of the value before Li but interestingly, recovers to the same value after the pulse. The same effect is seen in Fig. 4.2 and is thought to be related to the chemical binding shown in the TDS spectra in Fig. 5.8.

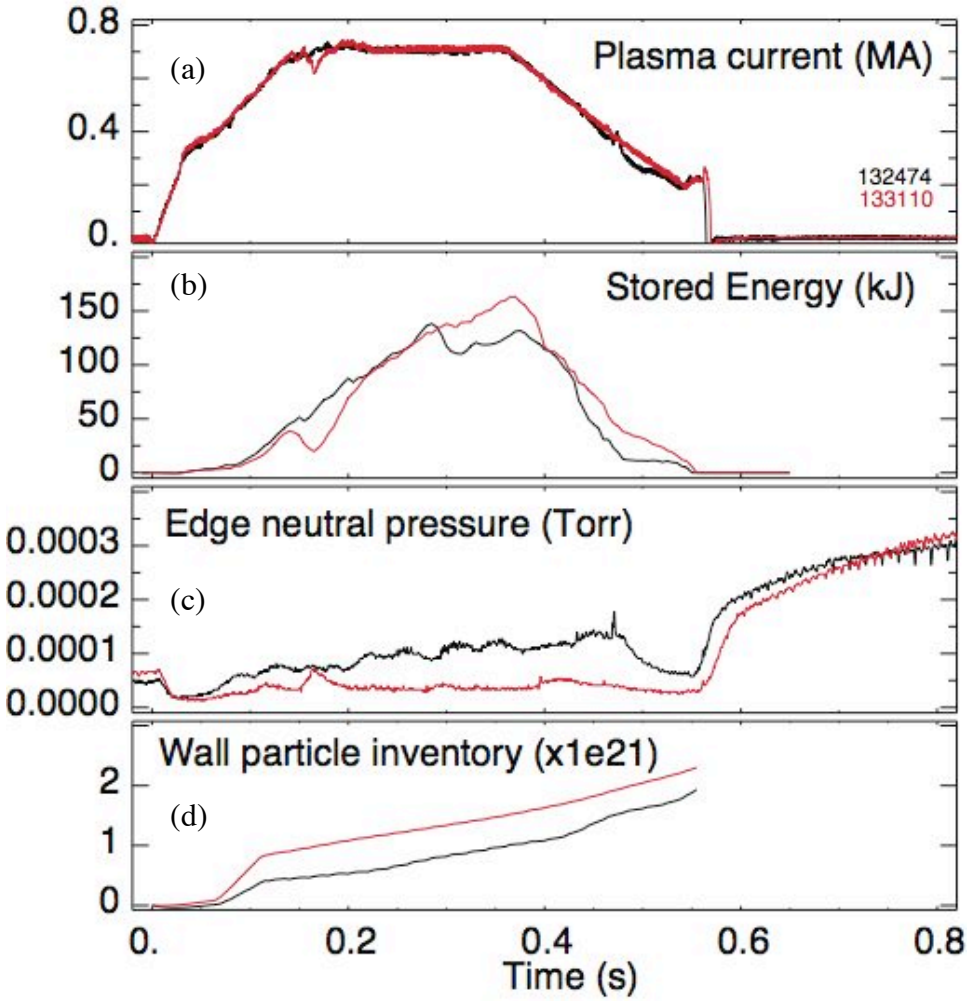


Figure 4.4 (a) plasma current, (b) stored energy (c) in-vessel pressure and (d) wall inventory calculated by dynamic particle balance model for pre-Li (black) and with-Li (red) neutral beam heated discharges.

A dynamic particle balance model was used to study the wall pumping and outgassing during the discharge. The model was based on the particle balance analysis previously developed on NSTX[4,5]. The model takes into account all measured particle sources, such as gas injection, NBI injection and the dynamic change in particle inventory, and calculates the wall loading rate. At present, the model used electron inventory as a proxy for plasma particle content, and does not take into account any electron contributions from the carbon source. The wall was found to

[4] V.A. Soukhanovskii et al., J. Nucl. Mater., 313-316 (2003) 73.
[5] R. Maingi et al., J. Nucl. Mater, 241-243 (1997) 672.

be in a pumping state in nearly all of the analyzed discharges. A significant difference was found in the cumulative wall inventory in lithium conditioned neutral beam heated discharges and is shown in fig. 4.4 pane (d).

In summary the end of pulse retention is high (~ 90%) and slightly higher with lithium conditioning. The difference with lithium is more noticeable with heavy lithium conditioning and parallels the discussion of minimum lithium 'thickness' based on surface analysis described in sect. 5.1. However after the discharge the additional deuterium retained with lithium is released. This may be further understood in the light of the lithium surface chemistry revealed by TDS and XPS surface analysis of samples exposed to these plasmas and will be discussed in section 5.

Long term outgassing.

The long term hydrogenic inventory build up is of most interest to ITER for safety reasons. Deuterium outgassing follows an NSTX discharge and reduces the retention. Previous Q2 and Q3 reports cited a preliminary estimate of long term retention of 50% - 60%. This was based on the overnight rise in total pressure due to outgassing with the pumping valves closed compared to the fueling of the last shot of the day. In this method the vessel acts as an integrator avoiding uncertainties due to the numerical integration of very low pressures over extended times. In the fourth quarter we have further calibrated the NSTX residual gas analysers (RGAs) and examined the rise in deuterium partial pressure. This has revealed a more complex situation with isotope exchange and wall pumping of deuterium.

Some of the outgassing following a discharge is from fueling from that discharge, but some is from earlier discharges. Deuterium outgassing continues for days at least after NSTX deuterium discharges (for TFTR, tritium outgassing continued for years). An additional difficulty with measuring long term deuterium retention is periodic helium glow discharge cleaning (He-GDC) which pumps out deuterium in a gas mix of He and $D_2$ which are very difficult to distinguish on the RGAs.

To look at overnight trends the NSTX the RGAs were calibrated and used to record the partial pressure rise of different mass gas molecules with the pumping valves closed (without any He-GDC). While mass 4 ($D_2$) dominates immediately following a discharge there is also a contribution from $H_2$ (protium molecules) that grows over time and isotope exchanges with $D_2$ to make a mass 3 HD peak that becomes comparable to the mass 4 peak after several hours. Figure 4.3 shows the combined $D_2$ + ½ HD partial pressures following ohmic discharges with- and without Li.

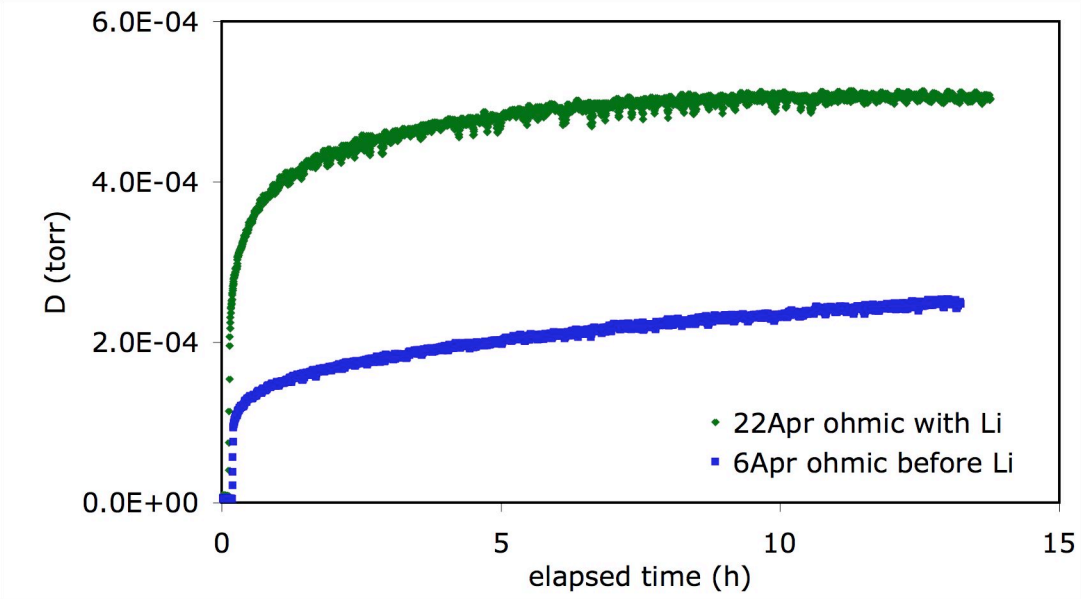


Figure 4.5 Deuterium partial pressure following ohmic discharges before Li (lower blue curve) and with Li (upper green curve).

We attribute the difference in magnitude between the curves to He-GDC. The discharges on 22 April prior to the time period of Fig. 4.5 had an average of 47 mg of Li evaporated into the vessel in-between discharges, and most had no intershot He-GDC. The prior discharges on 6 April used no lithium conditioning but did have 8 minutes of He-GDC in-between discharges that depleted the wall of deuterium, leaving less to outgas at the end of the day. The same behavior is seen in a comparison of neutral beam discharges. Outgassing after the before-lithium but with intershot He-GDC neutral beam discharges on April 3rd was a factor of three lower than the with-Li but no He-GDC sequence on April 24th.

One interesting result was evidence of wall pumping of molecular deuterium. Figure 4.6 shows the combined $D_2$ + ½ HD partial pressure following neutral beam heated discharges with Li. The neutral beam valve was closed immediately following the last discharge on 24 April and the D partial pressure peaks 10h later and then decreases slightly as the vessel cools (the lower outboard divertor tiles near the strike point cooled from 50°C to 30°C over this period). The NB valve is opened briefly to pump out the vessel at 26 h and the D pressure rises again once the valve is closed. The $D_2$ pressure in the vessel is the result of both outgassing and pumping by the wall. The outgassing term dominates immediately after pumpout but at higher pressures the deuterium behavior is more like a saturated vapor. A similar pressure decrease was seen after 10h following neutral beam heated discharges before Li. The data record does not extend past 13 h in the ohmic cases as the machine was needed for other experiments. The partial pressures of other potential D containing molecules such as mass 20 $CD_4$, or $D_2O$ was about 6% of the partial pressure of D from $D_2$ and HD and is smaller than the pumping effect.

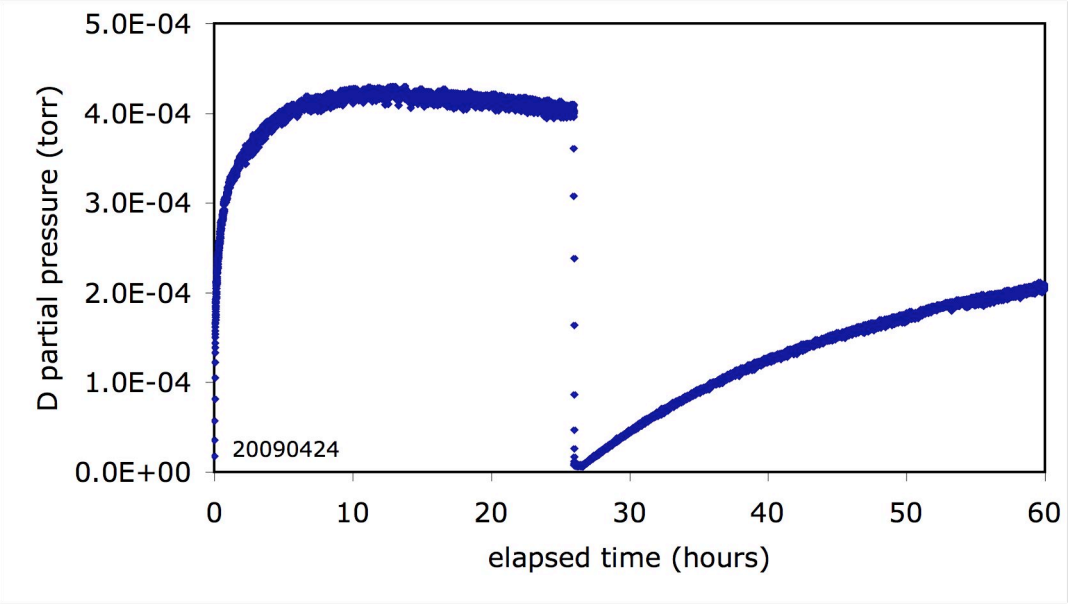


Figure 4.6 Deuterium partial pressure following neutral beam heated discharges with Li conditioning. The vessel is briefly pumped at 26 h.

## *5 Surface analysis for understanding hydrogenic retention in NSTX and controlled laboratory experiments*

A plasma-material interface (PMI) probe was used to study the fundamental mechanisms of deuterium retention in lithium-coated graphite surfaces. Purdue University in collaboration with PPPL used the PMI probe to expose samples to NSTX plasma discharges before- and with lithium wall conditioning. This particular PMI probe design is the first diagnostic on a tokamak device to have the capability in-vacuo to characterize the chemical state of lithium-deuterium interactions. For a full description of the PMI probe, including figures and diagrams, refer to the third quarter Joule Milestone report. The capability provided by the PMI probe is necessary due to the strong chemical reactivity of lithiated graphite surfaces [1]. Samples from the PMI probe are retracted in-vacuo and selected samples are heated for thermal desorption spectroscopy (TDS). The samples are then retrieved and shipped to Purdue University under argon atmosphere for further surface analysis, including XPS, TDS, 4-point probe, and SEM. Three primary techniques are utilized to investigate deuterium retention and chemical interaction with the lithium-coated graphite surface. Sects 5.1, 5.2 reports the use of X-ray photoelectron spectroscopy (XPS) for identification of chemical functionalities of deuterium with lithiated graphite indirectly by observation of the oxygen, carbon and lithium excitation states. Sect. 5.1 deals with NSTX tiles, and sect. 5.2 with samples from the NSTX PMI probe. Section 5.3 shows thermal desorption spectroscopy (TDS) results from NSTX conducted in-vacuo immediately after plasma exposure and ex-situ identification of bonding strengths and steady-state retention of deuterium in controlled laboratory experiments at Purdue University. This section also describes measurements of the adsorbed deuterium concentration by the 4-point probe technique that is based on electrical resistivity measurements. Section 5.4 summarizes the understanding gained of deuterium retention in lithiated graphite.

### 5.1 X-ray photoelectron spectroscopy (XPS) measurements of NSTX tiles and associated laboratory experiments

Laboratory measurements at Purdue University consist of X-ray photoelectron spectroscopy (XPS) and thermal desorption spectroscopy (TDS). X-rays from a Mg-K alpha source are used to excite photoelectrons and collected by an energy dispersive analyzer that

records a spectrum containing information on the chemical state of the exposed material. Three primary photoelectron spectra are analyzed: O1s, C1s and Li1s. Deuterium alone does not have enough electrons to produce an XPS spectra however, indirect interactions of deuterium with O, C and Li are measured by XPS and correlated to shifts in chemical bond energies.

Control studies at Purdue University have identified peak functionalities in XPS spectra of lithiated graphite surfaces that were exposed to energetic (~ 500 eV/amu) deuterium ions. These peaks have been correlated with similar functionalities in the XPS spectra of NSTX tiles exposed to plasmas and trace concentrations of air (during shipment), for example the strong carbonate peak[6] at 290 eV. A cleaning procedure, including Ar sputtering and annealing, was used to remove the passivated, amorphous layer as seen in Figure 5.1.

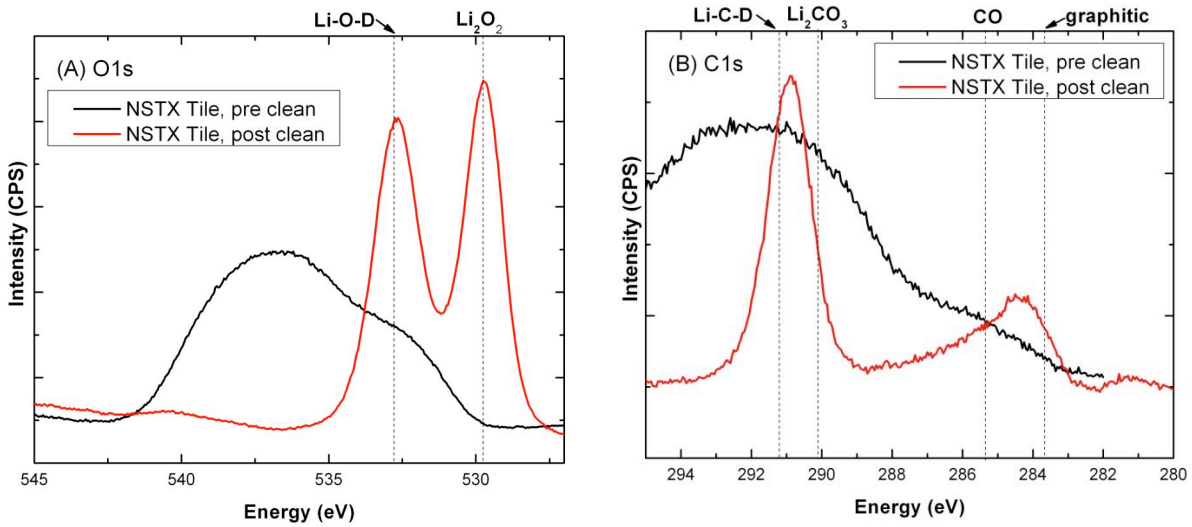


Fig. 5.1. XPS spectra from the NSTX lower divertor tile A408-002 in the (A) O1s, and (B) C1s energy ranges showing the primary bonding functionalities. The tile was exposed to plasmas throughout the 2008 campaign and to trace concentrations of air during shipment to Purdue. The black curves show the XPS spectra from samples as received from NSTX, and the red curves spectra from the same samples after an Ar sputtering and annealing cleaning procedure. The vertical lines refer to known binding energies discussed in this document and referenced literature [6,7,8].

[6] J.P. Allain, D. Rokusek, S.S. Harilal, M. Nieto, C.H. Skinner, H. Kugel, B. Heim, R. Kaita and R. Majeski, *J. Nucl. Mater*. **390–91** (2009), p. 942.

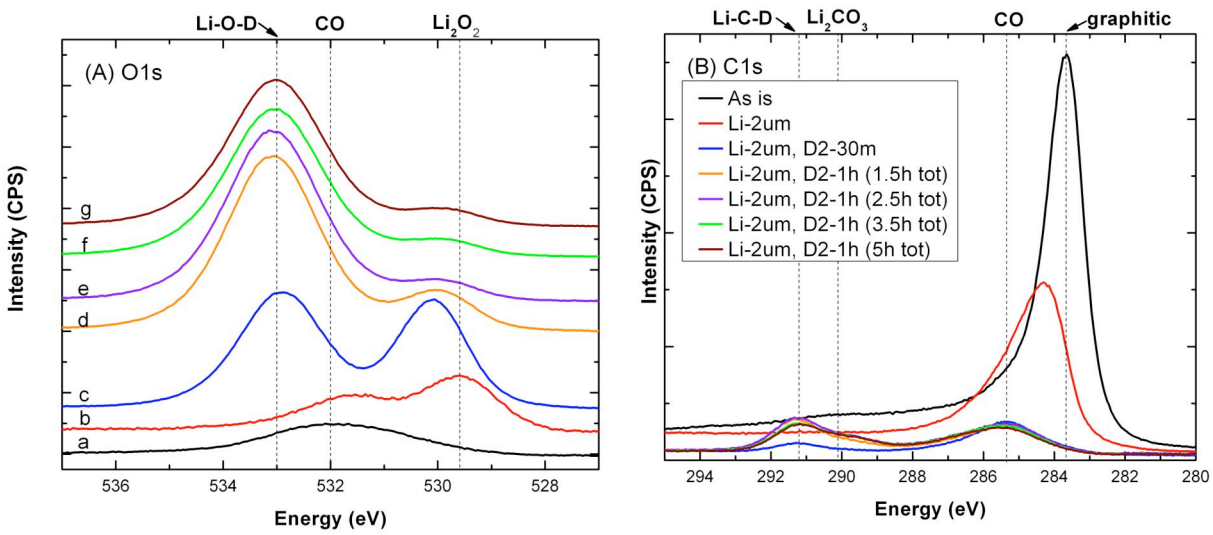


Fig. 5.2. XPS spectra showing binding functionalities of an ATJ graphite substrate for (A) O1s and (B) C1s photoelectron energy range. Spectra were obtained from (a) virgin ATJ graphite sample, (b) sample after 2μm nominal lithium deposition; and after cumulative deuterium irradiation of duration (c) 30 min, (d) 1.5 hr, (e) 2.5 hr, (f) 3.5 hr, and (g) 5 hr on the original 2μm nominal lithium film.

Controlled experiments at Purdue University partially replicate NSTX conditions by evaporating a controlled nominal thickness of lithium (typically 2.0 ± 0.13 μm) on ATJ graphite, followed by deuterium irradiation ($\Gamma \approx 7$ E13 $cm^{-2}s^{-1}$, 500 eV/amu) via an ion gun. (for a discussion of 'thickness' see sect. 5.2) Film deposition is calibrated prior to each experiment using a quartz crystal microbalance (QCM) and a Li density of 0.53 $g/cm^3$ is assumed. XPS peaks observed from these samples are at similar binding energies to those seen in the NSTX tiles (compare Figures 5.1 and 5.2). Harilal and Allain have attributed the peak located in Fig. 5.2A curve (c) at 529.5 eV to $Li_2O_2$ [7]. We attribute the peak located at 533 eV to Li-O-D interactions on a carbon substrate. Control studies isolate the influence of lithium in producing peak located at 533 eV. For a sample in which lithium is not deposited, as seen in Fig 5.4, deuterium irradiation does not result in a peak at 533 eV.

[7] S.S. Harilal, J.P. Allain, A. Hassanein, M.R. Hendricks, M. Nieto-Perez, *J. Nucl. Mater. Appl. Surf. Sci.*, 255 (2009), 8539

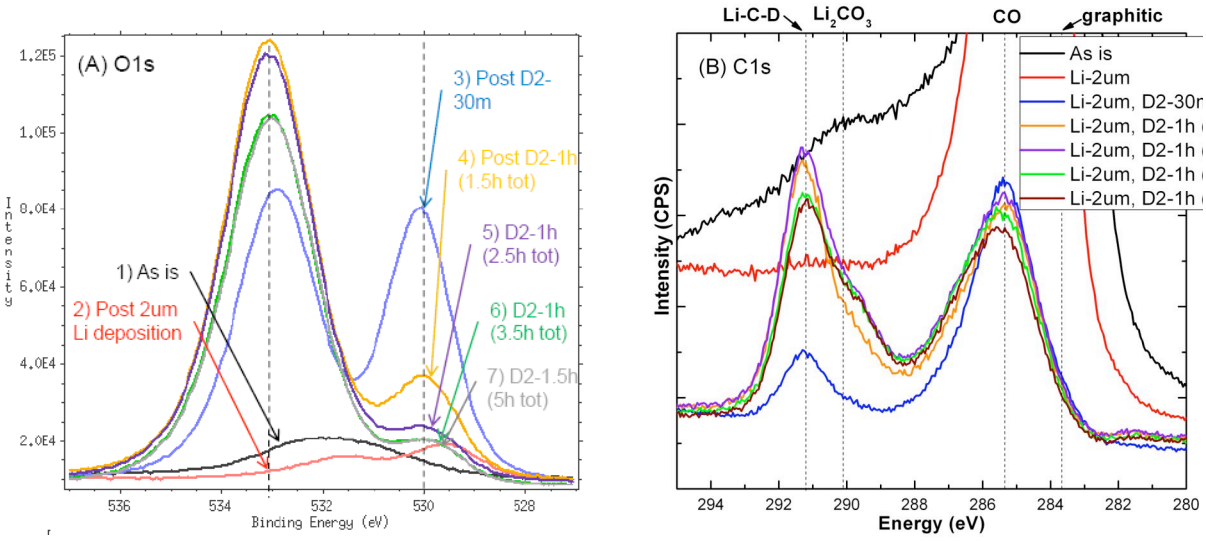


Fig. 5.3 (A) Overlay of O1s plots from Fig. 5.2. showing relative increase in peak intensity with increased deuterium exposure; (B) Close-up image of XPS C1s spectra showing correlation of functional peak growth with deuterium exposure.

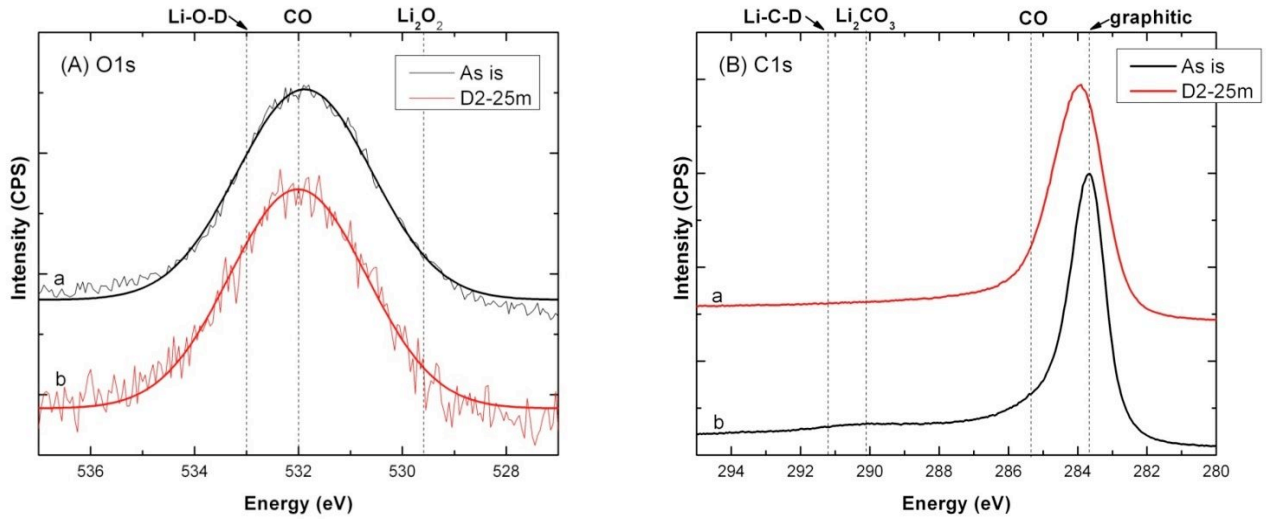


Fig. 5.4. (A) O1s and (B) C1s XPS photoelectron spectra ranges for non-lithiated ATJ graphite samples. Spectra obtained from (a) virgin graphite, and (b) 25 min deuterium irradiation without prior lithium deposition. No Ar cleaning was used.

In Fig. 5.3 (A) one can clearly see the correlation of peak shifts of O1s spectra to 533 eV and near 530 eV with deuterium fluence. In Fig. 5.3 (B) concurrently one observes a shift to 291.2 eV and the growth in the C1s peaks indicative of a clear correlation with deuterium

fluence. Since deuterium is not directly measured by XPS, this behavior relates to associated interactions of deuterium with either Li, C or O. The shifts observed are then related to interactions or functionalities of D and specific chemical states of lithium atoms in the carbon matrix. Our current working hypothesis is that the underlying mechanism for retention of deuterium particles is associated with "preferred interactions" with the graphite matrix. These preferred interactions or functionalities are strongly correlated with the presence of lithium. Recent ab-initio work on the Li-H-C system has observed that hydrogen is likely to bind in regions near lithium atoms in a graphite matrix. Similar behavior is expected for deuterium since there is no evidence of an isotopic effect. Electronic transfer from Li atoms to C atoms can induce dipole interactions with D and thus lead to relatively strong bonding/retention of deuterium in the vicinity of lithium atoms. Both O1s and C1s spectral shifts after deuterium irradiation correlate with functionalities found in post-mortem tile samples and provide strong evidence for this mechanism associated with D retention in the lithium-carbon matrix.

Further analysis of NSTX post mortem tiles has shown that a minimum thickness of Li is required before the Li-O-D functionalities are observed. Here 'thickness' means the thickness of the same amount of lithium if deposited on a perfectly flat surface. This minimum amount was measured in controlled laboratory experiments at Purdue to be in the range 100-400 nm. This is consistent with the gas balance results shown in Table 4.1 that shows a larger difference in deuterium retention with the higher amount of lithium evaporated in the neutral beam heated discharges.

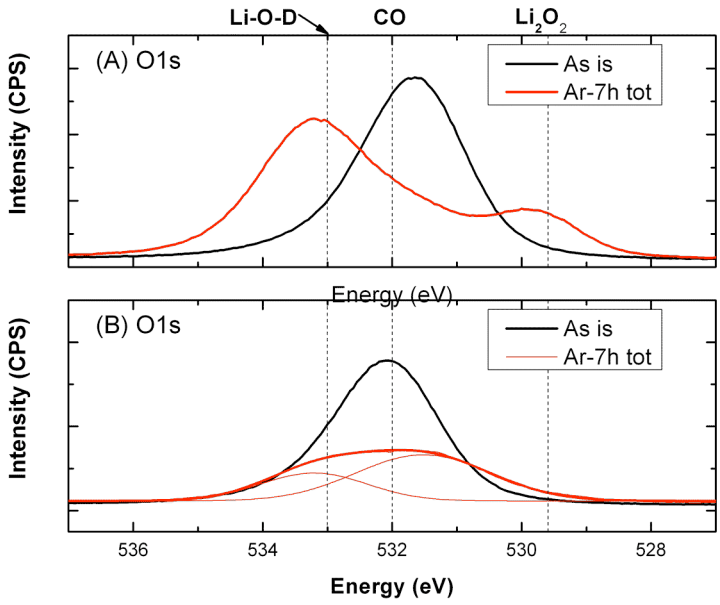


Fig. 5.5. XPS spectra for two opposing radial locations on the same NSTX post mortem tile A235-021. The location in (A) represents a location of high Li surface concentration (~4 x$10^{18}$ Li atoms/cm$^2$) while location (B) has a low Li surface concentration (~1 x$10^{18}$ Li atoms/cm$^2$). The thin lines in (B) represent multiple peaks that compose the primary (thick) peak.

NSTX tile A235-021 was removed from the upper outer divertor location near LiTER after the 2008 campaign, and XPS spectra are shown in Fig 5.5. It can be seen that the dominant XPS peaks occur at different energies in different regions of the tile. The Li surface concentration was measured by Wampler by ion-beam analysis (IBA)[8]. The XPS spectra represented in Fig 5.5a are from a surface region with a Li concentration ~ 4 times greater than the surface region shown in Fig 5.5b. IBA results also have shown that both locations have comparable deuterium concentrations. This is an interesting and important result, which elucidates on a particular aspect of deuterium retention mechanisms in lithiated graphite in NSTX. This point will be discussed in the summary section of this report.

[8] W. Wampler, et al., J. Nucl. Mater., 390-391 (2006) 1009.

## 5.2 XPS and thermal desorption spectroscopy (TDS) measurements of samples from the NSTX PMI probe.

Graphite, silicon, and palladium samples were exposed to NSTX deuterium plasmas during neutral beam heated and ohmic heated regimes using a PMI probe. The PMI probe is equipped with thermocouples connected to these samples to measure temperature ramps for thermal desorption spectroscopy (TDS). Once the samples are exposed to a selected number of shots, the probe can be retracted using a remote-controlled manipulator into an in-situ vacuum chamber equipped with a quadrupole mass spectrometer calibrated to measure hydrocarbon emission during a controlled temperature ramp. The four samples in the probe head are individually measured and thermally isolated (although there is about a 100-150 C increase in temperature for "non-heated" samples when the ramp reaches its maximum near 800 C). Samples not tested with in-situ TDS at NSTX are shipped in argon atmosphere to Purdue University for analysis using XPS and similar TDS.

Samples from both ohmic and neutral beam plasmas exhibited similar XPS spectra. The graphite sample XPS spectra shown in Fig 5.6 (A1) and (B1) are similar to those from tile regions with low-Li deposition as shown in Fig 5.5 (B). Based on NSTX lithium deposition monitors, and assuming that all deposited Li in NSTX is deposited on the divertor (25% of the vessel 40 $m^2$ surface, assuming lithium density of 0.53 $g/cm^3$), the sample shown in Fig 5.6 (A) had a nominal deposition thickness of ~214 nm Li. In a follow up PMI probe experiment, shown in panes (A2) and B2), much more lithium (~ 9x, total thickness of 1.84 μm) was deposited and resulted in XPS peaks characteristic of Li-D interactions, or retention.

It has been observed that deuterium retention is strongly correlated with deuterium recycling at the NSTX plasma edge. Furthermore, as discussed earlier there is strong correlation of peak functionalities associated with the interaction of D atoms in a lithiated graphite matrix. However, one key aspect of all this data has been the "effective minimum lithium thickness" necessary to influence D retention in lithiated graphite matrix. This is particularly important since the surface morphology of NSTX tiles can change greatly throughout a campaign, between NSTX and laboratory experiments and from sample to sample. Fig 5.7 shows scanning electron microscopy (SEM) images of various substrates, including (A) NSTX post mortem tile, (B) polished ATJ graphite for control experiment, (C) polished ATJ graphite for probe sample, and

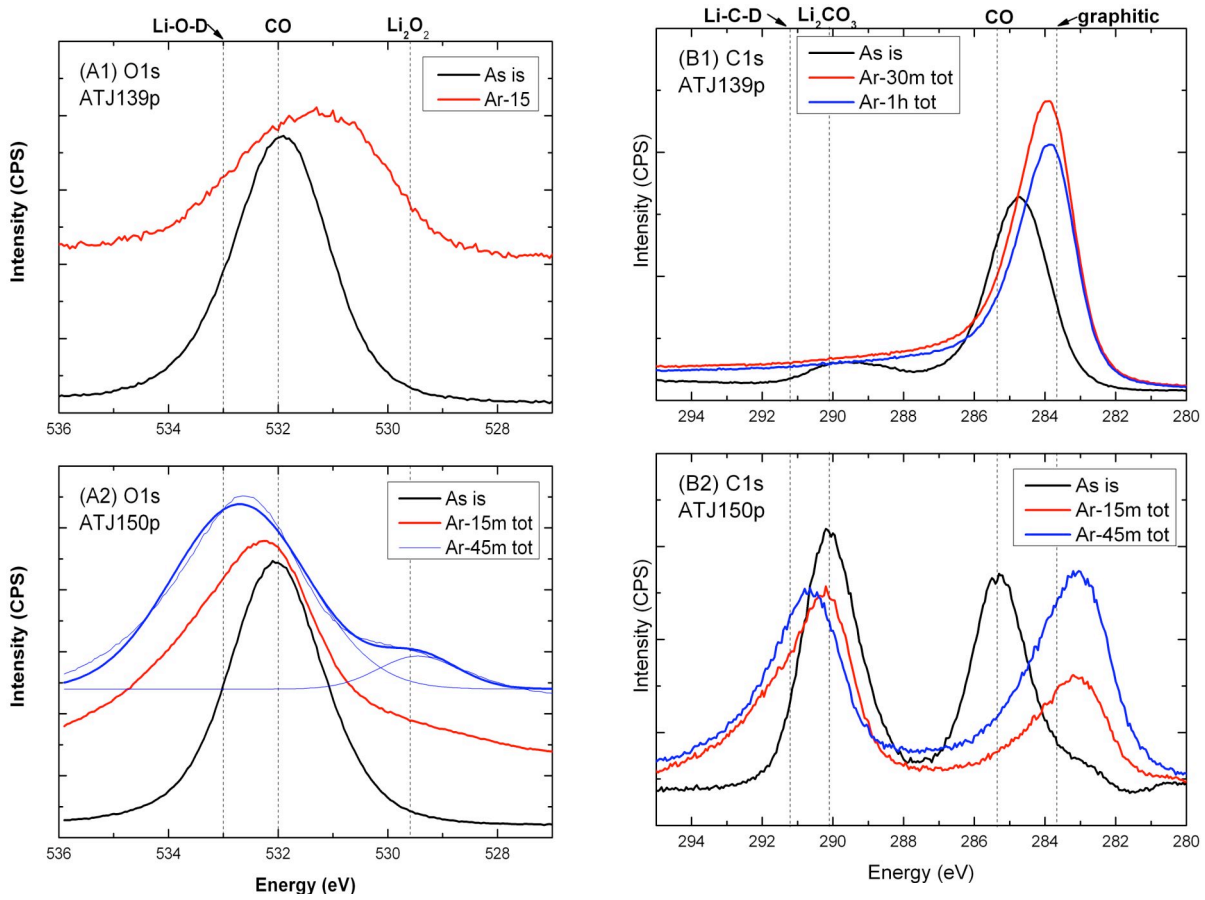


Fig 5.6. XPS spectra from two graphite samples exposed via the NSTX sample analysis probe. Panes A1 and B1 show XPS spectra from a sample with 214 nm Li that was exposed on April 24, 2009 to neutral beam heated plasmas with lithium conditioning before and after 15m, 30 m, 1h of argon cleaning. The two lower panes (A2 and B2) show XPS spectra from a sample with increased Li deposition to an equivalent thickness of 1.84 μm that was exposed on August 3-4, 2009. The thin lines in (A2) represent multiple peaks that compose the primary (thick) peak.

(D) Si used in probe sample. The SEM micrographs suggest that samples exposed to NSTX plasmas suffer radiation damage and dramatic surface morphology changes compared to the polished sample from (B) used in controlled experiments at Purdue. This poses two important observations: 1) even when morphologies are drastically different the D functionality is consistent and 2) lithium deposition on "rough" morphology can result in the effective Li layer thickness being much less than the ratio of areal mass deposited over the density. Further studies are necessary to understand the role of "lithium dose" and deuterium retention.

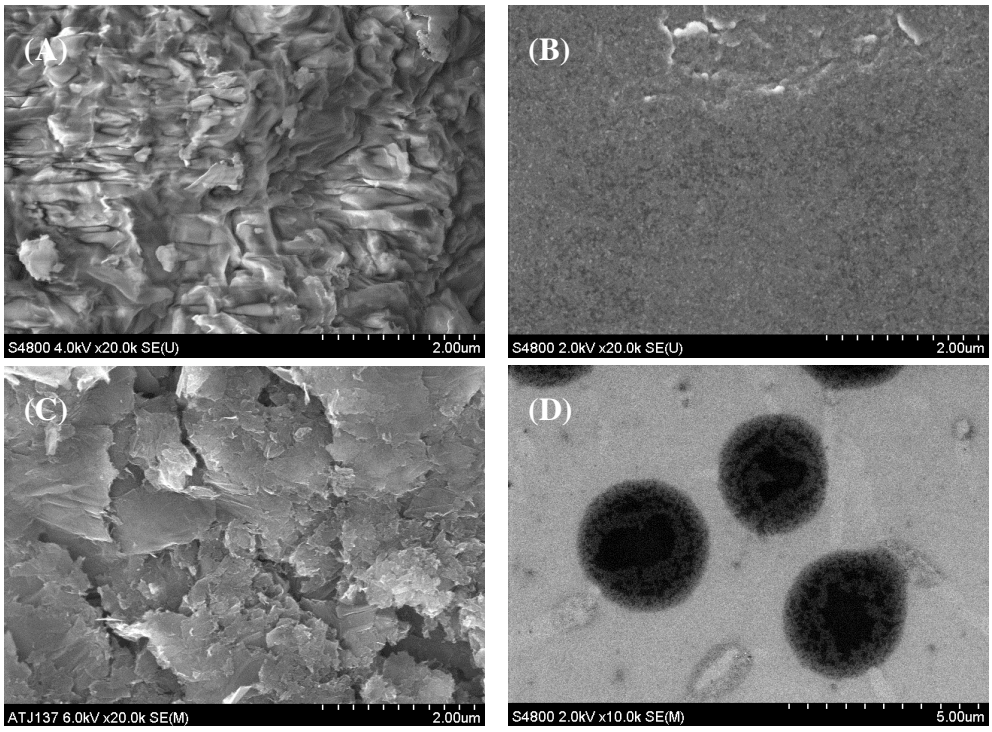


Fig 5.7. SEM images for various substrates, including (A) NSTX post mortem tile, (B) polished graphite used for control Li deposition and D irradiation, (C) polished graphite exposed to NSTX plasmas via sample analysis probe, and (D) Si exposed to NTSX plasmas via sample analysis probe. Note that the SEM scale refers to the complete marker made up of 10 sub-markers.

The PMI probe was used to expose samples during the NSTX gas balance experiments reported in sect. 4. Fig. 5.8 shows TDS spectra of samples exposed during the ohmic discharges for lithium and no-lithium deposition conditions. Fig 5.9 is for the neutral beam heated discharges. The TDS data is plotted as the partial pressure of all deuterium atoms desorbed by heating the sample to temperatures above 800 K. The data shows two peaks corresponding to effective release of deuterium. The peak near 600 K indicates a weak bonding state for D atoms in the presence of lithium. This is analogous to D bonding in lithium when bonded in solution. Higher peaks indicate stronger covalent bonding to Li, O, and/or C. This result is consistent with the post-discharge release of the additional deuterium retained with lithium in NSTX shown in Figs. 4.2 and 4.4. For sample ATJ135, the partial pressure of all D atoms was several orders of magnitude lower than other samples shown. This was due to a systematic experimental error in the TDS procedure for this sample. However, the peak locations at each temperature have similar signatures as the other three TDS samples.

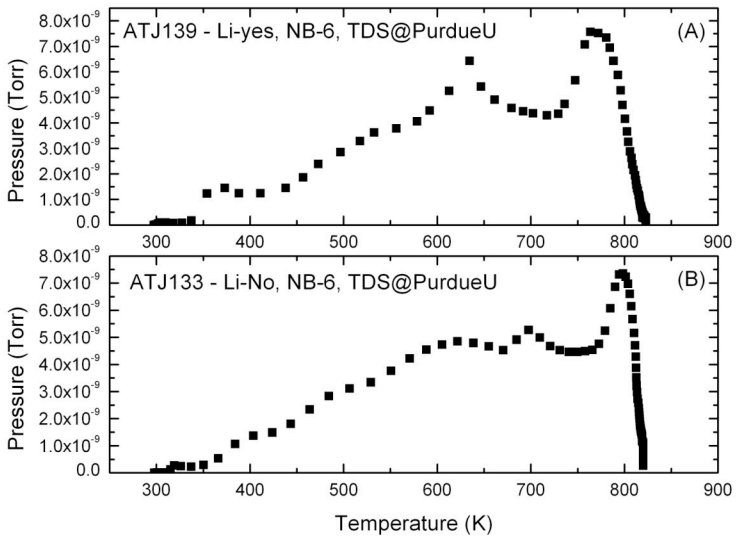


Fig 5.8. Temperature desorption spectroscopy (TDS) data of ohmic NSTX shots of PMI probe ATJ graphite samples with- and without lithium exposure.

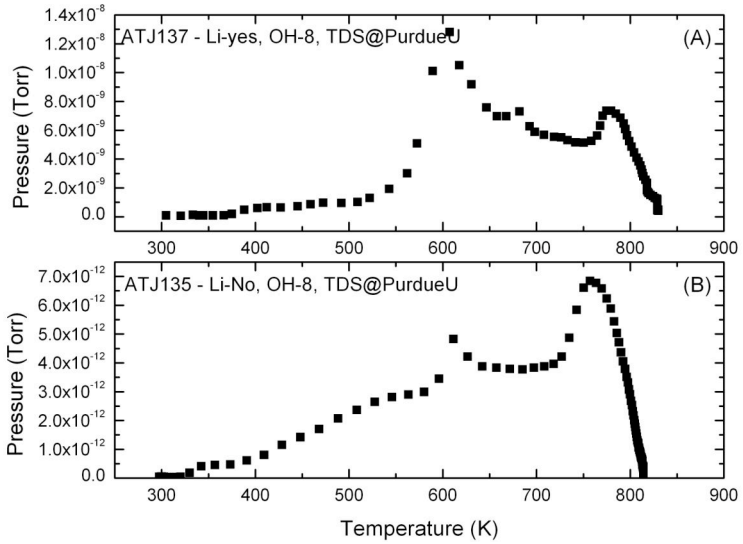


Fig 5.9. Temperature desorption spectroscopy (TDS) data of neutral beam heating NSTX shots of PMI probe ATJ graphite samples with- and without lithium exposure.

The quantitative amount of deuterium in a Pd witness sample on the PMI probe was measured using the 4-point probe method described in reference [9]. The 4-point probe technique compares the electrical resistivity of a control sample (in this analysis a 50 nm Pd film on a Si substrate) to a sample exposed to solute atoms (here, deuterium). Adsorption of solute atoms in a metallic matrix causes the resistivity to increase. The increase in resistivity is then related to an absolute atomic concentration. Using this method, an absolute D concentration of $5.16 \times 10^{20}$ $m^2$ was calculated for the pre-lithium NB discharges 132470-132475. The Pd sample was adjacent to the graphite sample heated to about 800 K for TDS measurements and heat conduction caused the Pd sample to reach temperatures near 400K releasing some of the D. It is likely this value would be a factor-of-ten higher if there had been complete thermal isolation of the Pd sample. For comparison, the sum of the gas balance retention for these discharges is $1.26 \times 10^{22}$ D atoms less outgassing between discharges.

The D flux to the Langmuir probe on the PMI probe was insufficient to measure D. Other Langmuir probe measurements located several cm inboard of the probe (R = 0.911 m) show a total particle flux of $1.16 \times 10^{22}$ $m^{-2}$ during the plasma shots to which the Pd sample was exposed. Considering that heating decreased the total D concentration on the Pd sample and that the Langmuir probe measurements from a location inboard of the PMI probe the two estimates of the D flux are in reasonable agreement and consistent with the exponential drop in D flux moving outboard from the location of the R = 0.911 m Langmuir probe to the PMI probe.

### 5.3 Summary: Implications to our understanding of deuterium retention in lithiated graphite

The above results provide insights into deuterium retention in lithiated graphite. Post-mortem NSTX tile analysis and controlled Purdue experiments using XPS have identified important chemical functionalities associated with deuterium irradiation in a graphite surface conditioned with lithium. These functionalities operate in both O1s and C1s spectra suggesting that the interaction of deuterium atoms is by indirect electrostatic interactions with Li atoms. This conjecture will be further tested in future work with techniques such as Raman spectroscopy

[9] Morris, D. R., L. Yang, X. Sun and F. R. Steward,“ The Electric Resistance of Dilute Solutions of Hydrogen or Deuterium in Palladium,” *Can. Met. Quart.* **40**, 91-96 (2001b).

and HR-EELS, that will measure the hybridization state of deuterium atoms in the Li-O-C matrix directly. The XPS data alone however do not describe the whole picture. The XPS data is complemented by two other important data sets, the ion beam measurement of D concentrations and thermal desorption spectroscopy. IBA analysis is sensitive to atoms in the top few microns. Although IBA does not resolve well the top 10-50 nm region measured in XPS, the lack of correlation between deuterium and lithium concentrations suggests that lithium is *not* increasing deuterium retention. The TDS data of the PMI probe samples aids in understanding the apparent discrepancy. The TDS fluence shows that steady-state retention is comparable for graphite surfaces conditioned with and without lithium. This is consistent with observations from NSTX gas balance measurements. The TDS spectra show that the binding energy for deuterium atoms in lithiated graphite can be a factor of 50% less than D bound in a graphite surface without lithium. This suggests the binding of D atoms in the lithiated graphite matrix is very different than in a non-Li conditioned graphite surface. NSTX operation with lithium-conditioned graphite surfaces show substantial operational differences compared to non-lithiated conditions. This suggests that retention mechanisms of D atoms *during plasma-surface interactions* are important and that the region of few 10-50 nm at the surface may play a key role in the way deuterium is bound (see also sect. 4). As noted from the controlled particle-beam experiments at Purdue using in-situ XPS, deuterium may be indirectly interacting with lithium atoms present during lithium conditioning in NSTX. Post-mortem and in-situ (but outside the NSTX plasma environment) experiments are not sufficient to clarify this point, however. One would need in-situ, real-time diagnosis of the lithiated graphite surface during D-plasma operation in NSTX with depth resolution between 10-50 nm to clearly identify the mechanism retaining deuterium to the lithium conditioned surface.

Therefore the key finding here is not *how much* deuterium is retained by conditioned and non-conditioned surfaces. The key is *how deuterium is bound during interaction of the plasma with the Li-conditioned graphite surface*. From the combination of IBS, XPS and TDS data, lithiated graphite and non-lithiated graphite surfaces can retain a comparable amount of deuterium in steady state. However, *during plasma interaction*, with *enough lithium dose (or amount near the surface)* the binding or retention of D atoms is *fundamentally different* from that of non-conditioned graphitic surfaces. In particular, D atoms are weakly bonded in regions near lithium atoms bound to either oxygen or the carbon matrix.

The ability for either conditioned and non-conditioned graphite surfaces to retain comparable amounts of deuterium in steady-state means that lithium alone is not responsible for retention of deuterium and in fact the surface morphology plays a very important role as well. With higher surface-to-volume ratio of "rough" graphite layers the higher surface energy and dangling bonds can quickly react and bind deuterium. This is evident in the TDS spectra shown in Fig. 5.8. For both lithium and non-lithium cases both peaks at low and high temperatures are measured with the notable difference in the lithiated case the low-energy (temperature) peak is observed higher than the peak at 750 K. The nature of the binding *substantially changes* when enough lithium is deposited. How much lithium is 'enough'? This at the moment is difficult to determine since the morphology is such that a given dose of lithium will effectively deposit a distribution of "layer thicknesses" by deposition of Li atoms in surface crevices and protrusions. It seems likely that the top few nm's of these protrusions become important sites for deuterium retention and lithium seems to make this interaction with the graphite matrix stronger. The TDS data also demonstrates that for non-conditioned surfaces the nature of the deuterium emission is also different due to the inherent binding of D atoms and possible chemical sputtering effects that are suppressed by lithium conditioning.